Janusz German

INTRALAMINAR DAMAGE IN FIBER-REINFORCED POLYMERIC MATRIX LAMINATES

KRAKÓW 2004

Praca habilitacyjna

CONTENTS

LIST OF IMPORTANT SYMBOLS

β	multiplier characterising crack opening displacement
β_m	average crack opening factor
$\boldsymbol{\varepsilon}$	strain tensor
ε_{Lult}	ultimate longitudinal strain
ε_{rst}	Ricci's symbol
ε_{Tult}	ultimate transverse strain
$\eta^L_{x,xy}$, $\eta^L_{y,xy}$	coefficients of mutual influence of the second kind
$\eta^L_{xy,x}$, $\eta^L_{xy,y}$	coefficients of mutual influence of the first kind
ν^L_{xy} , ν^L_{yx}	Poisson's ratios
θ	the angle of fibers orientation[1]
Θ_{tt} , $\Theta^{(k)}_{tt}$	invariant polynomial functions
ρ'	average crack density
$\boldsymbol{\sigma}$	stress tensor
σ^{∞}	remote tensile load of an infinite strip with a crack[1]
σ_{ult}	ultimate stress
(1, 2)	principal material coordinate system for a laminate ply[1]
$\boldsymbol{A}$	extensional stiffness matrix of the laminate
$A_1 - A_{10}$	material constants
$a_1 - a_8$	material constants
a_{ij}	second order kinematic matrix
$\boldsymbol{A}^d$	extensional stiffness matrix of a laminate in the damage state

[1] See Figure 1.7.

$\boldsymbol{A}^o$	extensional stiffness matrix of a laminate in initial (virgin) state
ATH	abbreviation for term ”Azzi-Tsai-Hill” criterion
$\boldsymbol{b}$	displacement jump vector[2]
$b_1 - b_8$	material constants
$\boldsymbol{C}$	stiffness matrix of a laminate ply in material axis
$c_1 - c_3$	material constants
$\overline{\boldsymbol{C}}$	transformed reduced stiffness matrix of laminate ply in reference coordinate system
$\overline{\boldsymbol{C}}^d$	transformed reduced stiffness matrix for a ply in damaged state
$\boldsymbol{C}^{\boldsymbol{d}}$	stiffness matrix of laminate ply in material axis, characterising the change of stiffness due to damage
CLT	abbreviation for term ”Classical Laminates Theory”
$\boldsymbol{C}^{\boldsymbol{o}}$	stiffness matrix of undamaged laminate ply in material axis
$\boldsymbol{d}'$	second order damage tensor (dyadic product)
$\langle \boldsymbol{d}' \rangle$	”average” damage tensor
$\langle \boldsymbol{d}' \rangle_n$	damage tensor of the normal discontinuities
$\langle \boldsymbol{d}' \rangle_t$	damage tensor of the tangential discontinuities
E	Young’s modulus
E_2	transverse Young’s modulus of a laminate ply
E_x^L	longitudinal Young’s modulus
E_y^L	transverse Young’s modulus
$\boldsymbol{e}$	strain tensor
e_{ij}	second order kinematic matrix
f	finite size correction function for stress intensity factor
$f_1 - f_3$	material constants

[2] See Figs 1.5 and 1.7.

F_{ult}	ultimate load
G_{xy}^{L}	shear modulus
$K_1 - K_{23}$	system of 23 invariants in contracted notation (Voigt's notation)
K_I	the stress intensity factor for crack in mode I
L	the length of representative volume element[3]
l	the crack length
LEFM	abbreviation for term "Linear Elastic Fracture Mechanics"
n	number of cracks
$\boldsymbol{n}$	unit outward vector normal to the surface S [4]
$\boldsymbol{P}^d$	matrix of transformation functions
$\boldsymbol{P}^o$	matrix of transformation functions
PPDM	abbreviation for term "Partial Ply Discount Method"
PR	abbreviation for term "Poisson's Ratio"
$R_{ij,k}$	polynomial functions of the set of invariants system (eq. 45)
RVE	abbreviation for term "Representative Volume Element"
S	crack surface[5]
s_m	average crack spacing within m-th damaged ply[3]
t	RVE thickness (the total thickness of a laminate specimen)[6]
t_m	thickness of m-th damaged ply (≡ intralaminar crack length)[3]
$\boldsymbol{T}^o$, $\boldsymbol{T}^d$	transformation functions
$\boldsymbol{u}$	displacements vector of crack surfaces
$\langle u \rangle$	average crack opening displacement
U_i	invariant functions of Tsai and Pagano
$V_1 - V_4$	geometrical coefficients for a laminate

---

[3] See Figs 1.6 and 1.7.
[4] See Figs 1.5 and 1.7.
[5] See Figure 1.5.
[6] See Figure 1.6.

v_m	the volume fraction of m-th laminate ply
W	the width of RVE[7]
(x, y)	reference coordinate system[8]
YM	abbreviation for term ”Young’s Modulus”

[7] See Figs 1.6 and 1.7.
[8] See Figure 1.7.

PART I
Theoretical Analysis

ABSTRACT

In the present paper, the damage of fiber-reinforced polymeric matrix laminates is considered with the aim to examine the change of their mechanical properties under external loading.

The damage mode in the form of intralaminar cracks (”primary matrix cracking”) has been described in terms of second order, symmetrical damage tensor by Vakulenko and Kachanov. It allows considering the orientation of the defects, which is determined by the orientation of the constituent layers. The crack discontinuity parameter is estimated in the frame of linear elastic fracture mechanics.

To describe the changes of the mechanical properties of a body caused by the damage – the constitutive relations, which take into account developing damage, along with stress and strain are needed. In order to derive an adequate description, the approach based on polynomial invariants functions and irreducible integrity basis by Adkins is employed.

Theoretical results are compared with the experimental data related to the longitudinal Young’s modulus, Poisson’s ratio and crack density, obtained for cross and, angle-ply laminates manufactured from carbon/epoxy Vicotex NCHR 174B prepreg tape.

The results related to the influence of developing intralaminar damage on ultimate strength are also shown and discussed.

1. THEORETICAL ANALYSIS

1.1. INTRODUCTION

One of the most important factors determining the load-bearing capacity of structural materials is the presence of internal defects (voids, micro-cracks, imperfections of the structure, etc.), which can exist as initial defects and/or can initiate and develop in response to the applied external load.

In case of the materials in a bulk form, for example metals, the failure assessment problem can be formulated in terms of fracture toughness, i.e. the resistance to growth of one, isolated crack driven by different mechanisms induced by e.g. fatigue, creep, corrosion process etc. Fracture mechanics provides now very efficient methods to solve the problems of this class.

In the case of composite materials the deterioration process is, however, much more complex, due to the existence of at least two constituents which

differ in properties. The main feature of composite material deterioration, contrary to a monolithic material, is the multiplicity of cracking in various shapes and forms which depend not only on the constituents' properties, but also on their geometrical arrangement. Therefore, considering deterioration of composites, one must take into account the multitude of cracks, instead of a single crack.

The composite materials damage, expressed in terms of fracture mechanics is, at the present time, at a relatively early stage (see e.g. [13]) and has limited usage. What is more, taking into consideration extremely complicated solutions of crack problem in an anisotropic body [120], one can conclude that the methods and models established by fracture mechanics are, in general, not very useful, or too unrealistic, or cumbersome. However, significant progress in fracture mechanics application to composite materials analysis has been noticed in recent years and one can expect further intensive development in this area, mainly due to the application of refined, specialized, professional numerical codes and methods (e.g. FRANC 2DL [123], IDEAS [115], [116]). The research activities are focused basically on the determination of stress intensity factors [30], [117], fracture toughness K_{Ic} and COD fracture criterion [65], as well as energy release rate [50], [97]. In most cases, the analysed cracks are assumed to originate at the boundary of stress concentrators in the form of circular and semi-circular notches.

The problem of composite laminates damage is considered on different platforms and different aspects are taken into account. Let us confine the basic issues to the following:

- load,
- plies stacking sequence and other laminate's geometrical features (e.g. notches),
- damage mechanisms,
- theoretical approaches,
- experimental verification.

It is obvious that the above issues are in most cases "coupled" to one another, therefore the review of up-to-date literature must be seen, more or less, as a reflection of the main trends only, and the personal choice by the author of the present work, probably far from complete and precise.

As regards the laminate's loading, fatigue load with tension-compression cycles is most often considered (it is typical not only of composites, but also of all other materials). One of the first and most comprehensive publications

in this field is the book by Talreja [124]. From the wide spectrum of current problems let us mention only some interesting examples, namely: fatigue damage induced composite's residual strength degradation model ([102], [142]) and residual stiffness degradation model ([102], [137], [138]), life period estimation of composite plate with damage [93], combination of orthotropic damage model and isotropic fatigue evolution model [2], the FEM based fast and computationally efficient composite's fatigue damage simulation [136]. An interesting review of fatigue damage of composite materials is reported in [19].

In the vast number of papers (e.g. [12], [15], [31], [53], [58], [63], [69], [76], [84], [102], [103], [107], [109], [115], [121]) the static load, i.e. monotonically increasing unidirectional and biaxial tensile load (with visible majority of the first one), and less frequently bending load [73] are analysed.

Taking into account laminates' plies stacking sequences one can state that most effort is devoted to cross-ply laminates, while other sequences are rarely analysed. It can be explained by the fact that in a cross-ply laminate damage is localized in 90° plies only and the overall picture of laminate's damage is quite clear from both theoretical and experimental point of view. It is also easier to formulate some general conclusions for different composite materials. An analysis of laminates of any configuration needs more effort, and it is difficult to get "universal" conclusions that are reliable and relevant for any plies stacking sequence and type of composite material.

In the last few years we have noticed a growing interest the notches induced damage; notches of different configuration (e.g. central and edge notches) and of different shape (e.g. circular and semi-circular) [15], [69], [74], [86].

Let us now discuss briefly (more detailed considerations are included in the next chapter "Problem Formulation") the basic damage mechanisms in composite laminates.

One can notice that the biggest interest is focused on delamination, though it need not necessarily be of primary importance in each case, when laminate's life period is considered. The probable reason is that delamination is a phenomenon easily visible with the naked eye, and therefore it is considered the crucial factor for determination of the laminate's serviceability. However, one must keep in mind that delamination is often very close to final massive failure (in such a case it is

too late for intervention!) and it is always preceded by a progressive process of matrix deterioration.

Matrix damage in off-axis plies, also called ”the transverse cracking”, is the first state in the progressive damage process, but it can cover a considerable part of the life period, and – what is equally important – it always initiates possible consecutive damage mechanisms. The direct, unfortunately invisible to the naked eye, result of matrix cracking is degradation of laminate's strength and stiffness. This can be seen as one of the basic reasons of interest in this phenomenon. The other reason is that the standard procedure – widely used in the frame of strength analysis of laminates – based on partial or total ply discount method coupled with one of many strength criterion [37], [47], [59], [66], [98] leads to unreasonable predictions of engineering moduli changes caused by progressive laminate deterioration (an example is given in Part II of the present work).

The problem of stiffness changes due to matrix cracking has been considered for 15 years very extensively by many authors, on the basis of different approaches. The main reason is that composite materials combine excellent strength and stiffness characteristics with low weight, therefore are specially predestined for lightweight, e.g. aerospace, structures. On the other hand, such structures need a careful inspection and adequate tools for design, which take into account limits of damage tolerance [89]. Despite the unquestionable importance and ”attractiveness” (from both the scientific and practical points of view) of the problem of laminate's stiffness degradation due to damage development, the number of papers in this branch of composite mechanics is not large in comparison with other current topics of the mechanics of composite materials. As a proof, let us show the results of searching in World Wide Web. The three most popular and reliable searching engines, namely Altavista, Yahoo and Google asked for a key-word ”*laminates*” gave 162.000, 190.000 and 198.000 results, respectively (searching was done in November 2003). Refining searching process by adding specific, more detailed key-words and phrases, one can obtain results which are shown in Figure 1.1. Even if not all results are adequate and part of adequate papers is not available in the web, it is evident that the number of findings regarding basic terms in composite mechanics as: *shear*, *delamination* and *stiffness* is substantially bigger than number of results obtained for the same terms, but coupled with key-word *damage* or key-phrase *stiffness reduction*. It is characterized, on average, by factor 2.3

and 1.7 for *shear* and *delamination*, respectively. However, for *stiffness* and *stiffness reduction* the factor is, on average, as big as 50 (!).

This result, drastically different from the two others, let us to conclude, that the problem of the influence of damage on composite laminates characteristics is still open and far from final solution, after about 20 years of research. It can be seen as an explanation of different methods and approaches used in the formulation and description of the considered problem.

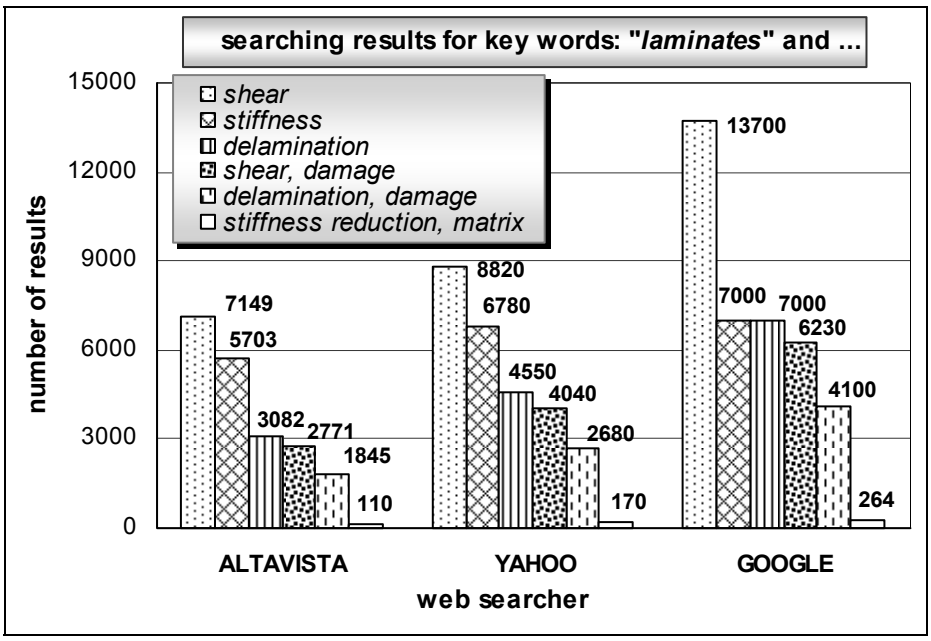

Figure 1.1. Results of searching in World Wide Web

The approaches used in the analysis of laminates damage are as follows:

1. Shear lag approach (see e.g. [57], [63], [70], [81], [115], [140]), which is based on the assumption that cracks exist only in a single ply, while the neighbouring material is undamaged.
   The serious weakness of this approximated approach is that the cracked ply is assumed to be constrained by homogenous material and therefore the laminate stacking sequence is ignored in the analysis.

2. Self-consistent approach (also called effective-medium approximation) is a tool for analysis of inclusions in a matrix.
   The basic idea is to embed a typical inclusion in a matrix that has an unknown effective property. The resulting expression for the effective property depends on the phase properties and volume fractions, and on the inclusion shape. Laws *et al*. [77] assumed that the stiffness of a cracked lamina can be approximated by the stiffness of an infinite isotropic body containing two sets of inclusions, one set being cylinders representing fibers and the other set being infinitely thin ellipses representing cracks. Using Eshelby's solution to the problem of an inclusion in an infinite elastic body combined with Hill's procedure for stiffness of multi-phase media measurement [56] they derived the approximated formula for the stiffness of a cracked lamina. This approach is fully analogous to classical micromechanical models for stiffness and strength computations, used in mechanics of composite materials (see e.g. [37]). The problem was refined by reducing the fibers and matrix to a single phase and embedding the cracks in this medium. Due to this approach, effective elastic properties of a cracked ply were determined and the laminate stiffness was then calculated using standard laminate theory. It has been shown that self-consistent approximations are exact for media that possess a type of topological symmetry that fiber-reinforced composites do not possess [132]. It is probably the reason why comparison of the stiffness estimates with experimental data available in the literature was not reported. Nonetheless, many researchers continue to apply self-consistent method because of its relative simplicity leading to close analytical solutions.
3. The micro-macro approach based on Mori-Tanaka's average model [92], reformulated later by Benveniste [14], [29].
   This approach is in fact based on micromechanical considerations, like self-consistent methods. The Mori-Tanaka approximation is obtained by assuming that the composite is a host material with imbedded inclusions and then choosing the host to serve as the reference material. The characteristics of individual phases can be linked to the overall composite response by the use of phases' local stress and strain in conjunction with the rule of mixtures. This model allows predicting damage initiation by comparing local stress field with the ultimate stress of the fiber or of the fiber/matrix interface. The advanced applications of Mori and Tanaka concept have been presented, recently, in e.g. [28], [119].

4. Minimum complimentary potential energy method introduced and developed by Hashin [52], [53].
   He considered a cross-ply laminate with transverse cracks in 90° plies. Assuming admissible stress fields in the cracked laminate which were approximated by employing the principle of minimum complementary energy, he derived the lower bounds for the laminate stiffness.
5. Variational mechanics approach which is mainly used in order to determine failure criterion based on energy release rate.
   This approach was successfully applied for rarely analysed composite laminates with outer 90° plies cracking under static load [95], for fatigue induced cracking [87], in analysis of transverse cracks leading to initiation of longitudinal cracks, delamination process [108], [109], stiffness reduction [141], as well as for more general analyses relating to stiffness reduction and crack opening displacement given in work by Praveen and Reddy [103].
6. Approach based on the average crack opening displacement (or more generally speaking – on displacement discontinuity) of a single, transverse and/or longitudinal matrix crack in the laminate [48], [49], [61], [63], [64], [90], [140], [143].
   This approach is often associated with analysis of delamination induced by matrix cracks. This approach needs, in most cases, sophisticated numerical FEM calculations, therefore it is a hard task to generalize obtained results.
7. Probabilistic approach (e.g. [29], [140]) which assumes that strength, fibers and matrix characteristics, fibers orientation, cracks density (in paper [18] a term ”statistical volume element” containing so-called critical defects leading to crack forming is introduced) etc. are random quantities.
   This approach is basically applied for statistical analysis of laminate failure, which is also defined in terms of probability.
8. Homogenisation method which, in general, deals with a cell [101] chosen from laminate’s ply including its constituents, i.e. matrix and fibers (and possibly damage [7]).
   For many researchers, e.g. [28], [119], the Mori-Tanaka model also belongs to homogenisation methods.
9. Continuum damage mechanics (CDM) approach [5], [6], [12], [124] – [128].
   The basic criterion for classifying any work as falling in the frame of CDM is description of cracks field with use of damage measures that are

inseparably associated with CDM concepts. Taking into account anisotropic properties of composite materials, the second order damage tensor is often used (see e.g. recent papers by Litewka *et al*. [83], [84] regarding damage in concrete, as well as paper [62] by Jiang *et al*. regarding impact load of laminate and paper [11] by Bai *et al*. on delamination).

This approach will be discussed in detail in chapter ”Continuum Damage Approach to Composite Body” of the present dissertation.

To supplement the above review let me add that brief, but quite complete survey of approaches related to composite laminates deterioration is given in [49] and quite recently in [96]. The review of theoretical and experimental research activity in one of the world leading centres in Cachan (France), regarding damage model for laminates is given in paper by Ladeveze and Lubineau [75].

Regarding the methods used in the analysis of composite laminates damage, they are like in other branches of engineering mechanics, either analytical or numerical. Advantages and disadvantages of both are well known. In case of composite laminates, due to the complexity of damage geometry, namely orientation and distribution of e.g. transverse cracks and unlimited possibilities of laminates forming, the result obtained for one configuration may be (and in many cases it is so) not appropriate for the other one. Taking it into account one may say that numerical methods have strong limitations from the point of view of generalization of obtained results. On the other hand, a number of sophisticated problems of composite mechanics can be solved solely with the use of numerical methods. The only conclusion to be made is that the method must be fitted to the considered problem. The current trends of numerical calculations in composite mechanics, including damage of composite materials, are reflected in e.g. report by Oñate *et al*. [100], and recent papers by Araújo dos Santos *et al*. [8], [9], Fiedler [31], Kilic *et al*. [72], Kato *et al*. [71].

In order to verify the theoretical model used in the composite laminates damage description adequate experimental procedures must be employed. A wide program of such experiments is presented in e.g. [76]. The basic task is to localize and to measure damage in form of e.g. matrix cracks. The basic methods are: optical method, acoustic emission method and electrical method based on AC/DC measurements. In chapter 2.4 ”Testing Instrumentation” of the present work, more detailed considerations regarding this aspect of laminates’ damage analysis are given.

To summarize briefly the above considerations regarding methods applied for laminate damage analysis, one can conclude that it is difficult, if possible at all, to point out the most effective or adequate approach. It is rather the question of researcher's individual choice and experience according to the motto: *the best tool is the tool you know how to use*, and which allows you to get reasonable results, of course.

1.2. PROBLEM FORMULATION

In the present publication, the problem of deterioration of a specific class of composite materials, namely fiber-reinforced polymeric matrix laminates, will be analysed on the base of damage mechanics concept, described in detail in the next chapter.

The main goal of the analysis of laminates' damaging process, by means of matrix transverse cracking, is to consider the influence of damage state on stiffness changes and, to some extent, also strength properties of composite laminates.

We confine our analysis to the laminates having combinations of unidirectional, cross-ply and angle-ply orientations under a monotonically increasing (nearly static) tensile load.

The theoretical model derived in this part of dissertation was verified in standard tensile tests. The testing procedures and their results together with detailed analyses are presented in Part II of the present work.

The mechanisms of damage in such laminates are quite well known and they have been reported by e.g. Reifsnider *et al.* [110] (an impressive review of Reifsnider's contribution to the development of composite materials mechanics, including composites' damage is given in the summary of his activities [111]). A schematic description of the fatigue damage development, recalled after [110], is shown in Figure 1.2.

The first stage of damage development is dominated by cracking of the matrix along fibers in off-axis layers which have fibers inclined in the direction of applied tensile load. This so-called primary matrix cracking results in a roughly periodic array of almost parallel cracks lying within off-axis lamina and spanning the entire width of a composite specimen. The cracks of this kind are also called intralaminar cracks. They are presented in

Figs 1.3 and 1.4, which show cracks within 90° ply of the cross-ply laminate.

The test observations of the polished specimen side surface show that the cracks density depends on the applied load level, orientation of the laminate, the stacking sequence of layers (see e.g. [95]) and the specimen thickness.

Reifsnider noticed that under fatigue loading after certain number of cycles the cracks density reaches a saturation level named Characteristic Damage State (CDS). In fatigue, CDS depends only on the laminate configuration irrespective of the stress level.

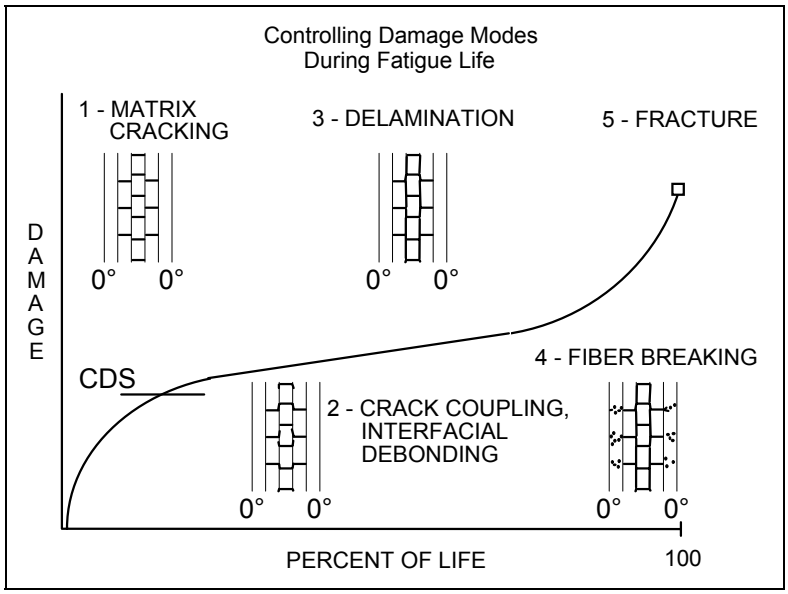

Figure 1.2. Fatigue damage development in composite laminates (from [110])

The subsequent damage stage is the initiation of cracks, transverse to the intralaminar cracks, lying in adjacent layers to those with primary cracks. These secondary cracks become initiators of the interlaminar cracks. Initially, they are small, isolated and sparsely distributed in the interlaminar planes. Subsequently, they grow and join together leading to a local loss of the laminate integrity.

Further development of damage involves large-scale fiber failures. In the final stage, the formation of a failure path through the locally damaged zones takes place.

The diagram shown in Figure 1.2 gives an overall picture of the laminate deterioration mechanisms, but it should be pointed out that not all of the mechanisms specified above must necessarily occur. Besides, some of those mechanisms can cover more or less wide range of laminate life period in comparison with indications shown in Figure 1.2. It depends mainly on laminate ply stacking sequence (for instance, that crack coupling may not be possible to occur and interfacial debonding as well as delamination will be present in a very limited range at a very late stage of laminate life).

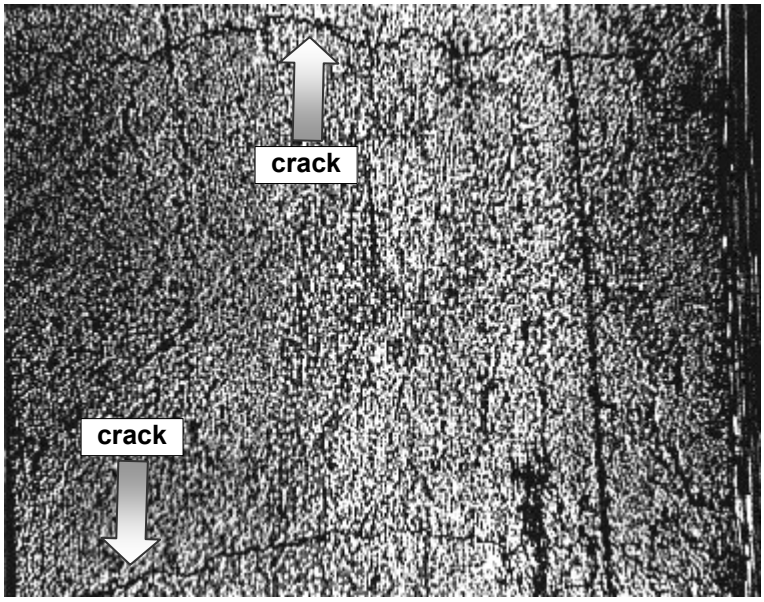

Figure 1.3. Transverse matrix cracking in [0, 90_8, 0] cross-ply laminate

The deterioration process is also influenced by the applied load. Reifsnider's diagram was obtained for fatigue load. In case of a monotonically increasing tensile load (nearly static load) and laminates with off-axis plies separated by on-axis plies, the predominant mechanism of laminate deterioration is intralaminar transverse matrix cracking (see e.g. [91], [95], [96], [99]). That first phenomenon, specified in Figure 1.2, is observed in a wide range of applied load. The delamination and fibers

breaking occur nearly simultaneously with a specimen failure. This observation has found confirmation in the author's experiments, carried out on symmetrical cross-ply and angle-ply specimens described in [36] and in more details in Part II of the present dissertation.

The process of intralaminar, transverse cracking is considered in the present publication with the aim to provide the description of the changes of mechanical properties of the composite laminate, caused by damage development. It was already reported by the author in the series of papers [35] – [38] and [40] – [45].

In order to describe the laminate matrix cracking, the CDM approach is utilised. Transverse matrix cracks are described in terms of damage concept with the use of tensorial damage representation, following Vakulenko and Kachanov's damage definition ([68], [135]).

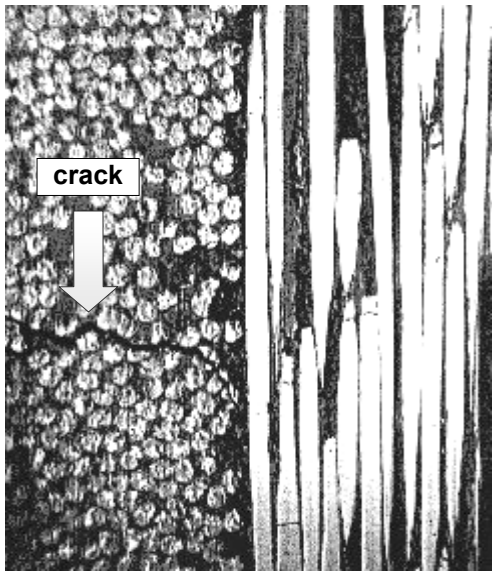

Figure 1.4. Transverse matrix cracking in [0, 90_8, 0] cross-ply laminate

The constitutive relations for damaged composite unidirectional lamina are derived in the frame of an approach based on polynomial representation of stress tensor as a function of the internal state variables [3], [4], [16] and [122].

Using those relations and employing concepts of the **C**lassical **L**aminates **T**heory (CLT) the changes of engineering moduli of a laminate are obtained as the final result.

They are related to the author's experimental data presented in Part II of the present dissertation.

1.3. CONTINUUM DAMAGE APPROACH TO COMPOSITE BODY

The term ”continuum damage” appeared in the 50's of 20^{th} century in the papers by Kachanov [67] and Rabotnov [105] related to the deterioration of homogeneous, isotropic continuum. However, the real development of CDM concept began in early 70’s, mainly due to activity of west European and Polish researchers.

The ”damage” in Kachanov’s formulation had no any physical, nor geometrical interpretation. It was characterised by the scalar quantity, called damage parameter which could change within the range <0, 1>.

In spite of the relative simplicity of the original damage measure formulation, it was successfully applied in many problems of mechanics, like e.g. interaction of creep and fatigue of metals [20], [21], creep crack propagation in bodies with dispersed damage [25], [33], [34], [54], [60], damage growth induced by stress concentrators [24], [26] and by strain energy [22]. Let us add that scalar damage measure is still used in the analysis of mechanical questions, as well as problems far from engineering at first glance, like modelling of heart attacks in terms of CDM [144]. A wide review of CDM achievements is given in published lectures by Chrzanowski [23] and Lemaitre [80].

For composite materials such an approach is rather useless, as in composites, which are in general anisotropic, the scalar representation of the damage state cannot reflect the orientation of defects. For instance, in composite laminates undergoing unidirectional tension, the orientation of the intralaminar cracks is determined by the orientation of the constituent layers (see Figs 1.6 and 1.7).

The continuum damage approach to the cracked composite materials is based on an element of the volume of homogeneous continuum, containing a representative sample of damage entities, called **R**epresentative **V**olume **E**lement (RVE).

By damage entity we understand a single micro structural change which in composite materials made of brittle constituents, under mechanical loads can take the form of a matrix crack, fiber break and fiber-matrix debonding.

In real composites, contrary to e.g. metals, we never observe a single dominant defect (for example crack), but a collection of damage entities. The collection of damage entities of the same, or at least similar geometrical features, is called a damage mode. In widely used laminated fiber composites, under tensile load, a set of almost parallel cracks can be observed, which are confined to layers of unidirectional fibers and have their planes normal to the laminate plane – these are so-called intralaminar cracks. Depending on the laminate stacking sequence, several damage modes can be distinguished in a given laminate.

A set of damage modes is simply called damage.

The damage state formed by a set of damage modes of any geometrical orientation (determined by the stacking sequence of the laminate composite) in the shape of intralaminar cracks will be analysed in the subsequent chapters of this publication.

1.3.1. Tensorial representation of damage

Let us consider, following [135], the two states of a body: the initial ”virgin” (i.e. without any damages) state and the actual one – the state in which internal damage is developing in the body in response to the applied external load. The transition from the first to the second state can be characterised by displacements vector of crack surfaces, $\boldsymbol{u}$, or strictly speaking discontinuity of displacements along crack surfaces. This is described by the displacement jump vector $\boldsymbol{b}$ across a crack surface S (see schematic Figure 1.5), which takes the form:

$$\boldsymbol{b} = \boldsymbol{u}_{+} - \boldsymbol{u}_{-} \ . \tag{1}$$

Vector $\boldsymbol{b}$ represents a certain influence of the considered single damage entity on the surrounding volume of the body.

Let vector $\boldsymbol{n}$ be a unit outward normal to surface S. Both $\boldsymbol{b}$ and $\boldsymbol{n}$ are in general different at each point of surface S.

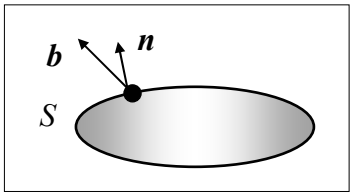

Figure 1.5. Displacement jump vector ***b*** and unit outward normal vector ***n***

Following classical papers by Vakulenko and Kachanov [68], [135] one can construct at any point of a single crack (i.e. damage entity) surface S, the second order tensor $\boldsymbol{d}'$ in the form of dyadic product of vectors ***b*** and ***n***, which fully defines the local geometry of a single defect and takes the form:

$$\boldsymbol{d}' = \boldsymbol{b} \otimes \boldsymbol{n}\, d\, S \ . \tag{2}$$

The components of a tensor $\boldsymbol{d}'$ are as follows:

$$d'_{ij} = b_i n_j \, dS \ . \tag{3}$$

In order to fully characterize the damage field by means of its total measure for "k" isolated defects – the summation of local damage, i.e. summation over k, must be carried out. We obtain the following relation:

$$\boldsymbol{d}' = \sum_k \boldsymbol{b}_k \otimes \boldsymbol{n}_k \, dS_k \ . \tag{4}$$

For the transition from discrete to the continuum model a standard averaging procedure must be employed by means of averaging the damage field described by (4) over a volume V of the representative volume element, containing representative sample of cracks. Denoting an average over volume V by symbol "<>", the damage tensor can be obtained as the sum of the integrals over the cracks surfaces S_k contained within the representative volume V, i.e. such a volume in which a representative sample of damage entities is contained. Thus, we can write the relation:

$$\langle \boldsymbol{d}' \rangle = \frac{1}{V} \sum_k \int_{S_k} \boldsymbol{b}_k \otimes \boldsymbol{n}_k \, d\, S_k \quad . \tag{5}$$

Discontinuity vector $\boldsymbol{b}$ can always be decomposed into the sum of two others, namely – vector $\beta\, \boldsymbol{n}$, which is parallel to vector $\boldsymbol{n}$ and the second one – $\boldsymbol{\tau}$ - which is normal to vector $\boldsymbol{n}$. Thus:

$$\boldsymbol{b} = \beta\, \boldsymbol{n} + \boldsymbol{\tau} \quad , \tag{6}$$

where β denotes a multiplier characterising crack opening displacement.

Inserting eq. (6) into eq. (5) we derive the decomposed averaged damage tensor in the form:

$$\langle \boldsymbol{d}' \rangle = \langle \boldsymbol{d}' \rangle_n + \langle \boldsymbol{d}' \rangle_t \quad , \tag{7}$$

where:

$$\langle \boldsymbol{d}' \rangle_n = \boldsymbol{d} = \frac{1}{V} \sum_k \int_{S_k} \beta_k \, \boldsymbol{n}_k \otimes \boldsymbol{n}_k \, d\, S_k \quad , \tag{8}$$

$$\langle \boldsymbol{d}' \rangle_t = \frac{1}{V} \sum_k \int_{S_k} \boldsymbol{\tau}_k \otimes \boldsymbol{n}_k \, d\, S_k \quad . \tag{9}$$

Damage tensor in form of eq. (8) characterises the normal discontinuity while tensor given by eq. (9) – tangential discontinuity. In terms of the 2-D crack behaviour considered here, the first tensor is suitable for description of the damage field with cracks in mode I (”normal mode”), the second one – in mode II (”shear mode”).

In further analyses, we retain only the normal tensor, since intralaminar cracks will be assumed active in mode I. The shear damage tensor will no longer be taken into consideration. It means that mode II (as well as mode III) is neglected.

The components of a symmetrical, second order, normal damage tensor are as follows:

$$d_{ij} = \left(d'_{ij}\right)_n = \frac{1}{V} \sum_k \int_{S_k} \beta_k \, n_{ki} \, n_{kj} \, d \, S_k \quad . \tag{10}$$

For the set of "*k*" identical (in fact nearly identical) damage entities, creating individual damage mode, with the restriction to normal component of ***b***, the damage tensor simplifies to the following form:

$$d_{ij} = \frac{1}{V} k \, b_i \, n_j \, S = \frac{1}{V} k \, \beta \, n_i \, n_j \, S \quad . \tag{11}$$

In successive analysis, surface *S* will be understood as the projection of the crack surface on a crack "midplane". Multiplier β is assumed as an averaged crack opening factor, depending on material stiffness, applied load, crack geometry and external geometrical constraints. The method of its determining lies within the framework of linear elastic fracture mechanics (LEFM) coupled with a new concept of "imaginary strip" proposed by the author. This concept is given in the next chapter.

1.4. INTRALAMINAR DAMAGE IN COMPOSITE LAMINATES

In order to determine damage tensor ***d***, let us consider the representative volume element (RVE) of the composite laminate, i.e. such a volume that contains complete information on damage representation within the laminate. The RVE is shown in Figure 1.6.

In the present work we confine the analysis to a specific damage mode, namely in the form of an array of parallel cracks lying along the direction of fibers and entirely spanning the width of RVE.

It is assumed that cracks are uniformly distributed along the RVE length with equal spacing, which is taken as the average cracks spacing under the applied load. Such a damage state is characteristic of the mechanism of intralaminar cracking of composite laminates. The crack surfaces are assumed to undergo a normal displacement only, which in terms of LEFM means that only mode I is taken into consideration. Modes II and III of the crack loading are neglected, as they are mostly related to delamination, which is not considered in the present work for reasons given in chapter 1.2.

It means, however, that the theoretical model gives a simplified picture of a real behaviour of the composite laminate, especially for high load levels.

The RVE shown in Figure 1.6 consists, for illustration, of three plies of different orientation and, as a consequence, of three damage modes named ”a”, ”b” and ”c”. The notation used in Figure 1.6 denotes: W – the width of RVE, L – the length of RVE, here understood as the length of a reference section of a specimen side surface along which the cracks are observed and counted in the corresponding experiment, t – the RVE thickness – meant further on as the total thickness of a laminate specimen, t_m – thickness of any damaged ply (as well as the intralaminar crack length) specified as m-th ply (alternatively put m-th damage mode) and s_m – average crack spacing within m-th ply.

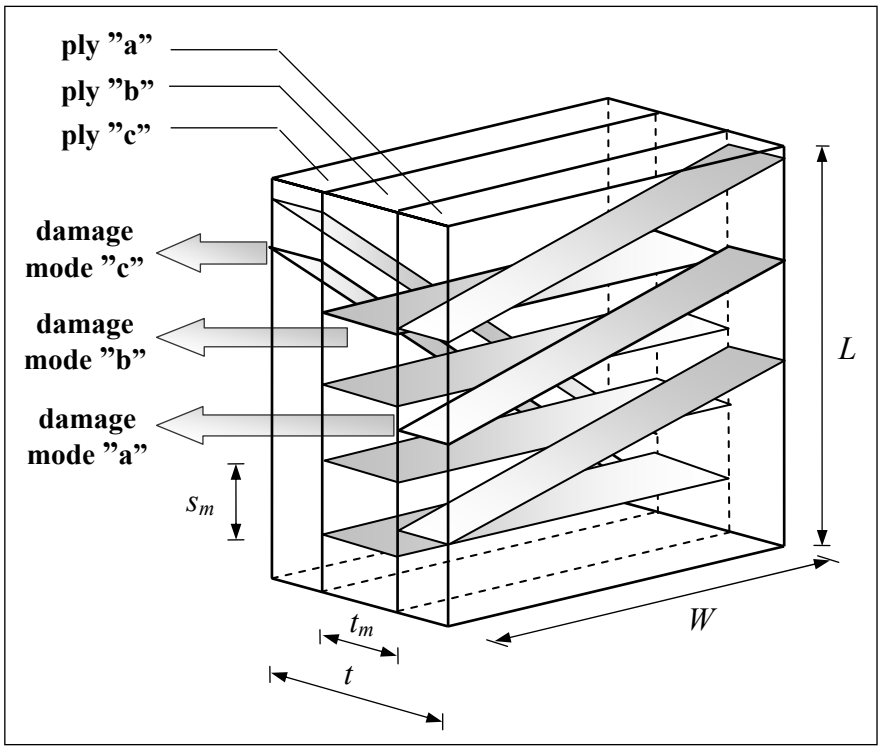

Figure 1.6. Representative volume element of damaged composite laminate with intralaminar cracks

Within the laminate volume V there are, in general, many cracking plies, specified by the angles of their orientation with respect to the chosen global reference coordinate system, thus many damage modes can be observed. It involves necessity of determining the damage tensors separately for each individual cracking ply.

In the present paper, another procedure will be employed. The damage tensor for any ply will be derived in the coordinate system which coincides with the principal material axis of orthotropy, i.e. on-axis configuration of a single ply will be a basis for determining components of damage tensor. Due to this approach, the common feature of all damaged plies is that they are formally indistinguishable from each other and the damage tensor for any ply is identical. Therefore, there is no reason to analyse every damaged ply of different angle orientation as the origin of separate damage mode, as was proposed in e.g. [5], [6], [124], [126] and [128].

The approach briefly presented above will be applied for a ply of arbitrary orientation given by angle θ_m with respect to the global reference coordinate system (x, y). It is chosen in such a way that the plane (x, y) is parallel to the mid-plane of a laminate ply. Principal material axes (1, 2) are taken in such a way that axis "1" coincides with the fibres direction, while axis "2" is perpendicular to the first one. The ply orientation is shown in Figure 1.7.

Using notation as in Figs 1.6 and 1.7, the volume V of RVE and crack surface S_m are equal, respectively, to:

$$V = W\,L\,t \ , \tag{12}$$

$$S_m = \frac{1}{\sin\theta_m} W\,t_m \ . \tag{13}$$

Since only the normal discontinuity of the crack surfaces is taken into consideration, we have:

$$\boldsymbol{b} \,||\, \boldsymbol{n} \ , \tag{14}$$

where unit normal vector $\boldsymbol{n}$ has in coordinate system (1, 2) the following representation:

$$\boldsymbol{n} = \left[0, \pm 1\right] . \tag{15}$$

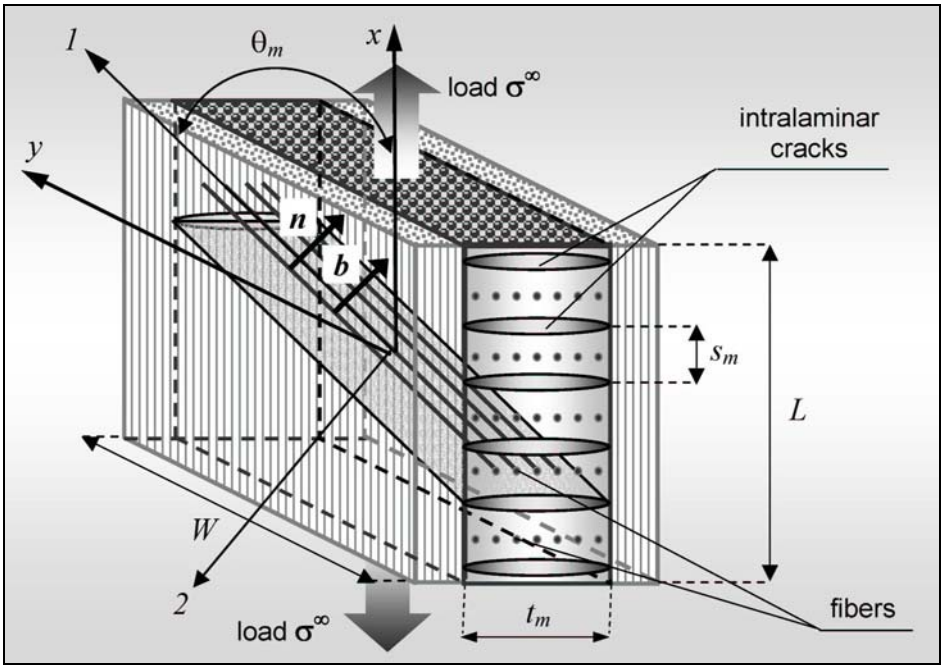

Figure 1.7. Orientation of damaged ply (*m*-th damage mode)

After elementary transformations, we derive the components of the damage tensor, expressed in principal material axis (1, 2) as follows:

$$d_{ij} = \frac{1}{\sin\theta_m} \rho_m \, v_m \, \beta_m \, n_i \, n_j \ , \tag{16}$$

where ρ_m denotes the crack density within *m*-th damaged ply, which is equal:

$$\rho_m = \frac{1}{s_m} = \frac{n}{L} \ , \tag{17}$$

and n denotes the number of cracks within section of length L, v_m means the volume fraction of *m*-th ply. Thus:

$$v_m = t_m / t \ . \tag{18}$$

The choice of an average crack opening factor β_m is an open question. There are two typical approaches to this problem.

Talreja in the series of papers [125] – [127] introduced a vector of the surface activity, which in fact plays the same role as vector $\beta \boldsymbol{n}$. Since crack opening displacement (COD) given by LEFM is proportional to the crack length and crack length is equal to the thickness of *m*-th ply of a laminate, he proposed to take as a crack opening factor β_m the product $\kappa\, t_m$ with κ to be assumed as a material constant. Thus, he considered in fact the flat crack of rectangular shape. The crack opening was controlled in this approach by a "new" constant κ only, and was independent of the applied load. The Talreja's concept is based on the simplistic assumptions and relations leading to relatively simple and easy to use results.

The approach employed in papers by e.g. Gudmundson and co-workers [49], [143] and Joffe *et al.* [64] allows, in turn, to avoid most of the simplifications of the Talreja's model, but needs using much more complicated analysis, based primarily on LEFM concepts and FEM calculations. However, the obtained results are probably more correct from the theoretical point of view and they are possible to be derived for any laminate's ply stacking sequence (in paper [64] – only 90 deg ply cracks are considered), though they lose the beauty of simplicity of Talreja's results.

In the present paper in order to evaluate the value of β the results of LEFM will be utilised. For the central crack of length $2l$ in an infinite strip loaded by remote tensile stress σ^{∞} (see Figure 1.8), the crack opening displacement u (in terms of Vakulenko - Kachanov's approach – displacement jump of crack surfaces) is given by the relation (see e.g. [32]):

$$u = \frac{2\sigma^{\infty}}{E}\sqrt{l^2 - r^2} \quad . \tag{19}$$

It can be easily rearranged to the form:

$$u = \frac{2K_I}{E\sqrt{\pi l}}\sqrt{l^2 - r^2} \quad , \tag{20}$$

where K_I denotes the stress intensity factor in mode I, which is equal:

$$K_I = \sigma^{\infty}\sqrt{\pi l} \quad . \tag{21}$$

Let us assume that the above relations can also be used for the central crack in a strip of a finite width $2c$ (see Figure 1.9) with replacing K_I in form (21) by the relation which includes the finite width correction factor. Thus:

$$K_I = \sigma^{\infty} \sqrt{\pi l}\, f(l/c) \,, \tag{22}$$

where the correction function f is taken in the form [32]:

$$f(l/c) = 1 + 0.128\,(l/c) - 0.288\,(l/c)^2 + 1.523\,(l/c)^3 \,. \tag{23}$$

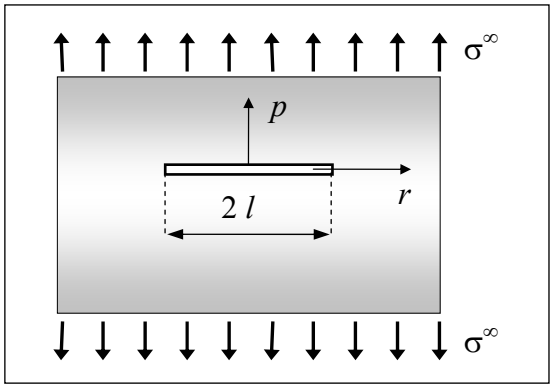

Figure 1.8. Central crack in an infinite strip

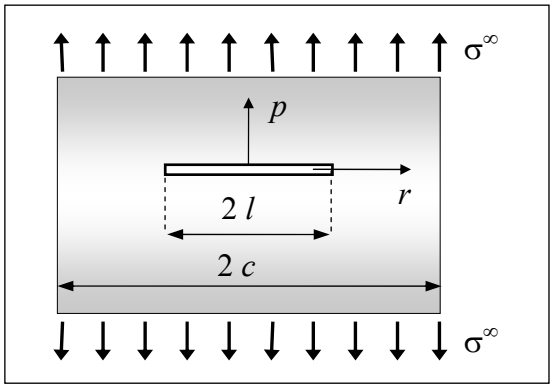

Figure 1.9. Central crack in a strip of finite width

The average crack opening displacement is defined as:

$$\langle u \rangle = \frac{1}{l} \int_0^l u \, dr \ . \tag{24}$$

Using eqs (19) and (22) we derive from eq. (24), after integration and simple transformations, the following relation for the average crack opening displacement:

$$\langle u \rangle = (1/E) b' \sigma^{\infty} \ . \tag{25}$$

The quantity *b'* denotes purely geometrical parameter equal:

$$b' = \frac{\pi l}{2} f\,(l/c) \ . \tag{26}$$

Let us introduce for a ply in *m*-th damage mode two vectors, namely an average discontinuity vector $\boldsymbol{b}'_m$ associated with parameter *b'* and a load vector $\boldsymbol{\sigma}^{\infty}_m$, both shown in Figure 1.10.

In principal material axis (1, 2) they take the following forms, respectively:

$$\boldsymbol{b}'_m = [0, \pm b'_m] \ , \tag{27}$$

$$\boldsymbol{\sigma}^{\infty}_m = \left[\pm \sigma^{\infty} \cos\theta_m \, , \pm \sigma^{\infty} \sin\theta_m\right] , \tag{28}$$

where b'_m, using the notation, as in Figure 1.10 and eq. (26), takes the form:

$$b'_m = \frac{\pi t_m}{4} f\,(t_m / c_m) \ . \tag{29}$$

Let us define an average crack opening factor β_m as a scalar product of the vectors $\boldsymbol{b}'_m$ and $\boldsymbol{\sigma}^{\infty}_m$, multiplied by $1/E$. Such a definition means in term of LEFM that mode III of crack load is not taken into account in the present model. Since β_m, characterising crack opening, must be positive, we take an absolute value of that product, therefore:

$$\theta_m = \frac{1}{E} b'_m \, \sigma^\infty \sin\theta_m \ . \tag{30}$$

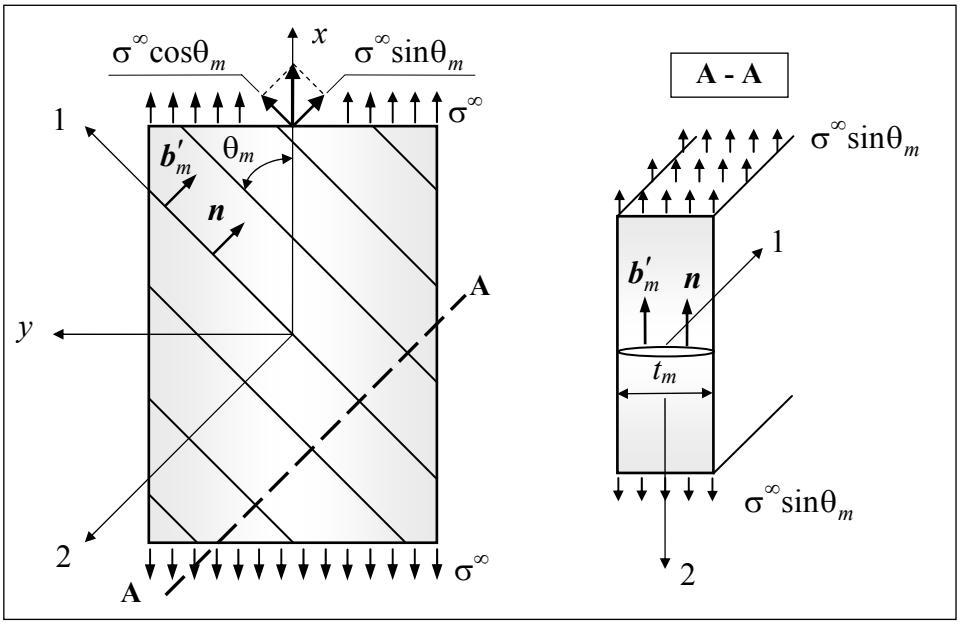

Figure 1.10. Geometrical characteristics for intralaminar crack

Thus, from eqs (29) and (30) we derive the following relation:

$$\beta_m = \frac{\pi t_m}{4E} f\left(t_m / c_m\right) \sigma^\infty \sin\theta_m \ . \tag{31}$$

As the intralaminar cracks are parallel to the fiber direction (direction of axis 1) and they are in mode I (opening displacement is parallel to the direction of axis 2), it is reasonable to replace in eq. (31) E by the transverse Young's modulus of a ply, i.e. E_2. We have:

$$\beta_m = \frac{\pi t_m}{4E_2} f\left(t_m / c_m\right) \sigma^\infty \sin\theta_m \ . \tag{32}$$

In order to use eq. (32) for a laminate which consists of a number of layers, in general of different orientation, we have to find any reasonable method of defining the width c_m.

Let us introduce an "imaginary" strip formed by the considered m-th ply with cracks and neighbouring plies, see Figure 1.11. In further analyses several simplifications are assumed, namely the interaction between the cracks within neighbouring plies as well as between cracks within one ply is neglected – only then eq. (19) and related relations are eligible. Another assumption is that the strip satisfies the requirement of symmetry with respect to the vertical symmetry axis of the cracks contained within m-th ply. Furthermore, the choice of a strip must take into account the stacking sequence of a laminate.

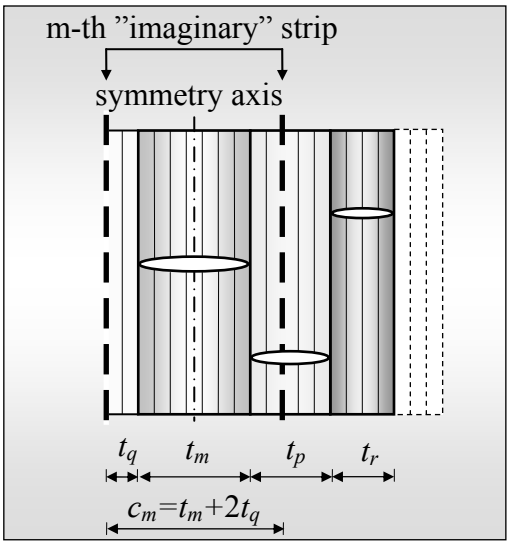

Figure 1.11. Modelling of imaginary strip

In order to satisfy both limitations the class of laminates has to be confined to laminates with undamaged outer plies. Only in this case the crack length of the last left-hand damaged ply (specified here as m-th ply) $t_m<c_m$ and the solution obtained by use of LEFM (eq. (22)) can be employed (the analogous observation relates also to the last right-hand damaged ply).

Let us now present the procedure of the division of a given laminate into "imaginary" strips. With every *m*-th damaged ply which is equivalent to *m*-th damage mode (note that within a laminate there can be a number of plies of the same damage mode) the *m*-th strip is associated. It is constructed from the *m*-th ply with cracks of length t_m and the adjacent plies (or their parts). In order to satisfy the requirement of strip symmetry, the thickness of left and right-hand adjacent plies must be the same and equal t_q, irrespective of their mechanical state, i.e. damaged or undamaged state. Let us note once more that possible cracks interactions are not considered.

In order to clarify the proposed procedure let us consider laminate, defined by the code e.g. $[0_1/\alpha_2/\delta_1/0_3/\alpha_2/\gamma_3/0_2]$, which is shown in Figure 1.12. We assume that the thickness of constituent single layers of each ply is the same and equal t_o, which in fact is quite common for most layered composites.

Let us notice that in this example the two plies α_2, identical from the geometrical point of view, are considered as different damage modes, namely mode "1" and mode "3", as corresponding to these plies strips are of different thickness and in result average crack opening factors β_1 and β_3 (eq. (32)) are different.

The proposed procedure allows, to some extent, taking into account the constraint effect of neighbouring plies on the cracking process developing in a given ply, contrary to e.g. Talreja's concept of a crack surface activity vector – see e.g. [126].

Let us consider two special orientations of the laminate plies, specified by the angles $\theta = 0°$ and $\theta = 90°$, i.e. a ply with fibers aligned along the direction of *x* axis in the first case and *y* axis in the second one (cross-ply). The values of factor β_m for these two cases follow from eq. (32) and are equal:

$$\beta_{90} = \frac{\pi t_m}{4E_2} f\left(t_m / c_m\right)\sigma^{\infty} \qquad \text{for } \theta = 90^{\circ}\ , \tag{33}$$

$$\beta_0 = 0 \qquad \text{for } \theta = 0^{\circ}\ . \tag{34}$$

The relation (33), as could be expected, is fully equivalent to eq. (25) supported by eq. (26), describing an average opening displacement of a central crack placed in a strip of finite width. The zero value of β_m for a ply

0° formally means a zero crack opening displacement, but physically it can be understood as a lack of any cracks in a ply with fibers aligned along the direction of applied load.

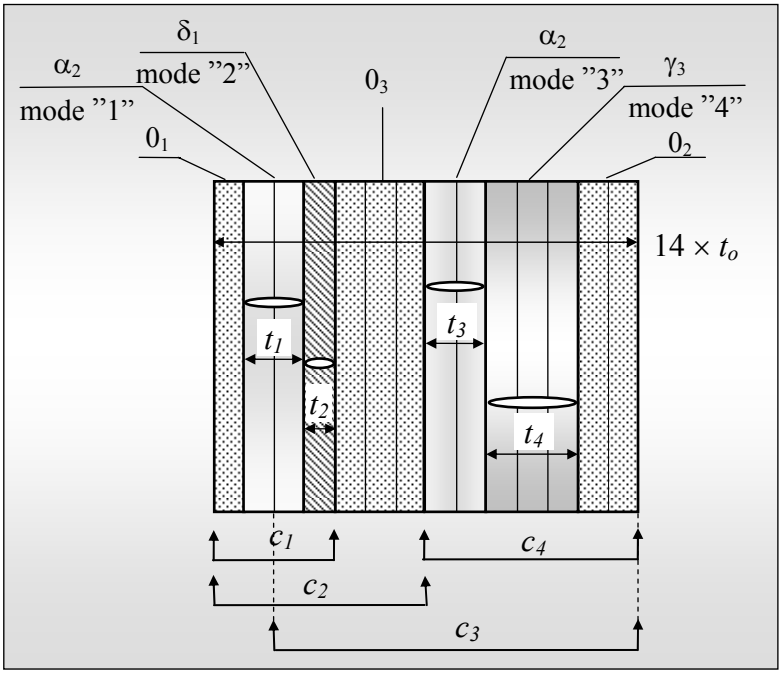

Figure 1.12. Procedure of a laminate separation into ”imaginary” strips with central cracks

This result is in agreement with the mechanism of intralaminar damage of layered laminates. For the plies orientations angles $\theta \in (0^\circ, 90^\circ)$, see Figure 1.10, the intralaminar cracks opening is then within the range (β_0, β_{90}).

One can easily see that the proposed definition of factor β_m, in the form of eq. (30) allows to connect the crack opening displacement with angle orientation of any ply, and at the same time the crack orientation.

Using eq. (16) together with eq. (32), we can finally obtain the damage tensor components for *m*-th mode of intralaminar damage expressed in the principal material axis (1, 2) of a ply in the following form:

$$d_{ij}^{m} = \frac{\pi t_m}{4 E_2} \rho_m \nu_m f(t_m / c_m) \sigma^{\infty} n_i n_j \ . \tag{35}$$

For the full clarity it must be noticed that relation (32) is derived in the frame of LEFM for an isotropic body. The orthotropic properties of a ply are incorporated in transverse crack opening displacement only by using the transverse Young's modulus of a ply. Thus, eq. (32) must be considered as an approximate one.

Varna *et al.* [140] verified experimentally different expressions for the transverse crack opening displacement and they found that predictions of linear elastic fracture mechanics for an isotropic body are in general agreement with measured crack face opening displacements of transverse matrix cracks, except relatively small regions placed between the vicinity of crack tips and crack centre. This observation together with averaging technique of crack opening displacement, see eq. (24), is seen as justification of the approach used in the present paper.

1.5. CONSTITUTIVE RELATION FOR AN ORTHOTROPIC BODY WITH DAMAGE

To describe the mechanical behaviour of a continuous body with damage it is necessary to define tensors specifying stress $\boldsymbol{\sigma}$, deformation $\boldsymbol{\varepsilon}$ and damage $\boldsymbol{d}$.

The crucial point for an analysis of a body with damage is to introduce appropriate constitutive relations which take into account the damage state.

The above goal can be achieved, among others, by employing the theory of invariants, using the irreducible integrity basis and polynomial functions.

1.5.1. The fundamentals of theory of invariants

In most problems in continuum mechanics the construction of proper constitutive relation is of primary importance, but at the same time it is also a source of difficulties. They can be overcome with the use of the algebraic theory of invariants. The modern development in the application of invariant theory in continuum mechanics was originated in 1948 by Rivlin in his work [113] on elastic strain-energy function. Another key work is by Rivlin

and Ericksen (1955) [114], concerning constitutive equations in which stress tensor components were expressed as polynomials of kinematic matrices, taking into account specific material symmetry (e.g. orthotropy). This trend was continued by Rivlin, Green, Noll, Pipkin, Adkins, Spencer, and in Poland by e.g. Litewka [82] – [84].

A brief review of basic definitions and ideas of invariant theory is given in subsequent sections of the present work. More details can be found in e.g. [122].

1.5.2. Orthogonal transformation

The matrix whose *ij*-th element is denoted by M_{ij} is considered to be the matrix of orthogonal transformation if it:

1) transforms rectangular cartesian coordinate system X_i into a new set of rectangular cartesian coordinates $\overline{X}_i$ by the relation

$$\overline{X}_i = M_{ij}\, X_i \ , \tag{36}$$

2) satisfies the relations

$$M_{ik}\, M_{jk} = \delta_{ij} \tag{37}$$

and

$$\left| M_{ij} \right| = \pm 1 \ , \tag{38}$$

where δ_{ij} is the Kronecker delta.

The set of all orthogonal transformations forms an orthogonal group.

1.5.3. The orthogonal groups of transformation

The importance of orthogonal groups in continuum mechanics lies in the fact that they may be used to describe material symmetries, strictly speaking material symmetry may be characterized by a finite group of orthogonal transformations.

For any material symmetry and its associated transformation group the material is transformed by any of the transformations of the group into a configuration, which is indistinguishable from its reference configuration.

For orthotropy (rhombic-dipyramidal symmetry) the orthogonal group consists of the following set of transformations:

$$\boldsymbol{I}, \boldsymbol{C}, \boldsymbol{R}_1, \boldsymbol{R}_2, \boldsymbol{R}_3, \boldsymbol{D}_1, \boldsymbol{D}_2, \boldsymbol{D}_3 \ , \tag{39}$$

where $\boldsymbol{I}$ and $\boldsymbol{C}$ describe relations of identity and central inversion, respectively:

$$\boldsymbol{I} = \begin{bmatrix} 1 & 0 & 0 \\ 0 & 1 & 0 \\ 0 & 0 & 1 \end{bmatrix} \quad , \qquad \boldsymbol{C} = -\boldsymbol{I} \ . \tag{40}$$

Transformations $\boldsymbol{R}_1$, $\boldsymbol{R}_2$ and $\boldsymbol{R}_3$ are reflections of the coordinate system in the plane normal to axes X_1, X_2, and X_3, respectively.

$$\boldsymbol{R}_1 = \begin{bmatrix} -1 & 0 & 0 \\ 0 & 1 & 0 \\ 0 & 0 & 1 \end{bmatrix} \ , \quad \boldsymbol{R}_2 = \begin{bmatrix} 1 & 0 & 0 \\ 0 & -1 & 0 \\ 0 & 0 & 1 \end{bmatrix} \ , \quad \boldsymbol{R}_3 = \begin{bmatrix} 1 & 0 & 0 \\ 0 & 1 & 0 \\ 0 & 0 & -1 \end{bmatrix} . \tag{41}$$

Transformations $\boldsymbol{D}_1$, $\boldsymbol{D}_2$ and $\boldsymbol{D}_3$ are rotations of the coordinate system by 180º around axes X_1, X_2 and X_3, respectively:

$$\boldsymbol{D}_1 = \begin{bmatrix} 1 & 0 & 0 \\ 0 & -1 & 0 \\ 0 & 0 & -1 \end{bmatrix} \ , \quad \boldsymbol{D}_2 = \begin{bmatrix} -1 & 0 & 0 \\ 0 & 1 & 0 \\ 0 & 0 & -1 \end{bmatrix} \ , \quad \boldsymbol{D}_3 = \begin{bmatrix} -1 & 0 & 0 \\ 0 & -1 & 0 \\ 0 & 0 & 1 \end{bmatrix} . \tag{42}$$

The above relations defining orthogonal group can be written briefly as:

$$\left(\overline{X}_1, \overline{X}_2, \overline{X}_3\right) = \left(\pm X_1, \pm X_2, \pm X_3\right) \ . \tag{43}$$

1.5.4. An invariant function

The following function:

$$f\left(U_i, V_i, ..., m_{ij}, n_{ij}, ...\right) \tag{44}$$

of the components of the set of vectors ***U, V***,...and tensors ***m, n***,...is said to be an invariant of these vectors and tensors under a given group of orthogonal transformation if:

$$f\left(\overline{U}_i, \overline{V}_i, ..., \overline{m}_{ij}, \overline{n}_{ij}, ...\right) = \left|M_{ij}\right| f\left(U_i, V_i, ..., m_{ij}, n_{ij}, ...\right), \tag{45}$$

for every transformation M_{ij} of the group.

An invariant is generally assumed to be an algebraic function, i.e. it can be expressed as a polynomial.

A polynomial invariant is said to be irreducible if it cannot be expressed as a polynomial in other invariants.

1.5.5. Classical invariant theory, integrity basis

The main problem in the theory of invariants is: for a given set of variables (vectors and tensors) and a given orthogonal group, determine a basic set of invariants from which all other invariants can be generated.

A set of polynomial invariants which has such property that any polynomial invariant can be expressed as a polynomial in members of the given set of variables is called an integrity basis. If all invariants are irreducible then the integrity basis is called irreducible.

An important role in the theory of invariants is played by Hilbert's theorem which says that: *for any finite system of vectors and tensors there exists an integrity basis which consists of a finite number of invariants.*

As a consequence of this theorem any polynomial function F of any number of vectors and tensors which is invariant under given orthogonal group can be expressed as a polynomial in members of integrity basis

$$F\left(U_i, V_i, .., m_{ij}, n_{ij}, ..\right) = F\left[f_1\left(U_i, .., n_{ij}, ..\right), .., f_m\left(U_i, .., n_{ij}, ..\right)\right]. \tag{46}$$

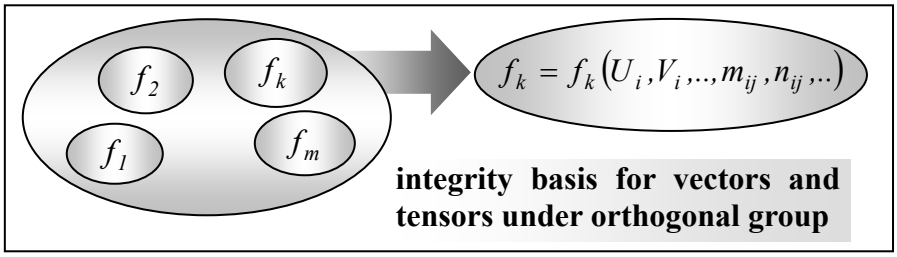

An irreducible integrity basis for orthotropy (orthogonal group ***I, C***, $\boldsymbol{R}_1$, $\boldsymbol{R}_2$, $\boldsymbol{R}_3$, $\boldsymbol{D}_1$, $\boldsymbol{D}_2$, $\boldsymbol{D}_3$) and two symmetrical second order tensors a_{ij}, e_{ij} was given by Adkins [4]:

$$\left.\begin{array}{lll} e_{ii}\,, & & a_{ii} \\ e_{ij}\,e_{ji}\,, & a_{ij}\,a_{ji}\,, & e_{ij}\,a_{ji} \\ e_{12}\,e_{23}\,e_{31}\,, & & a_{12}\,a_{23}\,a_{31} \\ e_{ij}\,e_{jk}\,a_{ki}\,, & & e_{ij}\,a_{jk}\,a_{ki} \end{array}\right\}. \tag{47}$$

and: $i, j, k = 1, 2, 3$; $i \neq j$, $i \neq k$, $j \neq k$; i, j, k are not summed.

1.5.6. Polynomial form of constitutive relation

Rivlin and Ericksen [114] proposed that the stress tensor components could be expressed as (or approximated by) polynomials in the components of certain kinematic tensors with suitable invariance properties. Material symmetries impose certain invariance requirements on the form of the constitutive relation.

The general polynomial form of constitutive relation is therefore as follows:

$$\sigma_{ij} = f_{ij}\left(a_{ij}, b_{ij}, ..e_{ij}\right) \quad \text{and} \quad f_{ij} = f_{ji}\,, \tag{48}$$

where a_{ij}, b_{ij}, ... are suitable kinematic tensors.

The specific form of eq. (48) depends on material symmetry, and number and form of kinematic tensors.

1.5.7. Adkins's approach to constitutive relation

It is common in the frame of approach based on the theory of invariants, irreducible integrity basis and polynomial functions to suppose that the stress tensor can be expressed as a polynomial in the elements of the tensors defining deformation and damage.

It is an important issue to construct a suitable polynomial in such a manner which takes into consideration any symmetry properties of an anisotropic material. In the present paper we confine the analysis to the orthotropic materials, since composite laminates belong to this class of materials. This problem was already reported in brief, in a paper [43].

Following Adkins's approach [3], [4], let us introduce the following quantities, expressed by their components:

- ϑ^i – a system of curvilinear coordinates associated with an element of a material,
- x^i ($\equiv x_i$) – rectangular Cartesian system,
- τ^{ij} – contravariant stress tensor referred to convected system ϑ^i,
- σ^{ij} – stress tensor referred to rectangular Cartesian system x^i which coincides with system ϑ^i,
- e_{ij}, a_{ij} – two symmetrical kinematic matrices formed in Cartesian system x^i.

The general relation (48) defines the stress tensor components for orthotropic material and two kinematic tensors as follows:

$$\sigma^{ij} = f^{ij}\left(e_{rs}, a_{pq}\right) \quad ; \quad \left(f^{ij} = f^{ji}\right), \tag{49}$$

where functions f^{ij} are polynomials in the arguments indicated.

The coefficients which appear in these polynomials are material constants that do not depend on the position through the body or on any deformation.

The relation between stress tensors is as follows:

$$\tau^{ij} = \frac{\partial \vartheta^i}{\partial x^r}\frac{\partial \vartheta^j}{\partial x^s}\sigma^{rs} = A^{ij}_{rs}\,\sigma^{rs} \ . \tag{50}$$

When the curvilinear system ϑ^i is such that it coincides with a rectangular Cartesian system x^i ($\equiv x_i$), i.e. ($\vartheta^i \equiv x_i$), we have:

$$A_{rs}^{ij} = A_{ijrs} = \begin{cases} 1 & \text{for} \quad i = r \ , \ j = s \\ 0 & \text{otherwise}. \end{cases} \tag{51}$$

Because of eq. (51) stress tensors have to satisfy the relation:

$$\tau^{ij} = \sigma^{ij} = \sigma_{ij} \tag{52}$$

and therefore the contravariant and covariant components of stress tensors are equal.

For the orthotropic body and two symmetrical, second order kinematic matrices e_{ij}, a_{ij} Adkins [3] derived the relation:

$$\tau^{ij} = A_{tt}^{ij}\,\Theta_{tt} + \varepsilon_{rst}\,\varepsilon_{rst}\,A_{rs}^{ij}\left[P_{rs;t}^{(1)} + P_{rs;t}^{(2)} + Q_{rs;t}^{(1)} + Q_{rs;t}^{(2)} + R_{rs;t}\right], \tag{53}$$

where:

$$P_{rs;t}^{(1)} = e_{rs}\,\Theta_{tt}^{(1)}\ , \tag{54}$$

$$P_{rs;t}^{(2)} = a_{rs}\,\Theta_{tt}^{(2)}\ , \tag{55}$$

$$Q_{rs;t}^{(1)} = e_{rt}\,e_{ts}\,\Theta_{tt}^{(3)}\ , \tag{56}$$

$$Q_{rs;t}^{(2)} = a_{rt}\,a_{ts}\,\Theta_{tt}^{(4)}\ , \tag{57}$$

$$R_{rs;t} = e_{rt}\,a_{ts}\,\Theta_{tt}^{(5)} + e_{st}\,a_{tr}\,\Theta_{tt}^{(6)}\ . \tag{58}$$

The symbol ε_{rst} denotes Ricci's symbol, defined as:

$$\varepsilon_{rst} = \begin{cases} +1 & \text{for } r \neq s \neq t \text{ and even permutation of suffixes } 1,2,3 \\ -1 & \text{for } r \neq s \neq t \text{ and odd permutation of suffixes } 1,2,3 \\ 0 & \text{otherwise}. \end{cases} \quad (59)$$

From eq. (59) it follows that in each of eqs (54) – (58) the conditions: $r \neq s$, $r \neq t$, $s \neq t$ must be satisfied. It is caused by the fact that functions given by left-hand sides of these equations are multiplied by Ricci's symbol when stresses are derived from eq. (53), besides t is not summed.

1.5.8. Constitutive relation for damaged laminate on-axis ply

The general Adkins's considerations regarding constitutive relation will be now reformulated for a specific case, namely for damaged ply of a laminate in its on-axis configuration defined by principal material co-ordinate system (1, 2).

The relation (53) is the form invariant under the group of transformations (43), describing the orthotropic symmetry of a material.

The functions $\Theta_{tt}, \Theta_{tt}^{(k)}$ (k=1,2,3,4,5,6) are invariant polynomial functions of a system of invariants (47) appropriate to the case where stress depends on two symmetric, kinematic matrices, namely e_{ij} and a_{ij}.

Taking into account the symmetry of matrices e_{ij} and a_{ij}, the set of invariants (47) has the following explicit form:

$$\left.\begin{array}{lll} e_{11}, & e_{22}, & e_{33} \\ a_{11}, & a_{22}, & a_{33} \\ e_{12}^2, & e_{13}^2, & e_{23}^2 \\ a_{12}^2, & a_{13}^2, & a_{23}^2 \\ e_{12}\,a_{12}, & e_{13}\,a_{13}, & e_{23}\,a_{23} \end{array}\right\} \quad (60)$$

$$\left.\begin{array}{ll} e_{12}\, e_{23}\, e_{31}\,, & a_{12}\, a_{23}\, a_{31} \\ e_{12}\, e_{23}\, a_{13}\,, & e_{13}\, e_{23}\, a_{12} \\ e_{12}\, e_{13}\, a_{23}\,, & e_{13}\, a_{12}\, a_{23} \\ e_{12}\, a_{13}\, a_{23}\,, & e_{23}\, a_{12}\, a_{13} \end{array}\right\}. \qquad \text{(60 cont.)}$$

Thus we have the system of 23 invariants, which with the use of more convenient contracted notation (Voigt's notation) can be rewritten in the form:

$$\left.\begin{array}{l} K_1 = e_{11} = e_1 \\ K_2 = e_{22} = e_2 \\ K_{12} = e_{33} = e_3 \\ K_4 = a_{11} = a_1 \\ K_5 = a_{22} = a_2 \\ K_6 = a_{33} = a_3 \\ K_3 = e_{12}^2 = e_6^2 \\ K_{13} = e_{13}^2 = e_5^2 \\ K_{14} = e_{23}^2 = e_4^2 \\ K_7 = a_{12}^2 = a_6^2 \end{array}\right\} \qquad (61)$$

$$
\left.
\begin{aligned}
K_8 &= a_{13}^2 = a_5^2 \\
K_9 &= a_{23}^2 = a_4^2 \\
K_{10} &= e_{12}\, a_{12} = e_6\, a_6 \\
K_{15} &= e_{13}\, a_{13} = e_5\, a_5 \\
K_{16} &= e_{23}\, a_{23} = e_4\, a_4 \\
K_{17} &= e_{12}\, e_{23}\, e_{31} = e_4\, e_5\, e_6 \\
K_{11} &= a_{12}\, a_{23}\, a_{31} = a_4\, a_5\, a_6 \\
K_{18} &= e_{12}\, e_{23}\, a_{13} = e_4\, e_6\, a_5 \\
K_{19} &= e_{13}\, e_{23}\, a_{12} = e_4\, e_5\, a_6 \\
K_{20} &= e_{12}\, e_{13}\, a_{23} = e_5\, e_6\, a_4 \\
K_{21} &= e_{13}\, a_{12}\, a_{23} = e_5\, a_4\, a_6 \\
K_{22} &= e_{12}\, a_{13}\, a_{23} = e_6\, a_4\, a_5 \\
K_{23} &= e_{23}\, a_{12}\, a_{13} = e_4\, a_5\, a_6
\end{aligned}
\right\} . \qquad \text{(61 cont.)}
$$

In the successive considerations we assume that stress is linearly dependent on both kinematic matrices e_{ij}, a_{ij}, therefore functions $Q^{(1)}_{rs;t}$ and $Q^{(2)}_{rs;t}$ can be neglected.

The other consequence of the assumed linearity is that functions $\Theta^{(5)}_{tt}$ and $\Theta^{(6)}_{tt}$ are reduced to a constant multiplier, as otherwise the function $R_{rs;t}$ (eq. (58)) would be at least a quadratic function of e_{ij} or a_{ij} or both, which obviously is in contradiction to the assumption. Thus, eq. (58) has now the form:

$$R_{rs;t} = g_1\, e_{rt}\, a_{ts} + g_2\, e_{st}\, a_{tr} \ , \tag{62}$$

where g_1 and g_2 are constants.

For $\vartheta^i \equiv x_i$, under this assumption, together with eqs (51) and (52), the stresses are as follows:

$$\sigma_{ij} = A_{ijtt}\,\Theta_{tt} + \varepsilon_{rst}\,\varepsilon_{rst}\,A_{ijrs}\left[P^{(1)}_{rs;t} + P^{(2)}_{rs;t} + R_{rs;t}\right]. \tag{63}$$

Let us further identify the symmetrical kinematic matrices e_{ij} and a_{ij} as strain tensor ε_{ij} and damage tensor d_{ij}, respectively. An assumption of linear dependence of stress on kinematic matrices is then equivalent to the assumption that strains and damage are small quantities.

We confine subsequent analysis to the in-plane behaviour of a laminate's ply by means of plane stress. Thus, the stress, strain and damage tensors in Voigt's notation are as follows:

$$\left.\begin{aligned} \boldsymbol{\sigma} &= \begin{bmatrix} \sigma_{11} \\ \sigma_{22} \\ \sigma_{12} \end{bmatrix} = \begin{bmatrix} \sigma_1 \\ \sigma_2 \\ \sigma_6 \end{bmatrix} \\ \boldsymbol{\varepsilon} &= \begin{bmatrix} \varepsilon_{11} \\ \varepsilon_{22} \\ \varepsilon_{12} \end{bmatrix} = \begin{bmatrix} \varepsilon_1 \\ \varepsilon_2 \\ \varepsilon_6 \end{bmatrix} \end{aligned}\right\} \tag{64}$$

$$\boldsymbol{d} = \left[\begin{array}{c} d_{11} \\ d_{22} \\ d_{12} \end{array}\right] = \left[\begin{array}{c} d_1 \\ d_2 \\ d_6 \end{array}\right] \Bigg\} . \qquad \text{(64 cont.)}$$

Plane stress analysis results in implied strain ε_3 which, however, is neglected in the classical 2-D theory of laminates. Due to this, the number of independent in-plane material constants for orthogonal material equals four, instead of nine, like for 3-D case [66].

Using eq. (63) and utilising eqs (51) and (59), we derive the following relations for stresses:

$$\sigma_1 = \Theta_{11} , \qquad (65)$$

$$\sigma_2 = \Theta_{22} , \qquad (66)$$

$$\sigma_6 = P^{(1)}_{12;3} + P^{(2)}_{12;3} + R_{12;3} , \qquad (67)$$

and from eqs (54), (55), (62) we get:

$$P^{(1)}_{12;3} = \varepsilon_6 \, \Theta^{(1)}_{33} , \qquad (68)$$

$$P^{(2)}_{12;3} = d_6 \, \Theta^{(2)}_{33} , \qquad (69)$$

$$R_{12;3} = 0 . \qquad (70)$$

Thus:

$$\sigma_6 = \varepsilon_6 \, \Theta^{(1)}_{33} + d_6 \, \Theta^{(2)}_{33} . \qquad (71)$$

Now we must define invariant polynomial functions Θ_{11}, Θ_{22}, $\Theta^{(1)}_{33}$ and $\Theta^{(2)}_{33}$ which in general are the functions of invariants set (61). For in-plane case considered here only the chosen invariants are of interest, namely K_1,

K_2, K_4, K_5 and K_{10}, i.e. ε_1, ε_2, d_1, d_2 and ε_6 d_6. Taking into account linearity of the stress vs. strain relations, as well as stress vs. damage, the relevant polynomials are:

$$\Theta_{11} = a_1 \varepsilon_1 + a_2 \varepsilon_2 + (a_3 d_1 + a_4 d_2)\varepsilon_1 + \\ + (a_5 d_1 + a_6 d_2)\varepsilon_2 + a_7 d_6 \varepsilon_6 + a_8 \ , \tag{72}$$

$$\Theta_{22} = b_1 \varepsilon_1 + b_2 \varepsilon_2 + (b_3 d_1 + b_4 d_2)\varepsilon_1 + \\ + (b_5 d_1 + b_6 d_2)\varepsilon_2 + b_7 d_6 \varepsilon_6 + b_8 \ . \tag{73}$$

Recalling again the linear stress vs. strain relation and the form of eq. (71), where function $\Theta_{33}^{(1)}$ is multiplied by ε_6, an adequate polynomial for $\Theta_{33}^{(1)}$ can be reduced to the form:

$$\Theta_{33}^{(1)} = c_1 d_1 + c_2 d_2 + c_3 \ . \tag{74}$$

The same reasoning, but with regard to damage instead of strain leads to the following polynomial for $\Theta_{33}^{(2)}$:

$$\Theta_{33}^{(2)} = f_1 \varepsilon_1 + f_2 \varepsilon_2 + f_3 \ . \tag{75}$$

The coefficients a_1–a_8, b_1–b_8, c_1–c_3, f_1–f_3 are material parameters.

Polynomial functions Θ_{11}, Θ_{22}, $\Theta_{33}^{(1)}$ and $\Theta_{33}^{(2)}$ cannot be independent one of another, as the stress derived with the use of these functions must satisfy the ”universal” constitutive equation of a general form:

$$\sigma_i = C_{ij} \varepsilon_j \qquad i, j = 1, 2, 6 \ , \tag{76}$$

where C_{ij} denotes the stiffness matrix which for in-plane case has the following components (in Voigt's notation):

$$\boldsymbol{C} = \begin{bmatrix} C_{11} & C_{12} & C_{16} \\ C_{12} & C_{22} & C_{26} \\ C_{16} & C_{26} & C_{66} \end{bmatrix} . \tag{77}$$

We decompose the stiffness matrix into two constituent matrices: the first one $\boldsymbol{C^o}$ relating to the undamaged state and the other one $\boldsymbol{C^d}$ characterising the change of stiffness due to damage. We get the following relation:

$$\sigma_i = C_{ij}^o \, \varepsilon_j + C_{ij}^d \, \varepsilon_j \ . \tag{78}$$

Now we can calculate stresses from eq. (78) and then compare them with those given by eqs (65), (66) and (71), with the use of polynomial functions (72) – (75). We obtain the following relations:

$$\left.\begin{array}{c} C_{11}^o = a_1 \\ C_{12}^o = C_{21}^o = a_2 = b_1 \\ C_{16}^o = C_{61}^o = 0 \\ C_{22}^o = b_2 \\ C_{26}^o = C_{62}^o = 0 \end{array}\right\} , \tag{79}$$

$$C_{66}^o = c_3 \ , \tag{80}$$

$$a_8 = b_8 = f_3 = 0 \ , \tag{81}$$

$$a_5 = b_3 \ , \qquad a_6 = b_4 \ , \qquad a_7 = f_1 \ , \qquad b_7 = f_2 \ , \tag{82}$$

$$\left.\begin{aligned} C_{11}^{d} &= a_3\, d_1 + a_4\, d_2 \\ C_{12}^{d} &= C_{21}^{d} = a_5\, d_1 + a_6\, d_2 \end{aligned}\right\}, \tag{83}$$

$$\left.\begin{aligned} C_{22}^{d} &= b_5\, d_1 + b_6\, d_2 \\ C_{66}^{d} &= c_1\, d_1 + c_2\, d_2 \\ C_{16}^{d} &= C_{61}^{d} = a_7\, d_6 \end{aligned}\right\}, \tag{84}$$

$$C_{26}^{d} = C_{62}^{d} = b_7\, d_6 \ . \tag{85}$$

From eqs (79) – (85) we get the following set of independent material constants:

$$\left.\begin{aligned} A_1 &= a_5\ , & A_2 &= a_6 \\ A_3 &= a_7\ , & A_4 &= b_7 \\ A_5 &= a_3\ , & A_6 &= a_4 \\ A_7 &= c_1\ , & A_8 &= c_2 \\ A_9 &= b_5\ , & A_{10} &= b_6 \end{aligned}\right\}. \tag{86}$$

Note that we have derived a stiffness matrix for the undamaged material with elements $C_{16}^{o} = C_{26}^{o} = 0$. This result was expected, since it is typical of orthotropic laminate in principal material axis (1,2) (so-called *special orthotropy*).

For a general case of arbitrary damage state we have obtained $C_{16}^{d} \neq 0$, $C_{26}^{d} \neq 0$ (see eq. (84) and eq. (85)), thus the initial special orthotropy is no longer retained and is replaced by so-called *general orthotropy*.

The damage tensor given by (35) together with (15), obtained for the intralaminar damage model considered in the present work, has the only non-zero damage tensor component:

$$d_2^m = \frac{\pi t_m}{4E_2} \rho_m v_m f(t_m/c_m) \sigma^{\infty} . \tag{87}$$

Using eqs (83) – (86) we finally get the stiffness matrix (so-called *reduced* stiffness matrix) associated with the damage state in *m*-th ply, expressed in the principal material axis in the form:

$$\boldsymbol{C}^{dm} = \begin{bmatrix} A_6 d_2^m & A_2 d_2^m & 0 \\ A_2 d_2^m & A_{10} d_2^m & 0 \\ 0 & 0 & A_8 d_2^m \end{bmatrix} . \tag{88}$$

It follows from eq. (88) that four unknown material constants, namely A_2, A_6, A_8, A_{10}, will be involved in further analysis.

The result in the form of eq. (88) obtained according to Adkins's approach is similar from the formal point view to the one derived by Talreja [124] in the frame of quite sophisticated considerations based on thermodynamics with internal state variables introduced by Coleman and Gurtin [27], [51]. It is shown in brief in chapter 1.9. Such an approach with regard to the orthotropic composite laminates has been utilized in a number of papers, e.g. [104] and [124] – [127].

The stiffness matrices $\boldsymbol{C^o}$ and $\boldsymbol{C^d}$ for a single "virgin" and damaged ply, respectively, are a basis for the evaluation of transformed stiffness matrices, i.e. matrices transformed from principal material axis (1, 2) to any reference coordinate system (*x*, *y*). Subsequently, they will be used in calculations of stiffness matrices for a laminate as a collection of plies, some of which can be damaged, while the remaining can remain intact.

The next steps will be to derive engineering constants, and finally to determine material constants on the basis of experimental data. In order to achieve these goals the **C**lassical **L**aminates **T**heory (CLT) will be employed.

1.6. TRANSFORMED STIFFNESS MATRIX FOR A PLY OF DAMAGED LAMINATE

In order to obtain the elements of stiffness matrix for a given single ply in an arbitrary reference coordinate system (x, y) (so-called *transformed reduced stiffness matrix*) we have to transform the components of stiffness matrix $\boldsymbol{C}$, determined in the previous chapter, in principal material axis (1, 2) of a ply. Since the stiffness matrix, which in fact forms a tensor of fourth order, "loses" its tensorial nature when written in Voigt's notation, we cannot use the classical tensorial transformation law. An alternative method of transformation is shown in [55]. In the present paper we utilise the classical straightforward transformation procedure proposed by Tsai and Pagano, described elsewhere (e.g. [37], [66], [134]). Due to their scheme the transformed reduced stiffness matrix $\overline{\boldsymbol{C}}$ can be expressed in the following form:

$$\overline{\boldsymbol{C}} = \boldsymbol{T}\,\boldsymbol{P}\ , \tag{89}$$

where:

$$\overline{\boldsymbol{C}} = \begin{bmatrix} \overline{C}_{11} \\ \overline{C}_{22} \\ \overline{C}_{12} \\ \overline{C}_{66} \\ \overline{C}_{16} \\ \overline{C}_{26} \end{bmatrix}, \tag{90}$$

$$\boldsymbol{T} = \begin{bmatrix} U_1 & \cos 2\theta & \cos 4\theta \\ U_1 & -\cos 2\theta & \cos 4\theta \\ U_4 & 0 & -\cos 4\theta \\ U_5 & 0 & -\cos 4\theta \\ 0 & (1/2)\sin 2\theta & \sin 4\theta \\ 0 & (1/2)\sin 2\theta & -\sin 4\theta \end{bmatrix}, \tag{91}$$

$$\boldsymbol{P} = \begin{bmatrix} 1 \\ U_2 \\ U_3 \end{bmatrix}, \tag{92}$$

with:

$$\left.\begin{aligned} U_1 &= \frac{1}{8}\left(3C_{11} + 3C_{22} + 2C_{12} + 4C_{66}\right) \\ U_2 &= \frac{1}{2}\left(C_{11} - C_{22}\right) \\ U_3 &= \frac{1}{8}\left(C_{11} + C_{22} - 2C_{12} - 4C_{66}\right) \\ U_4 &= \frac{1}{8}\left(C_{11} + C_{22} + 6C_{12} - 4C_{66}\right) \\ U_5 &= \frac{1}{8}\left(C_{11} + C_{22} - 2C_{12} + 4C_{66}\right) \end{aligned}\right\}. \tag{93}$$

Taking into account decomposition of stiffness matrix in the form:

$$C_{ij} = C_{ij}^{o} + C_{ij}^{d}, \tag{94}$$

one can easily show that material coefficients $U_1 - U_5$ can also be decomposed into two parts, namely U_i^o and U_i^d, which correspond to the virgin and damaged state of a ply, respectively. Thus, we have:

$$U_i = U_i^o + U_i^d. \tag{95}$$

Both U_i^o and U_i^d are given by eq. (93), but replacing C_{ij} by C_{ij}^o and C_{ij}^d, respectively.

Therefore, the transformed reduced stiffness matrix $\overline{\boldsymbol{C}}$ with the use of eq. (95) is given now by the relation:

$$\overline{\boldsymbol{C}} = \overline{\boldsymbol{C}}^{\boldsymbol{o}} + \overline{\boldsymbol{C}}^{\boldsymbol{d}} \ , \tag{96}$$

with:

$$\overline{\boldsymbol{C}}^{o} = \boldsymbol{T}^{o}\ \boldsymbol{P}^{o} \ , \tag{97}$$

$$\overline{\boldsymbol{C}}^{d} = \boldsymbol{T}^{d}\ \boldsymbol{P}^{d} \ . \tag{98}$$

Transformation matrices $\boldsymbol{T}^{o}$, $\boldsymbol{T}^{d}$, $\boldsymbol{P}^{o}$, $\boldsymbol{P}^{d}$ are as follows:

$$\boldsymbol{T}^{\boldsymbol{s}} = \begin{bmatrix} U_1^s & \cos 2\theta & \cos 4\theta \\ U_1^s & -\cos 2\theta & \cos 4\theta \\ U_4^s & 0 & -\cos 4\theta \\ U_5^s & 0 & -\cos 4\theta \\ 0 & (1/2)\sin 2\theta & \sin 4\theta \\ 0 & (1/2)\sin 2\theta & -\sin 4\theta \end{bmatrix}, \tag{99}$$

$$\boldsymbol{P}^{\boldsymbol{s}} = \begin{bmatrix} 1 \\ U_2^s \\ U_3^s \end{bmatrix} \quad \text{and} \quad "s" = \begin{cases} "o" & \text{for virgin state} \\ "d" & \text{for damaged state}. \end{cases} \tag{100}$$

Note that for a laminate manufactured from plies made of the same composite material, which is true in most cases, the reduced stiffness matrix $\boldsymbol{C}^{o}$ (*on-axis* stiffness matrix) is the same for each ply, and as a consequence, it relates also to all material coefficients $U_1 - U_5$. The reduced stiffness matrix and the coefficients U_i for a ply in virgin state are as follows:

$$\boldsymbol{C}^{o} = \begin{bmatrix} K E_1 & K \nu_{21} E_1 & 0 \\ K \nu_{21} E_1 & K E_2 & 0 \\ 0 & 0 & G_{12} \end{bmatrix} \tag{101}$$

$$K = \frac{1}{1 - \nu_{12}\nu_{21}},$$

$$\left.\begin{aligned} U_1^o &= (1/8)\{K[3(E_1 + E_2) + 2E_1\nu_{21}] + 4G_{12}\} \\ U_2^o &= (1/2)K(E_1 - E_2) \\ U_3^o &= (1/8)\left[K\left(E_1 + E_2 - 2E_1\nu_{21}\right) - 4G_{12}\right] \\ U_4^o &= (1/8)\left[K\left(E_1 + E_2 + 6E_1\nu_{21}\right) - 4G_{12}\right] \\ U_5^o &= (1/8)\left[K\left(E_1 + E_2 - 2E_1\nu_{21}\right) + 4G_{12}\right] \end{aligned}\right\}, \tag{102}$$

where E_1, E_2, G_{12}, ν_{12}, ($\nu_{21} = (E_2/E_1)\nu_{12}$) are on-axis, in-plane standard independent engineering elastic moduli for a composite material.

If damage is considered in a ply stiffness analysis, we have an other situation. Stiffness matrix $\boldsymbol{C}^{\boldsymbol{d}}$ is dependent not only upon material characteristics A_2, A_6, A_8, A_{10}, E_2, the same for each ply, but is also dependent on geometrical parameters (ply thickness t_m, its volume fraction v_m, crack density ρ_m, width of "imaginary" strip c_m associated with any ply), which in general are different for different plies. Therefore, material coefficients U_i^d, transformation matrices $\boldsymbol{T}^d$, $\boldsymbol{P}^d$ and finally transformed stiffness matrix $\overline{\boldsymbol{C}}^{\boldsymbol{d}}$ have to be determined for each single ply separately if they are of different geometry.

Material coefficients U_i^d with the use of eq. (88) can be written in the form:

$$U_i^d = d_2 \overline{U}_i , \tag{103}$$

where:

$$\left.\begin{aligned}
\overline{U}_1 &= (1/8)\left(3\,A_6 + 3\,A_{10} + 2\,A_2 + 4\,A_8\right) \\
\overline{U}_2 &= (1/2)\left(A_6 - A_{10}\right) \\
\overline{U}_3 &= (1/8)\left(A_6 + A_{10} - 2\,A_2 - 4\,A_8\right) \\
\overline{U}_4 &= (1/8)\left(A_6 + A_{10} + 6\,A_2 - 4\,A_8\right) \\
\overline{U}_5 &= (1/8)\left(A_6 + A_{10} - 2\,A_2 + 4\,A_8\right)
\end{aligned}\right\} . \qquad (104)$$

Let us notice that the coefficients given by eq. (104) are actually purely material characteristics of damaged ply and they are independent of its geometrical characteristics. Thus, they play the same role as coefficients U_i^o, (eq. (102)), for a ply in a virgin state.

The transformed reduced stiffness matrix for a ply in a damaged state (eq. (98)) with the use of eqs (100) and (103) can be rewritten in a matrix form:

$$\overline{\boldsymbol{C}}^{\,d} = \overline{\boldsymbol{T}}\,\overline{\boldsymbol{P}}\,d_2 \ , \qquad (105)$$

or in an explicit form as follows:

$$\begin{bmatrix} \overline{C}_{11}^{\,d} \\ \overline{C}_{22}^{\,d} \\ \overline{C}_{12}^{\,d} \\ \overline{C}_{66}^{\,d} \\ \overline{C}_{16}^{\,d} \\ \overline{C}_{26}^{\,d} \end{bmatrix} = \begin{bmatrix} \overline{U}_1 & \cos 2\theta & \cos 4\theta \\ \overline{U}_1 & -\cos 2\theta & \cos 4\theta \\ \overline{U}_4 & 0 & -\cos 4\theta \\ \overline{U}_5 & 0 & -\cos 4\theta \\ 0 & (1/2)\sin 2\theta & \sin 4\theta \\ 0 & (1/2)\sin 2\theta & -\sin 4\theta \end{bmatrix} \begin{bmatrix} 1 \\ \overline{U}_2 \\ \overline{U}_3 \end{bmatrix} d_2 \ . \qquad (106)$$

1.7. STIFFNESS MATRIX FOR A DAMAGED LAMINATE

The transformed reduced stiffness matrix $\overline{\boldsymbol{C}}$, already derived for any single ply, is a basis for determination of the laminate stiffness matrices which in general case are: extension, coupling and bending stiffness matrices. All these matrices can be obtained in the frame of CLT, presented briefly in Appendix.

In order to simplify the subsequent analysis we restrict the class of laminates of our interest to the most widely used symmetrical laminates.

Besides, we assume that the laminate is loaded by tensile force only, i.e. unidirectional tensile load is applied along x axis direction, see Appendix, Figure A.2.

With the above condition, the problem of laminate stiffness is limited to the analysis of extensional stiffness matrix $\boldsymbol{A}$ defined as follows:

$$\frac{\boldsymbol{A}}{t} = \sum_{k=1}^{N} \overline{\boldsymbol{C}}_k \, v_k \ . \tag{107}$$

Using eq. (96) we get from eq. (107) the relation:

$$\frac{\boldsymbol{A}}{t} = \boldsymbol{A}^o + \boldsymbol{A}^d \ , \tag{108}$$

where:

$$\boldsymbol{A}^o = \sum_{k=1}^{N} \overline{\boldsymbol{C}}_k^{\,o} \, v_k \ , \tag{109}$$

$$\boldsymbol{A}^d = \sum_{m=1}^{M} \overline{\boldsymbol{C}}_m^{\,d} v_m \ , \tag{110}$$

and N is the total number of laminate's plies, M is the number of plies containing intralaminar cracks $(M<N)$. Matrix $\boldsymbol{A}^o$ relates to the initial virgin state of a laminate, while matrix $\boldsymbol{A}^d$ is responsible for the influence of damage, arising within some plies, on the resulting laminate stiffness.

First, let us consider the procedure of the determination of matrix $\boldsymbol{A}^o$ elements. Setting eq. (98) into the eq. (109) we get:

$$\boldsymbol{A}^o = \sum_{k=1}^{N} \left(\boldsymbol{T}^o \boldsymbol{P}^o \right)_k v_k \ . \tag{111}$$

In order to use the summation convention for matrices $\boldsymbol{T}^o$ and $\boldsymbol{P}^o$ let us rewrite the elements of matrix $\boldsymbol{A}$ in the following manner:

$$\boldsymbol{A}^o = \begin{bmatrix} A^o_{11} \\ A^o_{22} \\ A^o_{12} \\ A^o_{66} \\ A^o_{16} \\ A^o_{26} \end{bmatrix} \overset{def}{=} \begin{bmatrix} A^o_1 \\ A^o_2 \\ A^o_3 \\ A^o_4 \\ A^o_5 \\ A^o_6 \end{bmatrix} . \tag{112}$$

Thus, the relation (111) can be expressed in an explicit form as follows:

$$A^o_i = \sum_{k=1}^{N} \left(T^o_{ip} \, P^o_p \right)_k v_k \qquad i = 1,2,3,4,5,6 \ ; \ p = 1,2,3 \ , \tag{113}$$

where summation over p must be carried out.

From the previous considerations it follows that matrix $\boldsymbol{P}^o$ (see eqs (100), (102)) is purely material dependent, therefore it does not change from one ply to another one. Consequently, the elements of that matrix included in eq. (113) are not summed over ply index "k". Finally, from eq. (113) with the use of eq. (100) we obtain:

$$A^o_i = \left(\sum_{k=1}^{N} \left(T^o_{i1} \right)_k v_k \right) + \left(U^o_2 \sum_{k=1}^{N} \left(T^o_{i2} \right)_k v_k \right) + \left(U^o_3 \sum_{k=1}^{N} \left(T^o_{i3} \right)_k v_k \right) . \tag{114}$$

Let us introduce the following purely geometrical coefficients:

$$\left.\begin{aligned} V_1^o &= \sum_{k=1}^{N} v_k \cos 2\theta_k \\ V_2^o &= \sum_{k=1}^{N} v_k \cos 4\theta_k \\ V_3^o &= \sum_{k=1}^{N} v_k \sin 2\theta_k \\ V_4^o &= \sum_{k=1}^{N} v_k \sin 4\theta_k \end{aligned}\right\} . \tag{115}$$

After some transformations of eq. (114) with the use of eq. (115) we get an extensional stiffness matrix $\boldsymbol{A}^o$ for a virgin laminate, which can be written in the following form:

$$\boldsymbol{A}^o = \overline{\boldsymbol{T}}^o \boldsymbol{P}^o \ , \tag{116}$$

where:

$$\overline{\boldsymbol{T}}^o = \begin{bmatrix} U_1^o & V_1^o & V_2^o \\ U_1^o & -V_1^o & V_2^o \\ U_4^o & 0 & -V_2^o \\ U_5^o & 0 & -V_2^o \\ 0 & (1/2)V_3^o & V_4^o \\ 0 & (1/2)V_3^o & -V_4^o \end{bmatrix} , \tag{117}$$

$$\boldsymbol{P}^o = \begin{bmatrix} 1 \\ U_2^o \\ U_3^o \end{bmatrix} . \tag{118}$$

The stiffness matrix $\boldsymbol{A}^{o}$ is fully determined for any laminate if only engineering moduli for a ply in the on-axis configuration, namely E_1, E_2, G_{12} and ν_{12} are known.

Now let us consider the part of an extensional stiffness matrix characterising the influence of the damage on the overall laminate stiffness, i.e. matrix $\boldsymbol{A}^{d}$, given by eq. (110). Following exactly the same procedure as already presented for matrix $\boldsymbol{A}^{o}$, we can write $\boldsymbol{A}^{d}$ in the form:

$$\boldsymbol{A}^{d} = \overline{\boldsymbol{T}}^{d}\, \overline{\boldsymbol{P}}^{d} \,, \tag{119}$$

$$\overline{\boldsymbol{T}}^{d} = \begin{bmatrix} \overline{U}_1 & V_1^d & V_2^d \\ \overline{U}_1 & -V_1^d & V_2^d \\ \overline{U}_4 & 0 & -V_2^d \\ \overline{U}_5 & 0 & -V_2^d \\ 0 & (1/2)V_3^d & V_4^d \\ 0 & (1/2)V_3^d & -V_4^d \end{bmatrix}, \tag{120}$$

$$\overline{\boldsymbol{P}}^{d} = \begin{bmatrix} V_0^d \\ \overline{U}_2 \\ \overline{U}_3 \end{bmatrix}. \tag{121}$$

Coefficients V_i^d ($i = 0, 1, 2, 3, 4$) are as follows:

$$\left.\begin{aligned} V_0^d &= \sum_{m=1}^{M} v_m d_2^m \\ V_1^d &= \sum_{m=1}^{M} v_m\, d_2^m \cos 2\theta_m \end{aligned}\right\} \tag{122}$$

$$\left.\begin{aligned} V_2^d &= \sum_{m=1}^{M} v_m\, d_2^m \cos 4\theta_m \\ V_3^d &= \sum_{m=1}^{M} v_m\, d_2^m \sin 2\theta_m \\ V_4^d &= \sum_{m=1}^{M} v_m\, d_2^m \sin 4\theta_m \end{aligned}\right\} . \qquad (122 \text{ cont.})$$

Note that the coefficients given by eq. (122), contrary to those given by eq. (115), are not only geometrical, but also material characteristics, as the damage term d_2 (see eq. (87)) depends on crack density which in fact is a material property feature, though not in an explicit way.

The stiffness matrix $\boldsymbol{A}^{\boldsymbol{d}}$ is unknown as long as material parameters A_2, A_6, A_8 and A_{10} remain not determined in appropriate experiments. Note that for an orthotropic laminate in the virgin state, to get full information on laminate stiffness four on-axis constants are needed. When the damage is included into considerations, we also need to know four constants which, however, cannot be derived from tests carried out on a single ply (like in the first case), but on a laminate as a whole. The first crack in a single ply means its final fracture and the damage in the sense used in the present paper cannot be defined. Therefore, in order to determine constants A_2, A_6, A_8 and A_{10} the plies stacking sequence must be chosen in such a way which makes the calculations possible, but on the other hand, as easy as possible. It will be discussed in the next chapter.

1.8. ENGINEERING MODULI FOR A DAMAGED LAMINATE

In order to derive so-called *engineering moduli* for any laminate, the compliance matrix $\boldsymbol{S}$ must be determined.

It can be shown on the basis of considerations presented in Appendix and under two restrictions already assumed, namely:

- symmetry of plies stacking sequence with respect to the laminate mid-plane,

- laminate loading by extensional load only,

that the constitutive equation for a laminate is given by the following equation:

$$\overline{\boldsymbol{\sigma}} = \frac{\boldsymbol{A}}{t}\boldsymbol{\varepsilon} \ , \tag{123}$$

where $\overline{\boldsymbol{\sigma}}$ denotes the global, average stress tensor for a laminate (for details see Appendix).

The invert relation to that given by eq. (123) is:

$$\boldsymbol{\varepsilon} = \boldsymbol{S}\,\overline{\boldsymbol{\sigma}} \ , \tag{124}$$

where compliance matrix $\boldsymbol{S} = \boldsymbol{A}^{-1}\,t \equiv \boldsymbol{A}'\,t$.

The engineering moduli for a laminate can be directly derived from the compliance matrix by the use of the following relations:

$$\left.\begin{aligned} E_x^L &= \frac{1}{A'_{11}\,t} \\ E_y^L &= \frac{1}{A'_{22}\,t} \\ G_{xy}^L &= \frac{1}{A'_{66}\,t} \\ \nu_{xy}^L &= -\frac{A'_{21}}{A'_{11}} \\ \eta_{x,xy}^L &= \frac{A'_{61}}{A'_{11}} \\ \eta_{y,xy}^L &= \frac{A'_{62}}{A'_{22}} \end{aligned}\right\} . \tag{125}$$

The remaining three moduli are dependent on those expressed by eq. (125) and have the forms:

$$\left.\begin{aligned} \nu_{yx}^{L} &= \nu_{xy}^{L}\frac{E_y^L}{E_x^L} \\ \eta_{xy,x}^{L} &= \eta_{x,xy}^{L}\frac{G_{xy}^L}{E_x^L} \\ \eta_{xy,y}^{L} &= \eta_{y,xy}^{L}\frac{G_{xy}^L}{E_y^L} \end{aligned}\right\}. \tag{126}$$

The notation used in the above equations is following: E_x^L – longitudinal Young's modulus, E_y^L – transverse Young's modulus, G_{xy}^L – shear modulus, ν_{xy}^L, ν_{yx}^L – Poisson's ratios, $\eta_{x,xy}^L$, $\eta_{y,xy}^L$ – coefficients of mutual influence of the second kind by Lekhnitski [78] and $\eta_{xy,x}^L$, $\eta_{xy,y}^L$ – coefficients of mutual influence of the first kind by Lekhnitski.

We will use the relations (125) and (126) with the aim of determining the residual, i.e. current engineering moduli for a damaged laminate of both cross-ply and angle ply stacking sequences. In a general case they cannot be expressed in explicit forms and numerical calculations are needed.

1.8.1. Engineering moduli for a damaged cross-ply laminate

Intralaminar cracking in cross-ply laminates develops in transverse, i.e. 90° plies only. It makes calculations of engineering moduli much simpler than in any other case and one can derive relations for moduli in a close, explicit form.

Let us consider symmetric cross-ply laminates with volume fraction equal v_0 for 0° plies and v_{90} for 90° plies. In order to get a stiffness matrix let us calculate all needed quantities. From eqs (115) and (122) we get:

$$\left.\begin{aligned} V_1^o &= v_0 - v_{90} \\ V_2^o &= v_0 + v_{90} = 1 \\ V_3^o &= V_4^o = 0 \\ V_1^d &= -\sum_{m=1}^{M} v_m \, d_2^m = -V_0^d \\ V_2^d &= V_0^d \\ V_3^d &= V_4^o = 0 \end{aligned}\right\} . \tag{127}$$

Matrix $\boldsymbol{A^o}$ derived from equations (116) and (118) together with eqs (102) and (127) has a form:

$$\boldsymbol{A}^o = \begin{bmatrix} K\left(v_0 E_1 + v_{90} E_2\right) & K E_1 \nu_{21} & 0 \\ K E_1 \nu_{21} & K\left(v_0 E_2 + v_{90} E_1\right) & 0 \\ 0 & 0 & G_{12} \end{bmatrix} . \tag{128}$$

Matrix $\boldsymbol{A^d}$ given by eqs (119) and (121), after substituting eqs (104) and (127) is as follows:

$$\boldsymbol{A}^d = \begin{bmatrix} A_{10} & A_2 & 0 \\ A_2 & A_6 & 0 \\ 0 & 0 & A_8 \end{bmatrix} V_0^d \ . \tag{129}$$

An important observation arises from eqs (128) and (129), namely stiffnesses $A_{16}^o, A_{26}^o, A_{16}^d, A_{26}^d$ equal zero. Thus, the symmetric cross-ply

laminates, which in virgin state are always characterised by *special orthotropy*, retain this feature even in the presence of intralaminar damage.

Due to this fact the relations for engineering moduli become significantly simplified. The current engineering moduli of a laminate can be directly derived from the compliance matrix by use of the standard relations given in e.g. [134]:

$$\left.\begin{aligned} E_x^L &= \frac{1}{t}\frac{A_{11}A_{22}-A_{12}^2}{A_{22}} \\ E_y^L &= \frac{1}{t}\frac{A_{11}A_{22}-A_{12}^2}{A_{11}} \\ G_{xy}^L &= A_{66}/t, \\ \nu_{xy}^L &= A_{12}/A_{22} \end{aligned}\right\}. \tag{130}$$

From the symmetry of the stiffness matrix it follows that $\nu_{yx}^L = \left(E_y^L / E_x^L\right)\nu_{xy}^L$, as well as the Lekhnitski's coefficients of mutual influence are equal zero.

Recalling that $\boldsymbol{A}=\boldsymbol{A}^{\boldsymbol{o}}+\boldsymbol{A}^{\boldsymbol{d}}$, and already made assumption of damage being a small quantity, we get, after transformations, the following formulas for residual engineering moduli:

$$E_x^L = E_x^{oL} + A_{11}^d + \left(\nu_{xy}^{oL}\right)^2 A_{22}^d - 2\,\nu_{xy}^{oL}\,A_{12}^d\ , \tag{131}$$

$$E_y^L = E_y^{oL} + A_{22}^d + \left(\nu_{yx}^{oL}\right)^2 A_{11}^d - 2\,\nu_{yx}^{oL}\,A_{12}^d\ , \tag{132}$$

$$\nu_{xy}^L = \nu_{xy}^{oL} + \frac{1}{E_y^{oL}}\left(1-\nu_{xy}^{oL}\,\nu_{yx}^{oL}\right)\left(A_{12}^d - \nu_{xy}^{oL}\,A_{22}^d\right), \tag{133}$$

$$G_{xy}^{L} = G_{xy}^{oL} + A_{66}^{d} \ , \tag{134}$$

where all quantities with superscript "*o*" are related to the initial values of engineering moduli (i.e. in virgin state) and can be derived from the following relations:

$$E_{x}^{oL} = A_{11}^{o} - \frac{{A_{12}^{o}}^{2}}{A_{22}^{o}} \ , \tag{135}$$

$$E_{y}^{oL} = A_{22}^{o} - \frac{{A_{12}^{o}}^{2}}{A_{11}^{o}} \ , \tag{136}$$

$$\nu_{xy}^{oL} = \frac{A_{12}^{o}}{A_{22}^{o}} \ , \tag{137}$$

$$G_{xy}^{oL} = A_{66}^{o} \ . \tag{138}$$

Let us rewrite eqs (131) – (134) in terms of the elements of matrix $\boldsymbol{A^o}$ (eq. (129)). We get:

$$E_{x}^{L} = E_{x}^{oL} + V_{0}^{d} \left[A_{10} + A_{6} \left(\nu_{xy}^{oL} \right)^{2} - 2\, A_{2}\, \nu_{xy}^{oL} \right] , \tag{139}$$

$$E_{y}^{L} = E_{y}^{oL} + V_{0}^{d} \left[A_{6} + A_{10} \left(\nu_{yx}^{oL} \right)^{2} - 2\, A_{2}\, \nu_{yx}^{oL} \right] , \tag{140}$$

$$\nu_{xy}^{L} = \nu_{xy}^{oL} + \frac{1 - \nu_{xy}^{oL} \nu_{yx}^{oL}}{E_{y}^{oL}} V_{0}^{d} \left[A_{2} - A_{6}\, \nu_{xy}^{oL} \right] , \tag{141}$$

$$G_{xy}^{L} = G_{xy}^{oL} + V_{0}^{d}\ A_{8} \ . \tag{142}$$

The effective calculation of engineering moduli needs material parameters A_2, A_6, A_8, A_{10} to be experimentally determined. All details regarding experimental specimens, their preparation and testing procedures are given in Part II of the present work. The next chapter delivers a brief description of calculations necessary to determine A_2, A_6, A_8 and A_{10}.

1.8.2. Determination of material parameters

Since quantities A_2, A_6, A_8, A_{10} are only material dependent, it is reasonable to determine their values using laminate plies stacking sequence as simple as possible. It follows from the previous chapter that cross-ply laminates have such a feature, therefore they will be a basis for further analysis.

It must be clearly stated that the forthcoming considerations are not limitation or simplification of a theoretical model; their only goal is to adapt the model to current needs regarding calculation of material parameters.

Let us solve the set of eqs (139) – (142) with respect to unknown parameters A_2, A_6, A_8, A_{10}. After some calculations, we finally get:

$$A_2 = -A^* \, \nu_{xy}^{oL} \left(\nu_{yx}^{oL}\right)^2 + B^* \, \nu_{xy}^{oL} + C^* \left(1 + \nu_{xy}^{oL} \nu_{yx}^{oL}\right) E_y^{oL} \,, \tag{143}$$

$$A_6 = -A^* \left(\nu_{yx}^{oL}\right)^2 + B^* + 2\, C^* \, \nu_{yx}^{oL} \, E_y^{oL} \,, \tag{144}$$

$$A_8 = \frac{1}{V_0^d} \left(G_{xy}^L - G_{xy}^{oL}\right), \tag{145}$$

$$A_{10} = A^* \left(1 - 2\, \nu_{xy}^{oL} \, \nu_{yx}^{oL}\right) + B^* \left(\nu_{xy}^{oL}\right)^2 + 2\, C^* \, \nu_{xy}^{oL} \, E_y^{oL} \,, \tag{146}$$

where:

$$A^* = \frac{1}{V_0^d} \frac{E_x^L - E_x^{oL}}{\left(1 - \nu_{xy}^{oL} \, \nu_{yx}^{oL}\right)^2} \,, \tag{147}$$

$$B^* = \frac{1}{V_0^d} \frac{E_y^L - E_y^{oL}}{\left(1 - \nu_{xy}^{oL} \nu_{yx}^{oL}\right)^2} , \tag{148}$$

$$C^* = \frac{1}{V_0^d} \frac{\nu_{xy}^L - \nu_{xy}^{oL}}{\left(1 - \nu_{xy}^{oL} \nu_{yx}^{oL}\right)^2} . \tag{149}$$

The scheme of a procedure for determining the parameters A_2, A_6, A_{10} is shown in Figure 1.13. Let us note that A_8 related to the shear modulus is not taken into account in this scheme.

Besides, it was assumed that for any load level transverse Young's modulus changes can be neglected (i.e. $E_y^L = E_y^{oL}$), since transverse cracks within 90° ply do not produce the change of transverse stiffness. Liu [88] made the same assumption and he confirmed experimentally, for ceramic matrix composites, that it is a reasonable assumption. As a consequence – parameter B^*=0.

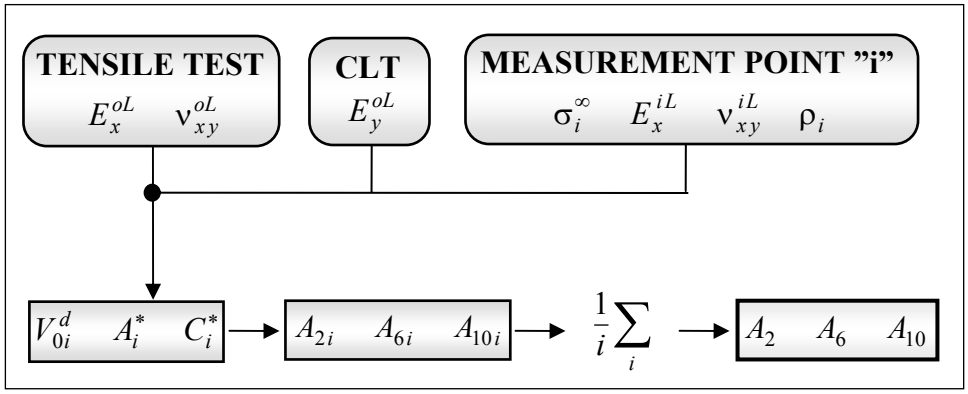

Figure 1.13. Procedure of the calculation of material constants

The three unknown parameters A_2, A_6, A_{10} can be determined in unidirectional tensile test described in Part II of the work. The measured quantities are longitudinal and transverse strains, and the number of transverse cracks within 90° ply. They are necessary to determine:

- initial longitudinal Young's modulus E_x^{oL} and major Poisson's ratio ν_{xy}^{oL}
- current values of Young's modulus E_x^{iL} and major Poisson's ratio ν_{xy}^{iL}
- cracks density ρ_i.

All quantities with index "*i*" are taken at different levels of applied load σ_i^{∞} (called in Figure 1.13 "measurement points").

The initial value of transverse Young's modulus is determined with the use of standard procedure in the frame of CLT (see e.g. [37]).

Applying the procedure shown in Figure 1.13 we finally get parameters A_2, A_6 and A_{10} as arithmetic means of the values calculated at several measurement points. It should be said that a specimen of arbitrarily chosen cross-ply laminate code, namely $[0/90_3]_s$, was used in the procedure discussed.

For a composite laminate manufactured from carbon/epoxy (Torayca T300 in the modified epoxy matrix Vicotex 174) "prepreg" tape Ciba-Geigy Vicotex NCHR 174B we obtain the following values for the requested parameters:

$$A_2 = -192.0 \text{ GPa}, \quad A_6 = -34.7 \text{ GPa}, \quad A_{10} = -258.0 \text{ GPa}. \tag{150}$$

The derived material parameters have been used for calculations of the current values of engineering moduli for different cross-ply and angle-ply carbon/epoxy NCHR 174B laminates. It allows a comparison of the values of engineering moduli predicted by the present model and those obtained from laminate specimens testing. It will be discussed in Part II of this publication.

1.9. THERMODYNAMICAL BASIS OF THE THEORETICAL MODEL

1.9.1. Thermodynamics with internal state variables

Following the concepts of thermodynamics with internal state variables, introduced by Coleman and Gurtin (for details see e.g. [27], [51]), let us introduce the following set of state variables:

$\boldsymbol{e}$ – strain tensor,

T– the absolute temperature,

$\boldsymbol{G}$ – gradient of the temperature,

$\boldsymbol{D}$ – vector of the internal variables.

The elements of vector $\boldsymbol{D}$ are internal variables (scalars, vectors, tensors) associated with any kind of microstructural changes within the body volume. In particular it can consist of the set of the second order damage tensors $\boldsymbol{D}^{(i)}$, where superscript "i" specifies damage tensor for i-th damage mode (i = 1, 2, ..., p).

The functions of thermodynamical response are as follows:

$\boldsymbol{\sigma}$ – stress tensor,

ψ – Helmholtz free energy,

s – specific entropy,

$\boldsymbol{q}$ – heat flux vector,

$\dot{\boldsymbol{D}}$ – vector of internal variables evolution.

According to Truesdell principle of equipresence the above five response functions form a set of constitutive equations, namely:

$$\boldsymbol{\sigma} = \hat{\boldsymbol{\sigma}}\left(\boldsymbol{e}, T, \boldsymbol{G}, \boldsymbol{D}\right), \tag{151}$$

$$\psi = \hat{\psi}\left(\boldsymbol{e}, T, \boldsymbol{G}, \boldsymbol{D}\right), \tag{152}$$

$$s = \hat{s}\left(\boldsymbol{e}, T, \boldsymbol{G}, \boldsymbol{D}\right), \tag{153}$$

$$\boldsymbol{q} = \hat{\boldsymbol{q}}\left(\boldsymbol{e}, T, \boldsymbol{G}, \boldsymbol{D}\right), \tag{154}$$

$$\dot{\boldsymbol{D}} = \boldsymbol{H}\left(\boldsymbol{e}, T, \boldsymbol{G}, \boldsymbol{D}\right). \tag{155}$$

The response functions must satisfy balance equations of linear and angular momentum, equation of energy balance (the first law of thermodynamics) and the second law of thermodynamics (called Clausius - Duhem inequality or reduced dissipative inequality).

If we assume that each process described by the response functions must satisfy dissipative inequality (so-called *theorem of thermodynamical restrictions imposed on the material described by the internal state*

variables), and we restrict formulation to the isothermal case, we get purely mechanical response in the form of following equations [51]:

$$\boldsymbol{\sigma} = \hat{\boldsymbol{\sigma}}\left(\boldsymbol{e}, \boldsymbol{D}\right) , \tag{156}$$

$$\psi = \hat{\psi}\left(\boldsymbol{e}, \boldsymbol{D}\right) , \tag{157}$$

$$\hat{\boldsymbol{\sigma}} = \rho \frac{\partial \hat{\psi}}{\partial \boldsymbol{e}} \qquad \Rightarrow \qquad \sigma_{ij} = \rho \frac{\partial \psi}{\partial e_{ij}} , \tag{158}$$

where ρ is mass density.

Eq. (158) has the following form in Voigt's notation:

$$\sigma_p = \rho \frac{\partial \psi}{\partial e_p} . \tag{159}$$

Taking into account eq. (76), we get a relationship between the Helmholtz free energy ψ and the components of a stiffness matrix $\boldsymbol{C}$ in the form:

$$C_{pq} = \rho \frac{\partial^2 \psi}{\partial e_p \, \partial e_q} \qquad p, q = 1, 2, 6 . \tag{160}$$

Now the crucial problem is to construct the function of Helmholtz free energy. It is possible on the base of the theory of irreducible integrity basis and polynomial functions.

1.9.2. Polynomial form of Helmholtz free energy

Helmholtz free energy, eq. (157), can be written as a polynomial in the arguments indicated. Let us assume that the vector of internal variables consists of symmetrical, second order damage tensor $\boldsymbol{d}$ only. Thus, it is given by:

$$\psi = \hat{\psi}\left(e_p, d_q\right) . \tag{161}$$

Besides, Helmholtz free energy must incorporate any symmetry properties of a material, therefore a relevant polynomial must be a form invariant under the group of coordinate transformations describing those properties. It is obtained by employing polynomial functions of an adequate system of invariants called an irreducible integrity basis. For an orthotropic body and two symmetrical, second order tensors, namely strain tensor ***e*** and damage tensor ***d***, the system of 23 invariants is given by eq. (61) replacing "*a*" by "*d*".

We confine our considerations to the in-plane behaviour of a laminate, described by eq. (64). Thus, the elements of irreducible integrity basis being of interest are as follows:

$$\left.\begin{array}{ll} K_1 = \varepsilon_1 , & K_2 = \varepsilon_2 \\ K_3 = \varepsilon_6^2 , & K_4 = d_1 \\ K_5 = d_2 , & K_7 = d_6^2 \\ K_{10} = \varepsilon_6 d_6 & \end{array}\right\} . \tag{162}$$

The most general form of a relevant polynomial for Helmholtz energy ψ with restriction to the second order terms in strain tensor components and first order terms in the damage tensor components is:

$$\begin{aligned} \rho\psi = {} & k_1\varepsilon_1 + k_2\varepsilon_2 + k_3\varepsilon_6^2 + k_4 d_1 + k_5 d_2 + k_6 d_6\varepsilon_6 + k_7\varepsilon_1^2 + k_8\varepsilon_2^2 + k_9\varepsilon_1\varepsilon_2 + \\ & + k_{10} d_1\varepsilon_1 + k_{11} d_2\varepsilon_1 + k_{12} d_6\varepsilon_1\varepsilon_6 + k_{13} d_1\varepsilon_2 + k_{14} d_2\varepsilon_2 + k_{15} d_6\varepsilon_2\varepsilon_6 + \\ & + k_{16} d_1\varepsilon_6^2 + k_{17} d_2\varepsilon_6^2 + k_{18} d_1\varepsilon_1^2 + k_{19} d_2\varepsilon_1^2 + k_{20} d_1\varepsilon_2^2 + k_{21} d_2\varepsilon_2^2 + \\ & + k_{22} d_1\varepsilon_1\varepsilon_2 + k_{23} d_2\varepsilon_1\varepsilon_2 + k_{24} , \end{aligned} \tag{163}$$

where k_1–k_{24} are the material constants.

It can be rewritten in the form:

$$\rho\psi = d_1\left(k_{16}\varepsilon_6^2 + k_{18}\varepsilon_1^2 + k_{20}\varepsilon_2^2 + k_{22}\varepsilon_1\varepsilon_2\right) +$$
$$+ d_2\left(k_{17}\varepsilon_6^2 + k_{19}\varepsilon_1^2 + k_{21}\varepsilon_2^2 + k_{23}\varepsilon_1\varepsilon_2\right) +$$
$$+ d_6\left(k_{12}\varepsilon_1\varepsilon_6 + k_{15}\varepsilon_2\varepsilon_6\right) + P_1\left(\varepsilon_p, d_q\right) + P_2\left(d_q\right) + P_3\left(\varepsilon_q\right) + P_o \ , \quad (164)$$

where:

$$\left.\begin{aligned} P_0 &= k_{24} \\ P_1\left(\varepsilon_p, d_q\right) &= d_1\left(k_{10}\varepsilon_1 + k_{13}\varepsilon_2\right) + d_2\left(k_{11}\varepsilon_1 + k_{14}\varepsilon_2\right) + k_6 d_6\,\varepsilon_6 \\ P_2\left(d_q\right) &= k_4 d_1 + k_5 d_2 \\ P_3\left(\varepsilon_p\right) &= k_1\varepsilon_1 + k_2\varepsilon_2 + k_3\varepsilon_6^2 + k_7\varepsilon_1^2 + k_8\varepsilon_2^2 + k_9\varepsilon_1\varepsilon_2 \end{aligned}\right\} \ . (165)$$

Setting the following conditions to be satisfied within the body:

1) for unstrained and undamaged material, the Helmholtz free energy ψ vanishes, i.e.:

$$\text{if } \varepsilon_p = 0 \text{ and } d_q = 0 \quad \Rightarrow \quad \rho\psi = 0 \ , \quad (166)$$

2) unstrained material is stress free at any damage state, i.e.:

$$\bigwedge_{d_q} \left\{\text{if } \varepsilon_p = 0 \ \Rightarrow \ \sigma_p = 0\right\} , \quad (167)$$

we get: P_0=0, P_1=0, k_1=k_2=0. Thus, Helmholtz energy is given by the relation:

$$\rho\psi = d_1\left(k_{16}\,\varepsilon_6^2 + k_{18}\,\varepsilon_1^2 + k_{20}\,\varepsilon_2^2 + k_{22}\,\varepsilon_1\,\varepsilon_2\right) +$$
$$+ d_2\left(k_{17}\,\varepsilon_6^2 + k_{19}\,\varepsilon_1^2 + k_{21}\,\varepsilon_2^2 + k_{23}\,\varepsilon_1\,\varepsilon_2\right) + d_6\left(k_{12}\,\varepsilon_1\,\varepsilon_6 + k_{15}\,\varepsilon_2\,\varepsilon_6\right) +$$
$$+ k_3\,\varepsilon_6^2 + k_7\,\varepsilon_1^2 + k_8\,\varepsilon_2^2 + k_9\,\varepsilon_1\,\varepsilon_2 + P_2\left(d_q\right). \tag{168}$$

1.9.3. Stiffness matrix for a damaged body

The elements of stiffness matrix derived with use of eqs (160) and (168) are:

$$\left.\begin{aligned}
C_{11} &= 2k_7 + 2k_{18}\,d_1 + 2k_{19}\,d_2 \\
C_{12} &= C_{21} = k_9 + k_{22}\,d_1 + k_{23}\,d_2 \\
C_{22} &= 2k_8 + 2k_{20}\,d_1 + 2k_{21}\,d_2 \\
C_{66} &= 2k_3 + 2k_{16}\,d_1 + 2k_{17}\,d_2 \\
C_{16} &= C_{61} = k_{12}\,d_6 \\
C_{26} &= C_{62} = k_{15}\,d_6
\end{aligned}\right\}. \tag{169}$$

Let us rewrite the material constants k_i (i = 3, 7, 8, 9, 12, 15–23) in terms of constants used in eqs (79) – (85) in the following way:

$$\left.\begin{aligned}
2k_3 &= c_3 = C_{66}^o, & 2k_7 &= a_1 = C_{11}^o \\
2k_8 &= b_2 = C_{22}^o, & 2k_9 &= a_2 = C_{12}^o \\
C_{16}^o &= C_{26}^o = 0, & k_{12} &= a_7 \\
k_{15} &= b_7, & 2k_{16} &= c_1
\end{aligned}\right\} \tag{170}$$

$$\left.\begin{array}{ll} 2k_{17} = c_2\,, & 2k_{18} = a_3 \\ 2k_{19} = a_4\,, & 2k_{20} = b_5 \\ 2k_{21} = b_6\,, & k_{22} = a_5 \\ k_{23} = a_6 & \end{array}\right\}. \qquad \text{(170 cont.)}$$

The stiffnesses given by eq. (169) can be now written in a general form as follows:

$$C_{ij} = C_{ij}^{o} + C_{ij}^{d}\,, \qquad (171)$$

where:

$$\left.\begin{array}{c} C_{11}^{o} = a_1 \\ C_{12}^{o} = C_{21}^{o} = a_2 \\ C_{16}^{o} = C_{61}^{o} = 0 \\ C_{22}^{o} = b_2 \\ C_{26}^{o} = C_{62}^{o} = 0 \\ C_{66}^{o} = c_3 \\ C_{11}^{d} = a_3\, d_1 + a_4\, d_2 \\ C_{12}^{d} = C_{21}^{d} = a_5\, d_1 + a_6\, d_2 \\ C_{22}^{d} = b_5\, d_1 + b_6\, d_2 \end{array}\right\} \qquad (172)$$

$$\left.\begin{aligned} C_{66}^{d} &= c_1\, d_1 + c_2\, d_2 \\ C_{16}^{d} &= C_{61}^{d} = a_7\, d_6 \\ C_{26}^{d} &= C_{62}^{d} = b_7\, d_6 \end{aligned}\right\} . \qquad \text{(172 cont.)}$$

To recapitulate the results being derived here in the frame of the thermodynamical approach, let us conclude as follows:

- relation (171) is fully equivalent to eq. (78) and thus the admissibility of the decomposition of a stiffness matrix into two parts, namely $\boldsymbol{C}^{o}$ relating to the undamaged state and $\boldsymbol{C}^{d}$ characterising the change of stiffness caused by damage is demonstrated,
- stiffnesses given by eqs (172), derived on the basis of thermodynamics with internal state variables, under additional assumptions (166) and (167), are equivalent to the stiffnesses derived in the present paper on the basis of Adkins's mathematical approach – eqs (79), (80), (83), (84) and (85).

1.10. FINAL REMARKS

In Part I of the present dissertation the transverse cracking of a composite fiber-reinforced polymeric matrix laminates was considered.

The stiffness matrix as well as engineering characteristics for a damaged, symmetrical orthotropic laminate of cross-ply and angle-ply stacking sequences have been derived on the basis of:

- tensorial damage representation by means of Vakulenko and Kachanov's damage definition,
- linear elastic fracture mechanics, supported by the proposed concept of "imaginary strip", allowing reasonable evaluation of average crack opening factor β,
- polynomial invariants functions and invariants integrity basis, as a useful tool in construction of appropriate constitutive equations, by means of Adkins's approach,

- classical theory of laminates, which made possible calculations of all needed stiffness matrices for damaged single ply in the on-axis and off-axis configuration, and finally for damaged laminate.

The procedure for determination of the ”new” unknown material parameters (with the use of one specific cross-ply laminate stacking sequence) related to the influence of a damage state on the stiffness matrix has been proposed.

The complete equivalence of a formal approach based on Adkins's equation, employed in the present paper, and the thermodynamical approach, based on the thermodynamics with internal state variables, has been fully displayed.

Let us consider once more the issues related to the calculation method of the average crack opening factor β, applied in the proposed theoretical model. One should keep in mind that the only way to evaluate the correctness of any model is its experimental verification. In the present analysis the damage tensor is constructed with the aim of its use in successive analysis of the changes of stiffnesses and engineering constants of a laminate due to the intralaminar damage evolution. Thus, the final verification is based on the comparison of the predicted and measured values of the quantities of interest.

With regard to that problem, three critical points have to be pointed out:

a. The first one relates to the experimental results. It is well known that in the case of composite laminates there is always a considerable scatter of measured values of engineering constants for the geometrically identical specimens manufactured from the same composite and tested with the use of the same testing procedure and instrumentation. The scatter can be as big as tens percent. Thus, the results obtained from an individual test cannot be seen as fully representative for the tested composite, therefore their comparison with predicted values should be considered with caution.
b. Another point is the technique used when the comparison of the theoretical and experimental results is performed. In most cases reported the methods of best fitting of theoretical results are employed and then constants introduced in the frame of the given theoretical model are calculated. It does not mean, however, that constants derived on the basis of the data obtained for a specific laminate stacking sequence, which in fact is common practice, would be the same for other laminate lay-outs.
c. The last but not least problem relates to the mechanical behaviour of composite laminates. One should keep in mind that the theoretical model

aimed e.g. at prediction of the changes of engineering constants which is adequate for some laminates sequences, need not be fully adequate for others. The author's experiments with laminates of different stacking sequences, which are presented in Part II of the present paper, confirm this observation. Kashtalyan and Soutis report similar observation in paper [70].

To recapitulate the above remarks it should be clearly stated that actually there is no evidence that sophisticated, e.g. numerical, models give a better correlation of the theoretical and predicted values of engineering constants than simplified analytical models. Another conclusion is that a general model adequate (by means of its fitting to the experimental data) for a given composite material and any laminate lay-out probably does not exist at the present time, what is more, if we take into account unlimited possibilities of laminate lay-out forming, it looks somewhat hopeless to search for such a general model. Finally, let us conclude that even if the predictions given by any model match the experimental results obtained for a specific laminate, the model should be seen as suitable for this specific laminate, but not necessarily for others.

The above discussion should not be seen, by any means, as a pessimistic opinion that the analysis of laminate's damage, as well as its results, is doubtful and it does not allow any general conclusions regarding laminate behaviour. The results discussed in the next chapter show that it is possible to get quite good agreement of the theoretical predictions and experimental data, despite all the issues mentioned above.

PART II
Experimental Analysis and Model Verification

2. EXPERIMENTAL ANALYSIS AND MODEL VERIFICATION

2.1. INTRODUCTION

One of the basic questions in the description of the behaviour of the fiber composite with a plastic matrix is how its strength and stiffness characteristics are influenced by different fracture mechanisms developing during increasing load.

In Part I of the present paper the laminate composites consisting of unidirectional fibers reinforced plies of different angle orientation of fibers have been considered.

For such class of composite materials the failure process is dominated by matrix cracking along fibers in the off-axis layers. The result of this deterioration mechanism is the formation of an array of nearly parallel cracks (called *intralaminar cracks*) lying within an inclined lamina and spanning the whole width of a specimen. The observations of this feature of laminate damaging process do not require any special equipment during the tests.

The class of composites considered here exhibits orthotropic symmetry, thus the independent in-plane elastic characteristics are in general longitudinal Young's modulus E_x, transverse Young's modulus E_y, major Poisson's ratio ν_{xy}, shear modulus G_{xy} and coefficients of mutual influence of the second kind by Lekhnitski $\eta_{x,xy}$, $\eta_{y,xy}$ (they can be, however, expressed in terms of four independent on-axis ply stiffness characteristics).

The in-plane strength of a laminate is fully characterised by longitudinal and transverse strength (in tension and compression), as well as shear strength.

It should be emphasised for clarity that a complete picture of stiffness and strength properties of damaged laminate would require experimental determination of all specified characteristics, as well as additional characteristics related to the developing damage (e.g. intralaminar cracks spacing). In case of stiffnesses determination the experimental procedure has to be invented to make possible the continuous measurements of characteristics in question. In the case of strength the only characteristic which is measured is ultimate strength when specimen is completely broken.

The unidirectional tensile tests presented in this paper were performed with the aim of examining the influence of developing intralaminar cracks on current (i.e. at any load level) values of longitudinal Young's modulus, major Poisson's ratio, and ultimate longitudinal (axial) strength. The basic motivation for analysing unidirectional tensile load only was the possibility to achieve the above goal. According to the classical theory of laminated plates (see Appendix) it is possible only in such a case when there is no coupling between bending and extension, i.e. coupling stiffness matrix equals zero (it is assured for symmetrical laminates). The second necessary condition is to determine the compliance laminate's matrix as matrix inverse to the stiffness matrix (see chapter 1.8). It means that the bending stiffness matrix has to be equal zero also (it is assured for in-plane unidirectional load).

The results of tests and their analysis will be given in this part of dissertation in order to provide some qualitative and, to some extent, also quantitative observations related to the change of elastic constants and axial strength in response to developing damages. The author has reported some of these results in [35] and [36].

In Part II of the dissertation, the engineering moduli predicted on the basis of the theoretical model proposed in Part I will be compared with the results of experiments carried out on carbon/epoxy laminate specimens of cross-ply and angle-ply orientations.

2.2. MATERIAL AND SPECIMENS

2.2.1. Composite material and its characteristics

All the prepared specimens used in the tests have been manufactured from carbon/epoxy composite, namely carbon fibers Torayca T300 in modified epoxy matrix Vicotex 174. The basic carbon/epoxy material had initial form of prepreg unidirectional carbon fiber tape with removable backing, indicating fibers' direction (commercial name Ciba-Geigy Vicotex NCHR 174B). The "net" thickness of a tape was 0.123 mm and the width – 300 mm.

Elastic constants, strength characteristics and coefficients of linear expansion for a unidirectional lamina in its principal material axis are given in Table 2.1. The notation used in this table is:

- LYM – **L**ongitudinal **Young's M**odulus,
- TYM – **T**ransverse **Young's M**odulus,
- SM – **S**hear **M**odulus,
- PR – **Poisson's R**atio,
- LTS – **L**ongitudinal **T**ensile **S**trength,
- LCS – **L**ongitudinal **C**ompressive **S**trength,
- TTS – **T**ransverse **T**ensile **S**trength,
- TCS – **T**ransverse **C**ompressive **S**trength,
- SS – **S**hear **S**trength,
- LCLE – **L**ongitudinal **C**oefficient of **L**inear **E**xpansion,
- TCLE – **T**ransverse **C**oefficient of **L**inear **E**xpansion.

Table 2.1. Characteristics of Vicotex NCHR 174B unidirectional lamina

STIFFNESS CHARACTERISTICS				**STRENGTH CHARACTERISTICS**					**COEFFICIENTS OF LINEAR EXPANSION**	
LYM	TYM	SM	PR	LTS	LCS	TTS	TCS	SS	LCLE	TCLE
E_1	E_2	G_{12}	ν_{12}	X_t	X_c	Y_t	Y_c	S	$\alpha_1 \times 10^7$	$\alpha_2 \times 10^5$
[GPa]			–	[MPa]					[1/°C]	
137.0	10.0	4.8	0.3	1531	1390	41	145	98	3.1	3.1

2.2.2. Preparation and lamination of specimens

The procedure for manufacturing specimens was as follows. From the prepreg tape rectangular pieces of size 60×220 mm were cut off. The sides of rectangular pieces were inclined to the axis (x, y) at a desired angle (it is shown in Figs 2.1 and 2.4). Afterwards the layers were placed on top of each other to form a sheet of a desired stacking sequence.

The next step was the lamination process. The sheet was pressed in a standard testing machine between two thick steel plates under the pressure of approx. 0.736 MPa (7.5 atm.). The steel plates were equipped with a

heating device and thermocouple. It was cured up to 120° C at the rate 2° C/min. The constant pressure and temperature were held over the period of 60 minutes and then the heating was switched off. When the temperature of steel plates (and of laminated plies) dropped below 60° C, the compression of the sheet stopped. In order to control the parameters of heating process precisely both the heating device and the thermocouple were connected *via* special interface unit to a microcomputer with appropriate software. All the parameters of the lamination process are shown in Figure 2.2.

After lamination process the laminate pieces were sawn with the use of a numerically controlled thin, diamond coated cutting wheel. In this manner two rectangular specimens of size 25×200 mm could be obtained from one piece of size 60×220 mm. It should be pointed out that cutting has to be done very precisely if one wants to get a specimen of desired and anticipated orientation. Finally, the end tabs made of cross-ply glass/epoxy laminate were glued to the specimens using an epoxy adhesive film. The geometrical details of the specimens are shown in Figs 2.3 and 2.4.

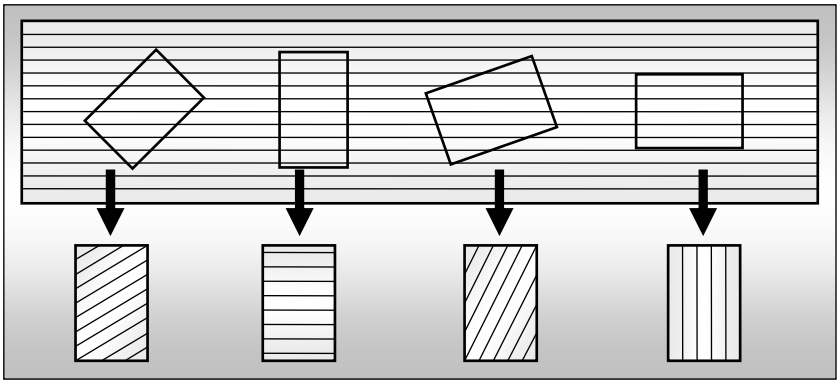

Figure 2.1. Procedure of cutting plies of desired orientation from the prepreg tape

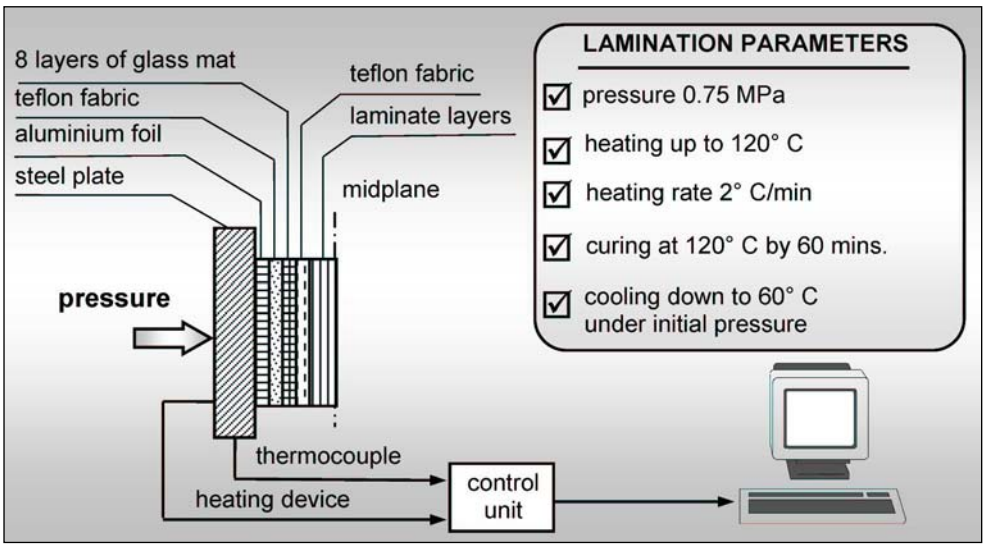

Figure 2.2. Lamination of the specimen material

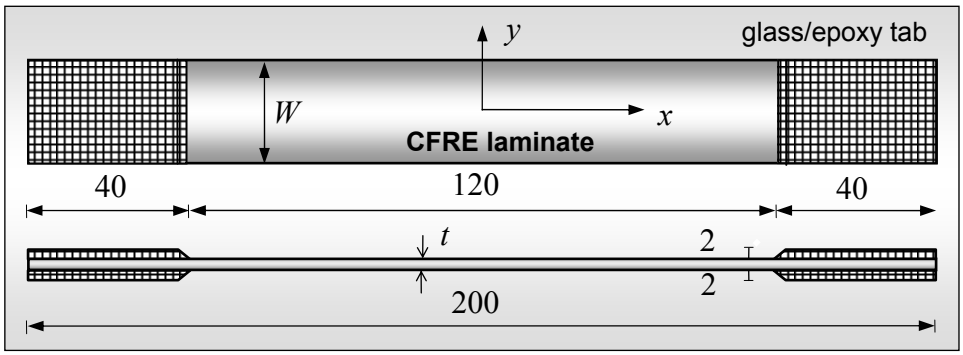

Figure 2.3. The specimen

Two sets of symmetric laminate specimens, cross-ply $[0,90_n]_s$ and angle-ply specimens of code $[-20,+20,-\theta_2,-20,+20,+\theta_2,-20,+20]_s$, were prepared for testing. The angle θ is equal 40°, 50°, 60°, 70°, 75°, 80° and 90°. Theoretical analyses for angle-ply specimens would be easier taking plies of angle 0° instead of ±20°. The reason is that in plies 0° the transverse intralaminar cracks cannot nucleate, and therefore analysis of angle $\pm\theta$

influence on damage evolution is more straightforward. On the other hand, specimens with 0° plies are stiffer than specimens with 20° plies. Due to this fact one can expect that higher load is needed to initiate cracking process within ± θ plies. Thus, the only reason for taking 20° was desire to "force" plies ± θ to undergo cracking under lower load. The plies with arbitrarily chosen angle orientation ±20° were also thought to remain undamaged under applied load (similarly to 0° plies); and in fact no cracks were observed within these plies in the performed tests.

The geometrical characteristics of both sets of specimens are shown in Figure 2.4 and Table 2.2.

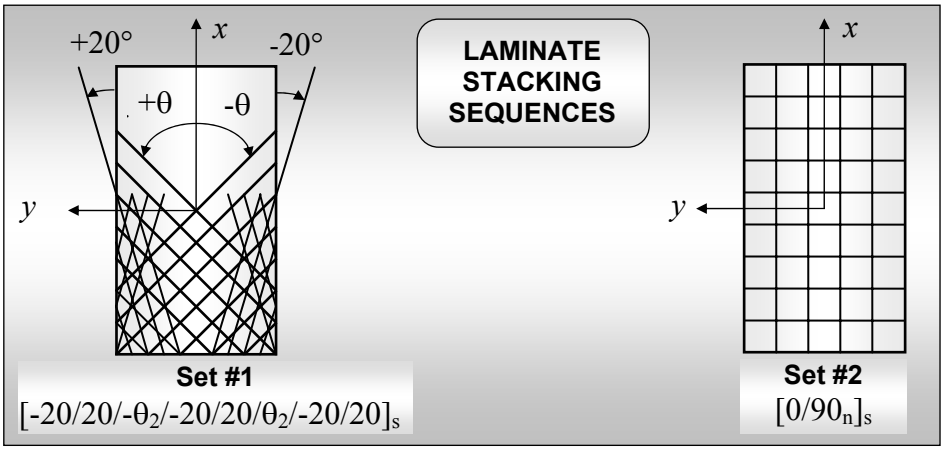

Figure 2.4. Two sets of test specimens

Table 2.2. Geometrical characteristics of test specimens

	SPECIMENS SET # 1							SPECIMENS SET # 2			
	A	B	C	D	E	G	H	1	2	3	4
t [mm]	2.46							0.48	0.74	0.98	1.22
W [mm]	24.38	23.74	24.66	24.54	24.75	23.56	23.46	24.86	24.96	24.88	24.98
θ [deg]	90	80	75	70	60	50	40	–			
n (set #2)	–							1	2	3	4
# of plies	20							4	6	8	10

2.2.3. Preparation of specimens' edges

The final, but of primary importance, step in the procedure of specimens preparation is connected with the method used to reveal any defects (and the structure of the material and fibers orientation, also) occurring before fragmentation of a specimen.

The present method is based on observation of specimen's edge with the use of standard microscope during the tensile test. It requires glossy edge surface which has to be nearly as a mirror surface to be able to distinguish scratches from cracks. In order to achieve the above aim a special procedure of grinding and polishing specimen's edge must be used. The method based on recommendations given in [131] is briefly described below. A similar method is also reported in [76].

The specimens were subjected to machine grinding and polishing on DP-U4/Pedemax-2, machine manufactured by STRUERS A/S (Denmark) equipped with lower rotary disc for grinding paper and mechanical clutch, allowing to attach a holder with specimens to the upper rotor. A special triangle shaped holder of aluminium, invented at DTH (The Technical University of Denmark, Lyngby) was used. It allows polishing of three specimens at the same time, which makes polishing significantly less time consuming. Water and lubricant are distributed uniformly and continuously through the channels drilled in the holder.

In order to obtain clear and glossy specimens' edge surfaces a "step-by-step" polishing procedure was applied with the use of SiC papers of grit 500, 1200 and 4000, Petrodisc-M with 6μm diamond spray, and finally, medium-hard cloth DP-Dur and 1μm DP-spray. Water and the STRUERS DP-Blue Lubricant were used as lubricants during polishing.

It should be clearly stated that selection of SiC paper grit, polishing time duration, the relative rotational speed of a specimen and disc with paper grit (range 50–300 rpm), as well as applied pressure (range 60–120 N) must be selected for a given group of specimens individually.

The last step in specimens manufacturing procedure was placing of strain gauges on their surfaces. Special care must be taken not to allow any contact between gauges leads and specimen surface, as it is a source of erroneous read-out since carbon/epoxy composite is an electrically conducting material.

2.3. SPECIMENS' LOADING

In all tests the monotonically increasing tensile load was applied to the specimens. The programmed and automatically controlled load rate was 0.2 kN/min. (ca 2 percent of ultimate load/min.) for set #2 and 0.5 kN/min. (ca 1.5 percent of ultimate load/min.) for set #1. It was kept constant up to the final failure of each specimen.

The chosen, relatively slow rate, allowed to count the number of cracks during tests at any, almost fixed load level.

2.4. TESTING INSTRUMENTATION

The tensile tests (load controlled) were performed with the use of INSTRON standard machine of 50 kN capacity. The longitudinal and transverse strains in the specimen were measured with strain gauges HBM 10/120 LY 11, HBM 6/120 LY 11, HBM 10/120 XY 91 (0/90 orientation) and strain bridges Brüel & Kjær 1526 (strain reading). The"displacement vs. applied load" curves were also recorded with the use of x–y plotters. Very good agreement of results obtained from both methods was noticed (analogous conclusion is reported in papers e.g. [106] and [107]).

The intralaminar microcracks (with length equal to the thickness of cracking ply – thickness of single ply was approx. 0.123 mm) and their current number were monitored *in situ* through the standard optical microscope equipped with the camera holder. The microscope and camera were mounted on a special translation stage, allowing their vertical shift necessary for observation of the chosen reference section (in presented tests its length was 48 mm). The configuration of testing instrumentation is shown in Figure 2.5.

The above system allows almost continuous observation of the specimens' edge surface and direct *in situ* measurement of cracks number at any load level (unlike the plastic replicas technique frequently used).

The weakness of the system is that the basic "apparatus" used for cracks number counting is the human eye, supported by the microscope. In order to determine the current (i.e. for fixed load) number of cracks, counting them within reference section has to be done very efficiently, particularly at high

load levels, when the number of cracks is large. The appropriate selection of load rate allows reaching this goal easier; still it is troublesome. It is also a source of possible errors, but this is of less importance, as we are mostly interested in the overall process of cracks number growth and not only in the current number of cracks at a single measurement point.

Another problem is connected with the applied method of observation, namely the results cannot be electronically recorded and analysed.

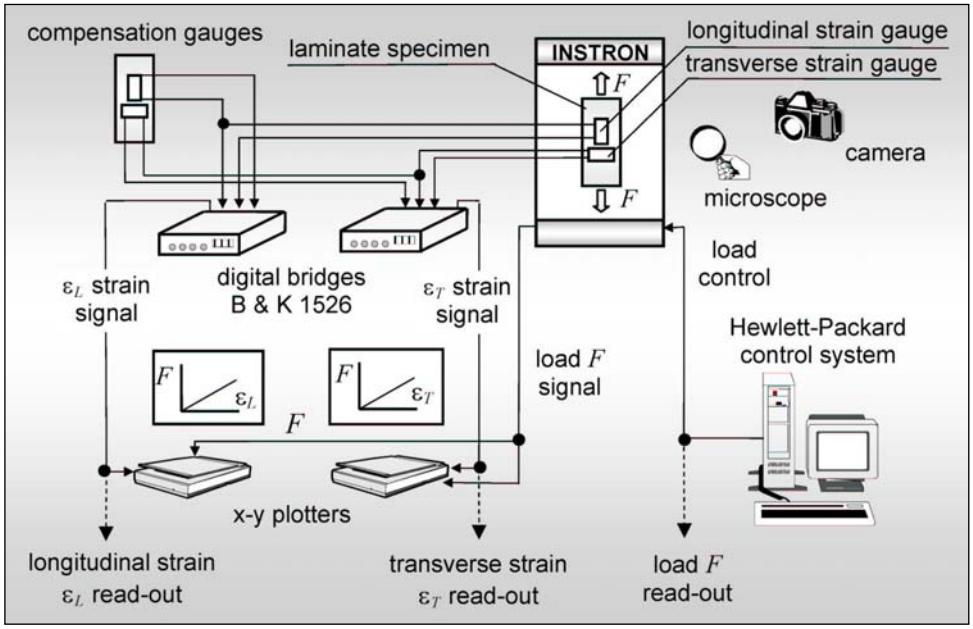

Figure 2.5. Testing equipment

Over the last few years the problem of non destructive testing (NDT), or precisely speaking *in situ* monitoring, the systems and methods designed for elements made of composite laminates has been in permanent progress. In CFRP laminates three basic methods are used, i.e.: optical method [58], acoustic emission (AE) method and electrical method based on AC/DC measurements. The modern optical methods which allow surface observation only, are based, as a rule, on computer controlled digital camera-video recorder system [17], [85]. This method is suitable mainly for laboratory conditions and especially prepared experimental specimens. The AE method [88], [91], [112], [129], [133] is free of that disadvantage. It is

able to predict easily the final fracture, while the analysis of earlier damage stages is still difficult, though newly designed sensors and systems are promising. Methods based on AC and/or DC measurements have limited usage, as they can be used only for composite laminates which satisfy the demand of the electric conduction, as e.g. CFRP laminates. It is discussed in [1].

2.5. RESULTS AND DISCUSSION

2.5.1. Initial Young's Modulus and Poisson's Ratio – classical theory of laminates versus experiment

The values of initial **Y**oung's **M**odulus (YM) and major **P**oisson's **R**atio (PR) are given in Table 2.3. There are both experimental data and theoretical predictions derived on the basis of classical lamination theory (CLT) (for details of calculations see e.g. [37]).

The dimensionless values (experimentally determined values are related to the theoretical ones) of initial longitudinal YM and major PR are shown in Figure 2.6. The results for specimens of cross-ply orientation are presented in Figure 2.6a, and for angle-ply orientation in Figure 2.6b.

Straight lines are linear regression fits to dimensionless data. Both slope and intercept of best fitting lines show that in case of Young's modulus theoretical predictions are in very good agreement with experiment – slightly better results are for cross-ply specimens.

For angle-ply specimens (set #1), CLT calculations and experimental results are very close to each other. Disagreement lies within the range approx. $-2.5 \div +3.0$ % for PR, and $3.5 \div 4.5$ % for YM, which is quite a satisfactory result.

For cross-ply specimens (set #2) theoretical values of YM are somewhat underestimated (approx. $2 \div 3$ %). Predictions of major Poisson's ratio given by CLT are not so close to the test results. Disagreement varies from 20% to 90 % (the thinner specimen the bigger disagreement). For instance, if we exclude from analysis the specimen $[0/90]_s$, the slope of best fitting straight becomes very small (slope tangent is equal -0.055), but disagreement is still significant, i.e. approx. $30 \div 40$ %.

Table 2.3. Initial Young's modulus (theoretical E_{oth} and measured E_{oex}) and Poisson's ratio (theoretical ν_{oth} and measured ν_{oex})

SPECIMEN			INITIAL YOUNG'S MODULUS AND POISSON'S RATIO			
#	Name	Code	E_{oex} [GPa]	E_{oth} [GPa]	ν_{oex}	ν_{oth}
1	A	$[-20/20/90_2/-20/20/90_2/-20/20]_S$	71.6	68.4	0.176	0.170
	B	$[-20/20/-80_2/-20/20/80_2/-20/20]_S$	67.4	67.9	0.198	0.203
	C	$[-20/20/-75_2/-20/20/75_2/-20/20]_S$	69.6	67.2	0.251	0.244
	D	$[-20/20/-70_2/-20/20/70_2/-20/20]_S$	66.3	66.3	0.307	0.305
	E	$[-20/20/-60_2/-20/20/60_2/-20/20]_S$	64.4	64.1	0.483	0.489
	G	$[-20/20/-50_2/-20/20/50_2/-20/20]_S$	64.6	62.2	0.741	0.763
	H	$[-20/20/-40_2/-20/20/40_2/-20/20]_S$	66.0	63.7	1.067	1.089
2	1	$[0/90]_S$	79.8	73.9	0.087	0.041
	2	$[0/90_2]_S$	53.5	52.6	0.046	0.032
	3	$[0/90_3]_S$	42.1	42.0	0.038	0.029
	4	$[0/90_4]_S$	35.9	35.6	0.036	0.027

2.5.2. Ultimate tensile strength

In Table 2.4 ultimate values of load F_{ult}, stress σ_{ult}, longitudinal strain ε_{Lult}, transverse strain ε_{Tult}, and average cracks density ρ'_{ult} are given for both specimens sets. For specimens set #2 average cracks density ρ'_{ult} is equal to ρ defined by (17) and it is taken at failure. For specimens set #1 the numbers of cracks in outer plies ($-\theta_2$) and inner plies ($+\theta_2$) are different. Therefore average cracks density ρ'_{ult} is defined as follows:

$$\rho'_{ult} = \frac{1}{t_d} \int_{-t/2}^{t/2} \rho(z)\, dz \quad , \tag{173}$$

$$\rho(z) = \frac{n(z)}{L_{obs}} , \tag{174}$$

where t_d denotes the sum of thicknesses of all plies containing intralaminar cracks, ρ – cracks density in a given ply, n – the number of cracks within the observation section of length L_{obs} of a ply. Elementary calculation gives $\rho'_{ult} = (\rho_{out}+\rho_{inn})/2$, where ρ_{out} and ρ_{inn} denote cracks density at failure in outer plies ($-\theta_2$) and inner plies ($+\theta_2$), respectively.

Ultimate cracks density for set # 2 depends strongly on 90° ply thickness – the bigger thickness the lower cracks density. It stabilizes when total thickness of 90 deg layer increases.

However, the ultimate tensile load is nearly the same for all four specimens. The reason is quite clear – load bearing capacity in this case is determined by the longitudinal tensile strength of two outer 0° plies, which is much bigger than transverse strength ($X_t/Y_t \cong 37$). The inner transverse layer (irrespective of its thickness) is of secondary importance from the point of view of longitudinal strength analysis. Consequently, the longitudinal strength should not be influenced by damage of inner 90° ply, as strength is determined mainly by undamaged, outer 0° plies.

Confrontation of the ultimate load and ultimate cracks density which represents damage state in 90° layer confirms the above observation.

Experimental data of longitudinal strength have also been compared with standard evaluations based on the partial ply discount method and Azzi-Tsai-Hill criterion [10] with regard to temperature effect caused by the difference between lamination and testing temperatures (see e.g. [37]). The temperature was taken into analysis as specimens were laminated at 120° C, while tested at 20° C.

The ultimate strength is shown in Figure 2.7 along with the ultimate crack density. The theoretical predictions match experimental data irrespective of ultimate cracks density.

The ultimate stresses for all specimens of the set #1 are a little different, which reflects the angle dependence of specimens' strength, but differences are almost negligible (less than 4.5 %). It is probably caused by the fact that volume fraction of damaging plies with alternating angle is 0.4, while volume fraction of undamaged plies of fixed angle (the same for all specimens) is 0.6. There is also no clear relationship between the strength and average ultimate crack density presented in Figure 2.8.

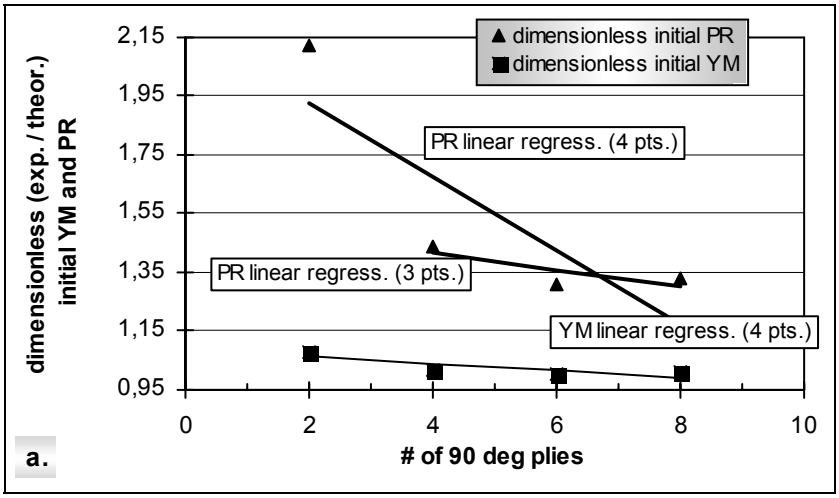

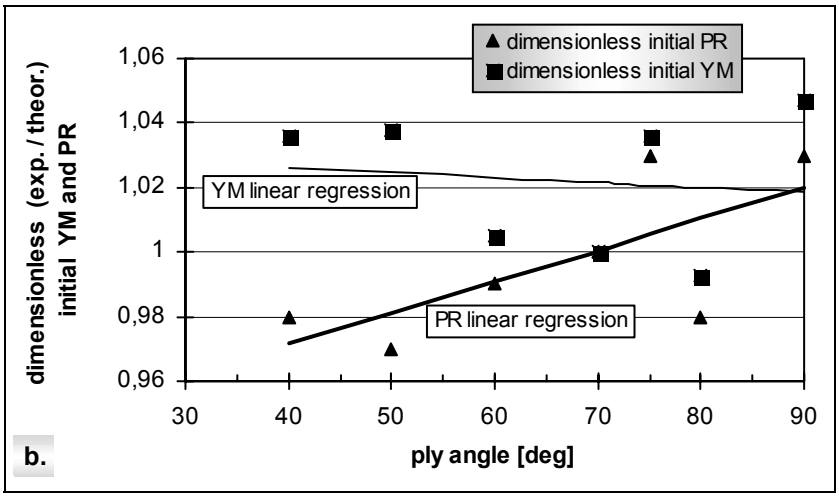

Figure 2.6. Dimensionless initial YM (E_{oex}/E_{oth}) and PR (ν_{oex}/ν_{oth}) versus: a) number of 90° plies (set #2), b) ply angle (set #1)

Table 2.4. Ultimate tensile load F_{ult}, stress σ_{ult}, longitudinal strain ε_{Lult}, transverse strain ε_{Tult} and average crack density ρ'_{ult}

SPECIMEN			ULTIMATE LOAD, STRESS, STRAINS AND AVERAGE CRACK DENSITY				
#	Name	Code	F_{ult} [kN]	σ_{ult} [MPa]	ε_{Lult} [%]	ε_{Tult} [%]	ρ'_{ult} [1/mm]
1	A	$[-20/20/90_2/-20/20/90_2/-20/20]_S$	35.0	582.7	0.82	0.148	1.310
	B	$[-20/20/-80_2/-20/20/80_2/-20/20]_S$	33.9	580.0	0.85	0.166	0.960
	C	$[-20/20/-75_2/-20/20/75_2/-20/20]_S$	35.1	579.0	0.83	0.219	0.812
	D	$[-20/20/-70_2/-20/20/70_2/-20/20]_S$	34.6	573.6	0.86	0.271	0.573
	E	$[-20/20/-60_2/-20/20/60_2/-20/20]_S$	36.5	599.5	0.93	0.495	0.440
	G	$[-20/20/-50_2/-20/20/50_2/-20/20]_S$	34.3	592.2	0.99	0.816	0.333
	H	$[-20/20/-40_2/-20/20/40_2/-20/20]_S$	34.5	598.1	1.00	1.298	0.125
2	1	$[0/90]_S$	10.9	914.3	1.12	0.045	2.020
	2	$[0/90_2]_S$	10.3	557.1	1.10	0.016	1.083
	3	$[0/90_3]_S$	10.2	416.7	1.07	0.011	0.860
	4	$[0/90_4]_S$	10.2	335.0	1.07	0.004	0.710

It seems that for the angle-ply specimens analysed here the strength is not influenced by damage of $\pm\theta_2$ plies. It should be noticed that they are strongly constrained (especially inner $+\theta_2$ plies) by the intact plies. Together with the volume fraction aspect mentioned earlier, it may be an explanation of this supposition. On the other hand, there is no way to determine experimentally how damage of some plies influences the strength of specimen, as in order to do it we should know, from test, the strength of entirely intact specimen and then compare it with the strength of the damaged specimen. It is obviously impossible, as due to the applied load the specimen is always more or less damaged. Thus, the only possibility is to compare the experimental values with the theoretical ones (e.g. based on CLT and any strength theory), as was previously done for specimens set #2.

In Figs 2.9 and 2.10, the ratio of **F**irst **C**rack **A**ppearance (FCA) stress to the ultimate tensile strength, as a function of number of transverse plies (for

set #2) and angle of damaging plies (for set #1), respectively, are presented. For specimens set #1 the graphs are shown for both outer and inner plies $\pm\theta$.

In order to get the best fits to the experimental data the linear regression lines have been drawn. The approximation by linear regression method has been chosen for two reasons. Firstly, there is no visible tendency in data distribution, therefore it is no clear indication, regarding more adequate approximation method. Secondly, the linear regression lines are the simplest, for both data interpretation and possible practical application.

For all the tested cross-ply specimens of set #2 the above ratio is within the range approximately $0.5 \div 0.4$. It is visible that the thicker specimen the less ratio of FCA to the stress at fracture, therefore laminates with thicker 90° ply are more susceptible to cracking [96]. Another observation is that together with the growth of thickness of 90° ply the ratio stabilizes – it is almost constant and equals approximately 0.4.

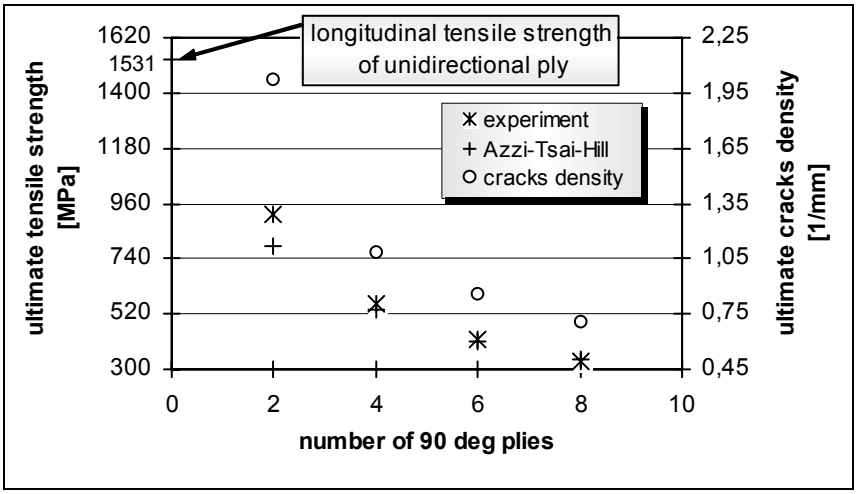

Figure 2.7. Ultimate longitudinal tensile strength and crack density versus number of transverse plies in $[0/90_n]_s$ specimens

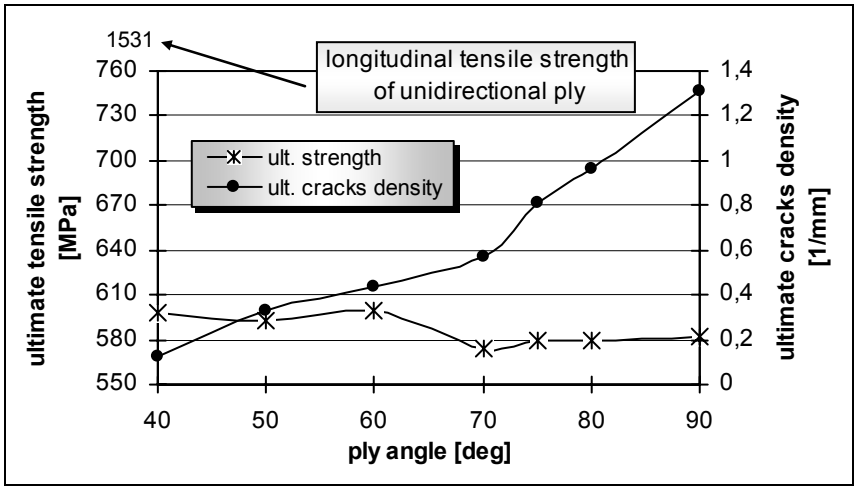

Figure 2.8. Ultimate longitudinal tensile strength and crack density versus damaging ply angle (specimens set #1)

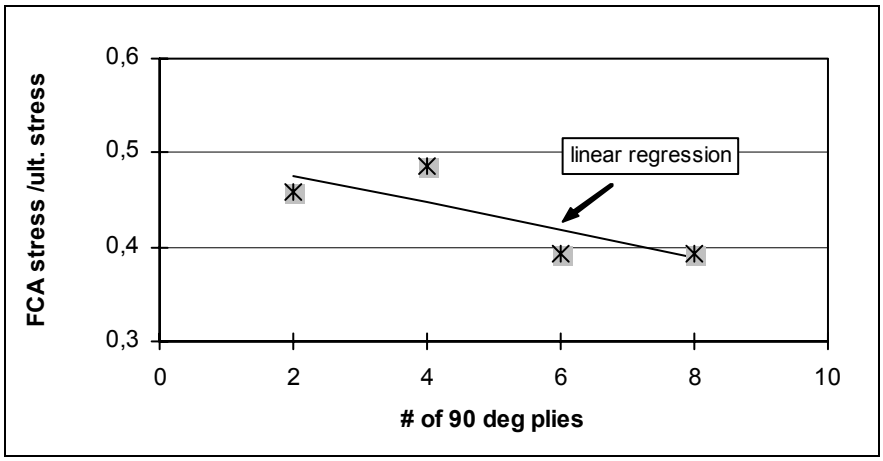

Figure 2.9. Ratio of FCA stress to fracture stress versus number of transverse plies in $[0/90_n]_s$ specimens

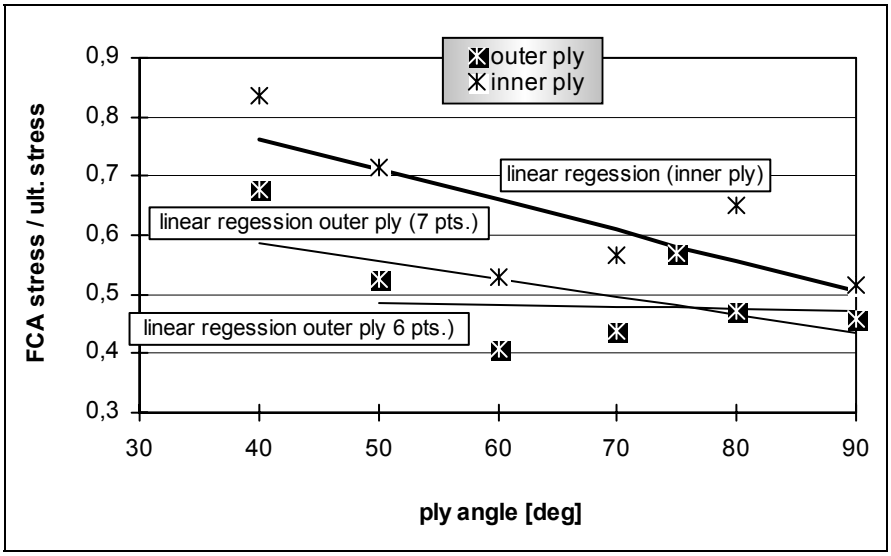

Figure 2.10. Ratio of FCA stress to fracture stress versus ply angle for outer and inner cracking plies in angle-ply specimens

For the angle-ply specimens of set #1 (completely different with regard to thickness and orientation in comparison with set #2), the ratio is within range 0.6 ÷ 0.45 for outer cracking plies and 0.8 ÷ 0.5 for inner cracking plies. Smaller values relate to bigger angles. It should be noted that the first cracks in angle-ply specimens always occurred in outer plies, as they are less constrained by neighbouring intact plies ±20°, therefore outer plies are relevant for analysis of the cracking process initiation. Excluding specimen H ($\theta=\pm 40^{\circ}$), for which, in fact, we observed only several cracks, we find the ratio of FCA stress to tensile strength in outer plies somewhat below 0.5. It is very close to the ratio obtained for the cross-ply specimens.

Therefore, the value 0.4 can be regarded as a conservative estimation of this ratio. It should not be seen as a general rule, since it is based on a very limited number of test data only, and further investigations are needed to confirm (or not) the above estimation, which probably is more credible for $[0/90_n]_s$ orientation.

In order to use in practice the FCA stress to tensile strength ratio and thereby to predict the early stage of matrix cracking we need to know longitudinal strength of a laminate. It can be obtained directly from the test,

but it is obviously time and cost consuming procedure. Instead, the theoretical prediction of strength based on known strength theories, e.g. maximum stress, maximum strain, Tsai-Hill or Tsai-Wu approaches (an interesting extension of classical Tsai-Wu criterion for progressive failure is presented in [139]) and one of the methods of strength determination (e.g. **F**irst **P**ly **F**ailure (FPF), **L**ast **P**ly **F**ailure (LPF), total ply discount, partial ply discount) can be employed. The disadvantage of this last procedure is that it can be relatively easily performed only for simple laminate orientations, e.g. cross-ply, while for most orientation a computer code is necessary.

2.5.3. Ultimate longitudinal and transverse strain

In Figs 2.11a and 2.11b the ultimate longitudinal and transverse strains are shown, respectively, together with the ultimate crack density for cross-ply specimens.

Longitudinal fracture strains ε_{Lult} are large, slightly less for specimens with thicker 90° ply (approx. 4.5%), but they are nearly independent of the inner ply thickness and cracks density within this ply. Therefore, only outer 0° plies decide about ε_{Lult}. Ultimate transverse strain ε_{Tult} changes significantly with inner ply thickness – the thicker ply the smaller ε_{Tult}. However, their values (0.045%÷0.004%) are drastically smaller when compared with the longitudinal strains. It is a direct result of big stiffness of 90° ply (increasing with the growth of its thickness) in transverse direction to the direction of applied load, which does not allow transverse deformations. They cannot be influenced by 90° ply matrix cracking, as the basic role is played by the intact fibers, not a damaged matrix.

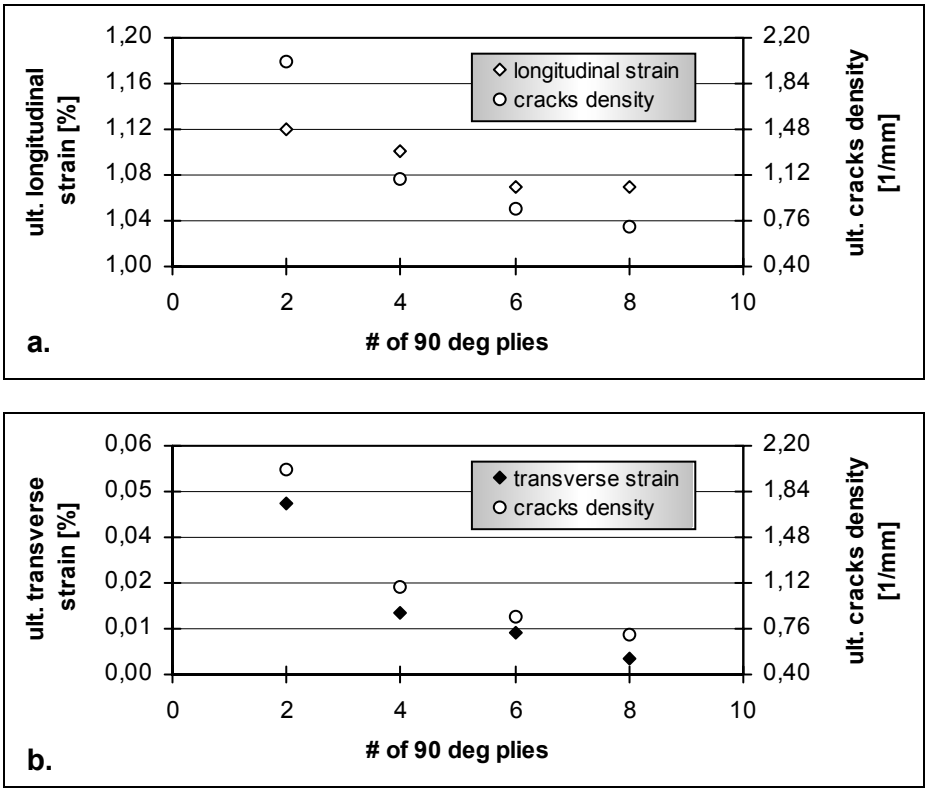

Figure 2.11. Ultimate longitudinal strain (a.), transverse strain (b.) and crack density versus number of transverse plies in $[0/90_n]_s$ specimens

In Figure 2.12 the ultimate longitudinal and transverse strains are shown together with the ultimate cracks density for the angle-ply specimens. The smaller angle θ of damaging ply, the bigger ultimate longitudinal strain (for ply 40° ε_{Lult}=1%, and for 90° ply ε_{Lult}=0.82%), which can be explained by the natural tendency of the inclined fibers to reducing angle of inclination under the tensile axial load. It is confirmed by the values of transverse fracture strains. Their angle relation is similar to that for longitudinal strains, but sensitivity of ε_{Tult} to angle decrease is significantly stronger in comparison with ε_{Lult} (for ply 40° – ε_{Tult}=1.3%, whereas for 90° ply ε_{Tult}=0.15%).

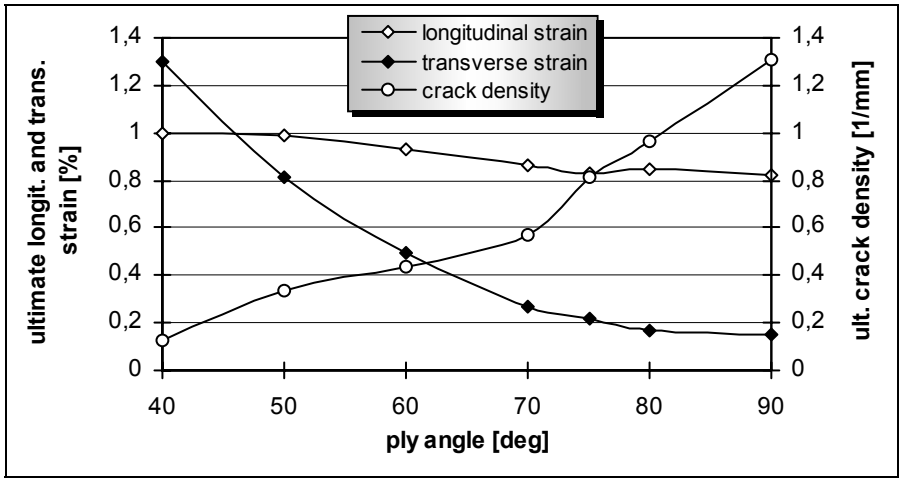

Figure 2.12. Ultimate longitudinal strain, transverse strain and cracks density versus damaging ply angle (specimens set # 1)

Another observation is that transverse fracture strains for small angles can be greater than longitudinal strains (for ply 40° it is about 30%). It is a completely different result from that in the case of cross-ply specimens.

From the comparison of Figs 2.11 and 2.12 one more interesting conclusion can be drawn. It is visible that in the case of specimens set #2 the reduction of both longitudinal and transverse fracture strains is accompanied by decreasing of the crack density, while in the case of set # 1 the behaviour is opposite. It can be seen as an indirect confirmation of the independence of fracture strains of damage within some layers.

2.5.4. Longitudinal Young's Modulus and Poisson's Ratio – cross-ply orientation

In Figs 2.13, 2.15, 2.17 and 2.19 dimensionless (ratio of the actual value to the initial one) values of longitudinal Young's modulus (YM) and Poisson's ratio (PR) along with the cracks density within transverse plies are plotted as functions of applied stress. The above figures relate to cross-ply specimens $[0/90]_s$, $[0/90_2]_s$, $[0/90_3]_s$ and $[0/90_4]_s$, respectively.

In Figs 2.14, 2.16, 2.18 and 2.20, the graphs of longitudinal and transverse strains versus applied stress are shown for the same specimens set.

The first group of figures exhibits several common features. One of them is that cracks density depends strongly on 90° ply thickness – the bigger thickness the smaller crack density. Comparing the crack density at failure in the thinner and thicker specimen, one can see that it is three times less for thicker specimen. It is visible that crack density stabilizes for high load level, especially for thicker specimens. One can also notice that the onset stress (threshold stress) for matrix cracking initiation is bigger for the thinner specimens. It means that threshold stress is inversely related to the thickness of cracking 90° ply. The theoretical and experimental analysis presented in paper [96] by Nairn confirms this conclusion.

The most important observations are related to the changes of engineering constants. It is well known from a number of papers (e.g. [45], [110]) that, in fact, they should not be called ”constants”, as they are changing under applied load. This effect is much stronger in the case of Poisson’s ratio. Irrespective of the specimen thickness, the actual values of PR significantly decrease with load increase. The reduction in PR is up to 50% for $[0/90]_s$ specimen (it is similar to the results reported in e.g. [121] and reaches 90% for $[0/90_4]_s$. For the two other specimens of set #2 PR is within the range specified by the above limits. The basic and direct factor causing such substantial reduction of Poisson’s ratio is the nonlinearity of the relation between transverse strain and stress, which is shown in Figs 2.14–2.20. Direct dependence of a degree of PR reduction with nonlinearity of transverse strains is easily visible if relevant pairs of figures are compared (e.g. Figure 2.13 and Figure 2.14 for specimen $[0/90]_s$ etc.).

An open question is the reason of progressive nonlinearity (the thicker specimen the stronger nonlinearity) of transverse strains. It is probably due to stacking sequence and on-axis properties of a CFRE ply, but there is no doubt that transverse cracks also influence this phenomenon. Initiation and evolution of the process of 90° ply cracking make the nonlinearity stronger. The above effect is reflected by the degradation of Poisson’s ratio. It takes place from the very beginning of the loading process, but the detailed analysis of the experimental data presented in Figs 2.13–2.20 shows that the reduction of PR is stronger when the growth of load is accompanied by growth of crack density.

The analysis of the graphs of longitudinal Young's modulus shows that it is much less sensitive to the stress level and cracks density than Poisson's ratio, nevertheless the dependence of the YM reduction on cracks density in the cases of specimens #2, #3 and #4 is evident. The biggest reduction of YM was 13% for the thickest $[0/90_4]_s$ specimen. For the specimens #2 and #3 the reduction was nearly the same and equal to approx. 7%. Allen *et al*. [6] reported very similar values for graphite/epoxy AS4/3502.

The only exception from the above tendency was the thinnest specimen $[0/90]_s$. Instead of the reduction, we observe a very small increase of Young's modulus, which was the biggest at the final stage of loading (approx. 2.5%). We have a very similar result for the second specimen $[0/90]_s$. Both specimens were cut from the same laminate sheet, which also means that both specimens were laminated in the same conditions. The strain gauges used in these specimens were the same as well as the other test instrumentation. Therefore, a random error can not be considered as the reason of this unexpected result and can be rejected. The possible explanation can be as follows. During careful observation of the specimen edge surface and transverse cracks developing in 90° ply we noticed that very short interlaminar cracks at cracks tips, at the boundary of 0° and 90° plies were created. The direct result of this effect was partial delamination at the free edges of the specimen. Taking into account the multitude of cracks in $[0/90]_s$ specimen and their growth with load increase, the delamination effect intensified too. It is known from the laminates theory that longitudinal YM for specimen with the given volume fraction of 0° plies decreases if the volume fraction of 90° plies increases. If we recall that strain gauges are placed on the outer surface, i.e. surface of 0° ply and we confront it with the partial delamination, we can conclude that the influence of "weak" 90° ply on global Young's modulus decreases with the load increase. The possible result of this mechanism may be a slight increase of measured longitudinal Young's modulus. It is in accordance with the graphs shown in Figure 2.13. One can notice that Young's modulus growth is correlated with crack density growth.

Let us recall once more Figs 2.13, 2.15, 2.17 and 2.19. It is worth noticing, irrespective of the previous analysis, that the reduction of the actual values of engineering characteristics is the biggest for the specimen with the thickest 90° ply, while the number of observed cracks in this specimen is the smallest. Thus, in order to estimate the degradation of

elastic characteristics of a cross-ply laminate, the number of intralaminar cracks has to be taken into consideration along with the thickness of cracking ply.

From the above analysis, together with earlier discussion regarding the threshold stress, one can conclude that for the given load in the laminates' operating range it seems reasonable to separate 90° plies of a cross-ply laminate in groups of thin plies, instead of grouping them in one thick ply.

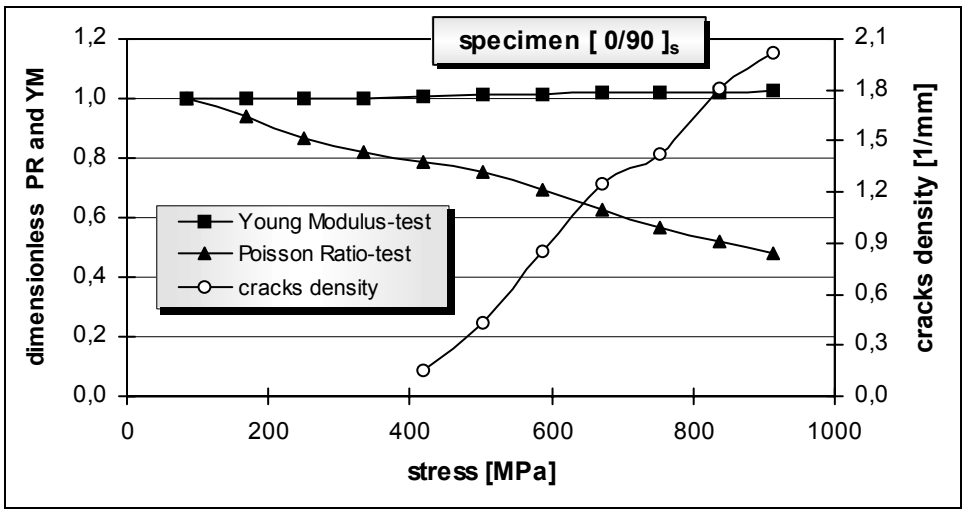

Figure 2.13. Dimensionless YM, PR and cracks density vs. stress for specimen $[0/90]_s$

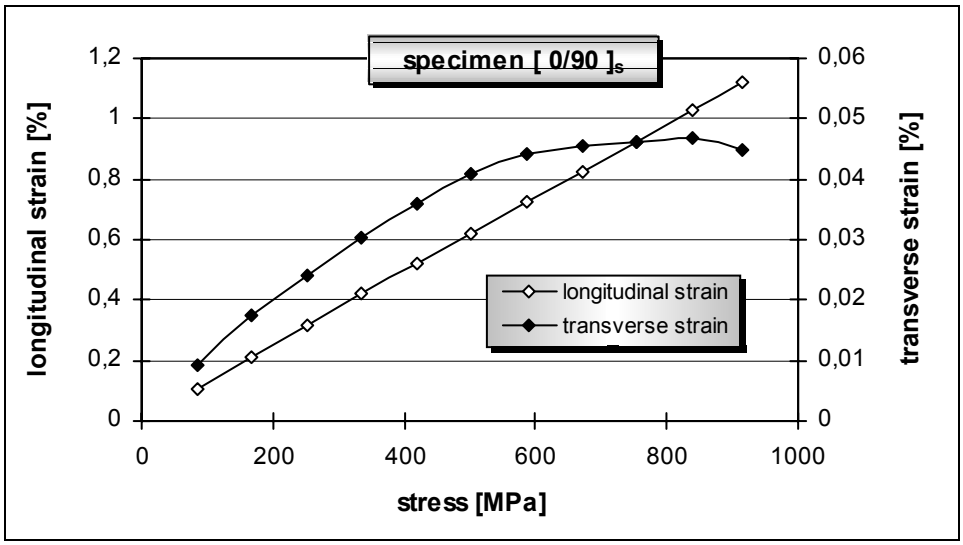

Figure 2.14. Longitudinal and transverse strains vs. stress for specimen $[0/90]_s$

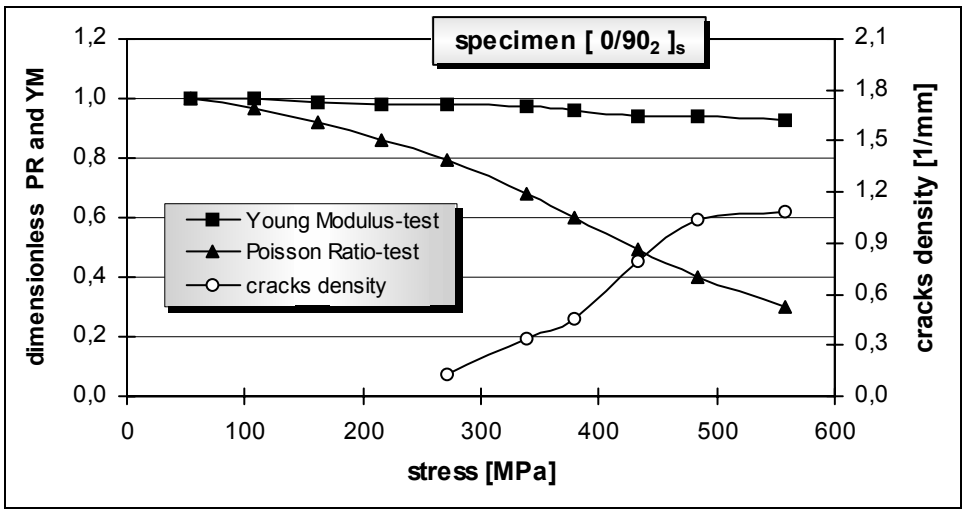

Figure 2.15. Dimensionless YM, PR and cracks density vs. stress for specimen $[0/90_2]_s$

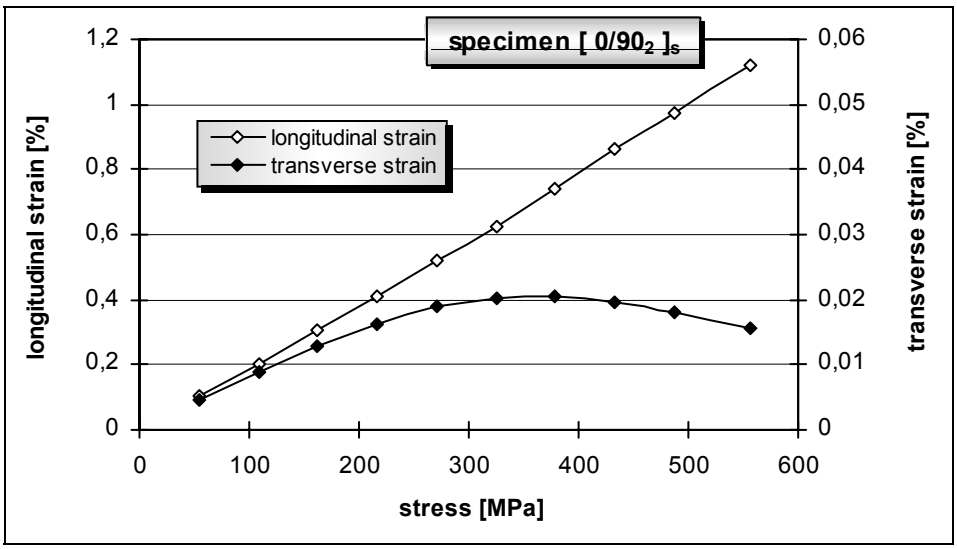

Figure 2.16. Longitudinal and transverse strains vs. stress for specimen $[0/90_2]_s$

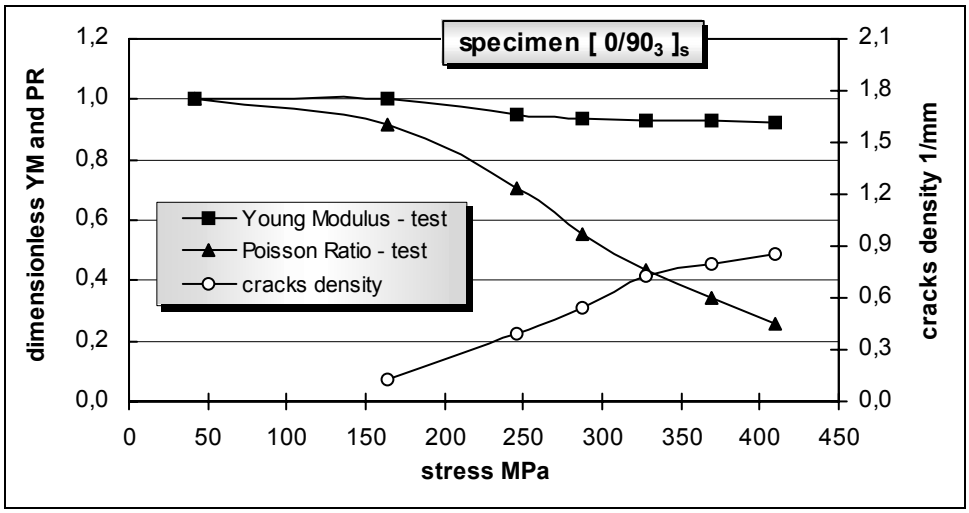

Figure 2.17. Dimensionless YM, PR and cracks density vs. stress for specimen $[0/90_3]_s$

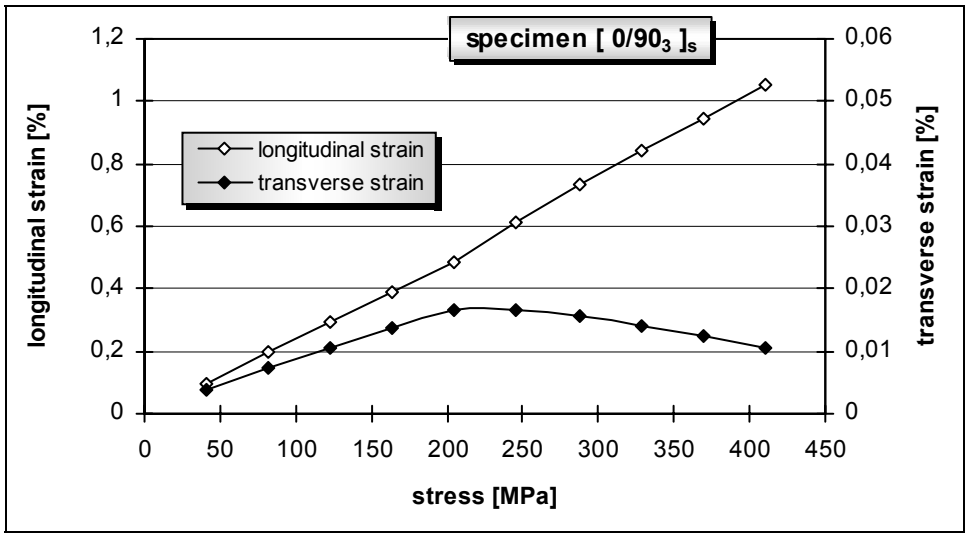

Figure 2.18. Longitudinal and transverse strains vs. stress for specimen $[0/90_3]_s$

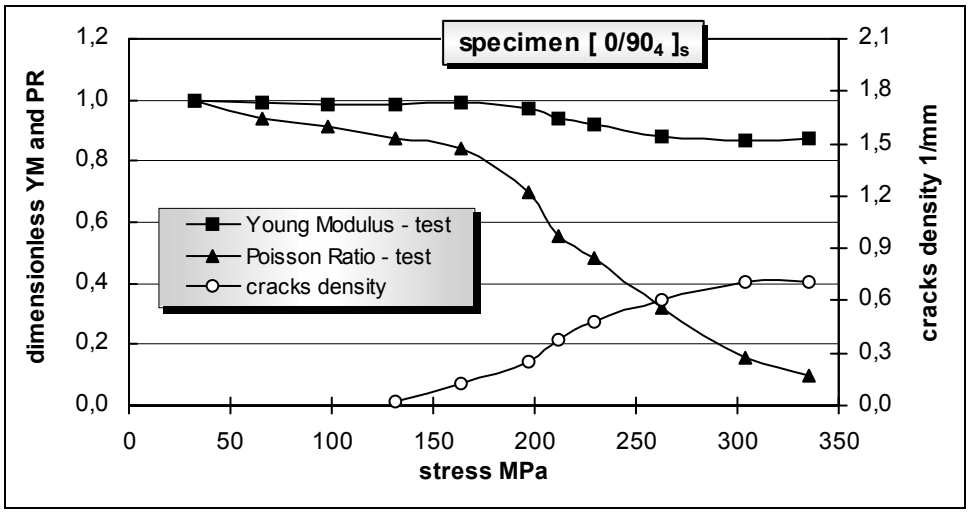

Figure 2.19. Dimensionless YM, PR and cracks density vs. stress for specimen $[0/90_4]_s$

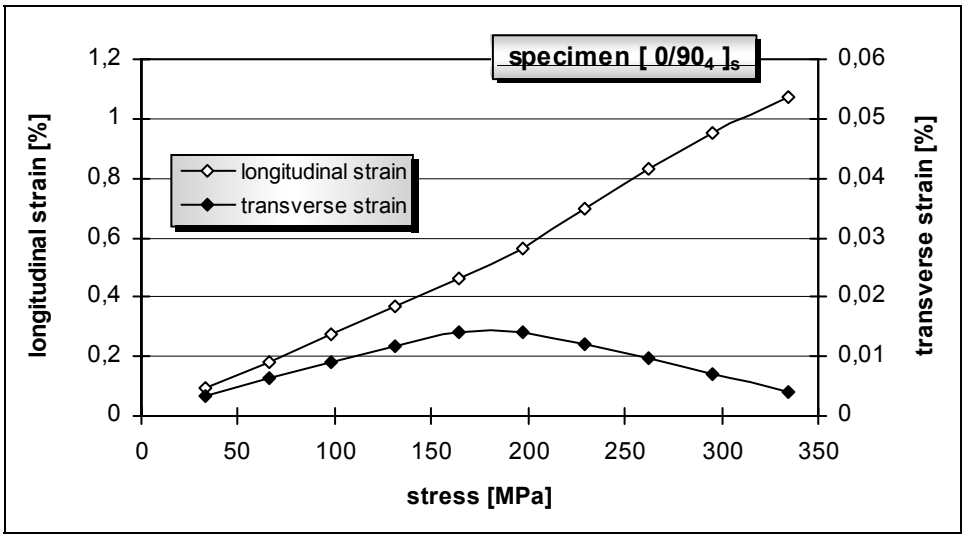

Figure 2.20. Longitudinal and transverse strains vs. stress for specimen $[0/90_4]_s$

2.5.5. Longitudinal Young's Modulus and Poisson's Ratio – angle-ply orientation

The mechanical behaviour of the specimens specified as set #1, with angle plies stacking sequence $[-20/20/-\theta_2/-20/20/+\theta_2/-20/20]_s$ is, in general, quite different in comparison with the cross-ply specimens. Experimental results related to engineering characteristics, represented by dimensionless axial Young's modulus and major Poisson's ratio, cracks density, longitudinal and transverse strains, are shown in the series of Figs 2.21 ÷ 2.34, successively from specimen A to H (θ changes from 90° to 40°).

First, let us notice some common features for all tested specimens. We have never observed any intralaminar cracks, even at the load near to its ultimate value, in plies with a fixed angle of fiber orientation ± 20°. If we confront this observation with very low cracks density within plies ±40° (specimen H, Figure 2.33), we can conclude that in the considered case the damage mechanisms connected with the formation of intralaminar cracks can not develop in plies inclined to the load direction with angles less than approx. 40 degrees. The upper angle limit is undoubtedly dependent on many factors (specimen thickness, volume fraction of damaging and intact plies, on-axis strength characteristics of single composite ply), therefore the above conclusion has only qualitative meaning, but one can expect the existence of that threshold angle also for other laminate configurations. The results given in papers [94] and [118] confirm this conclusion.

Another common observation for all specimens is that cracks in the outer $-\theta_2$ plies nucleate always at the lower load than in inner $+\theta_2$ plies and their density at any load is significantly higher (specimen H is the only exception for reasons mentioned earlier). It is a result of the influence of the constraining effect of intact plies on damage development in adjacent plies. This effect can be characterised for outer plies by the sequence $[-20/20/-\theta_2/-20/20]$, while for inner plies by $[-20/20/+\theta_2/-20/20/20/-20]$ one. The bigger number of adjacent intact plies in the second case is reflected by lower crack density within plies $+\theta_2$.

The next similarity of the behaviour of specimens A ÷ H is reflected by the changes of Poisson's ratio. In all cases the measured Poisson's ratio increases with the growth of applied load and the resulting cracks density

increment. It is very different from cross-ply orientations analysed previously. Instead of expected reduction of Poisson's ratio accompanying the damage growth we observed its progressive growth. This phenomenon is confirmed by the results derived by Kashtalyan and Soutis [70] for composite laminates of stacking sequence $[\Theta_1/\Theta_2]_s$

In order to find an explanation of this phenomenon, let us compare the results for specimen A and H. In the first case, cracks density was the biggest and maximum growth of Poisson's ratio was approx. 3.5%, while in the second specified specimen, in which we observed single cracks only, it was as big as 18%. Taking into account the ply layout in both specimens, one can say that growth of Poisson's ratio is caused by specimen layout and resulting deformations – both longitudinal and transverse strains for specimen H are slightly nonlinear, as shown in Figure 2.34. It follows from the above considerations that even if intralaminar cracks cause the reduction of Poisson's ratio (which in fact is only speculation based on experience with cross-ply specimens), its growth arising from laminate nonlinear deformations determines the overall macroscopic behaviour of considered laminates.

Now let us make some remarks regarding the Young's modulus. In the case of specimens A the Young's modulus was nearly constant and equal to the initial value in spite of numerous cracks (see Figure 2.21) within the entire range of applied load. The relation between longitudinal strain and stress was linear (see Figure 2.22). Thus, actual values of the modulus were not influenced by damage state. The graphs of Young's modulus for specimens B, C, D, E presented in Figs 2.23, 2.25, 2.27 and 2.29 show a slight positive slope for almost the entire load range. However, the maximum growth of Young's modulus is less than 2.5 % (generally less than 1%) and can reflect a scatter in experimental data, which is quite common in testing of composite materials. Therefore, we assume that Young's modulus for these specimens is not influenced by the damage. For specimens G and H (Figure 2.31 and Figure 2.33, respectively) we observed a reduction of Young's modulus equal to approx. 7% and 9%, respectively. However, it cannot be explained, by evolution of cracks, as their density for these two specific specimens was, in comparison with the remaining specimens of set # 1, the smallest. It is also hard to explain the results obtained for those specimens by measurements errors.

The above considerations resulting from experimental data allow us to conclude that in the case of specimens set #1 the influence of developing

intralaminar cracks on engineering characteristics is insignificant, if any. It is in contrast to the results previously reported for cross-ply laminates. What is more, the results obtained for two types of specimens, namely G and H, are distinctly different from all others. Taking into account the foregoing considerations it is reasonable to assume that for relatively thick laminates of specific angle orientations changes in mechanical properties are probably controlled strongly by different damage mechanisms from these considered in the present work. It should be seen as a problem worth further research.

The qualitative observations are quite important since they show that in the case of orthotropic laminates (or anisotropic materials, generally speaking) the change of engineering moduli cannot be considered as the ”universal” feature and the appropriate, in each case, measure of the damage state. It is an important issue, as it is a basically different picture from that for isotropic materials. In case of isotropic materials, e.g. Young’s modulus changes are very often considered as the damage measure and it is well proven experimentally [79].

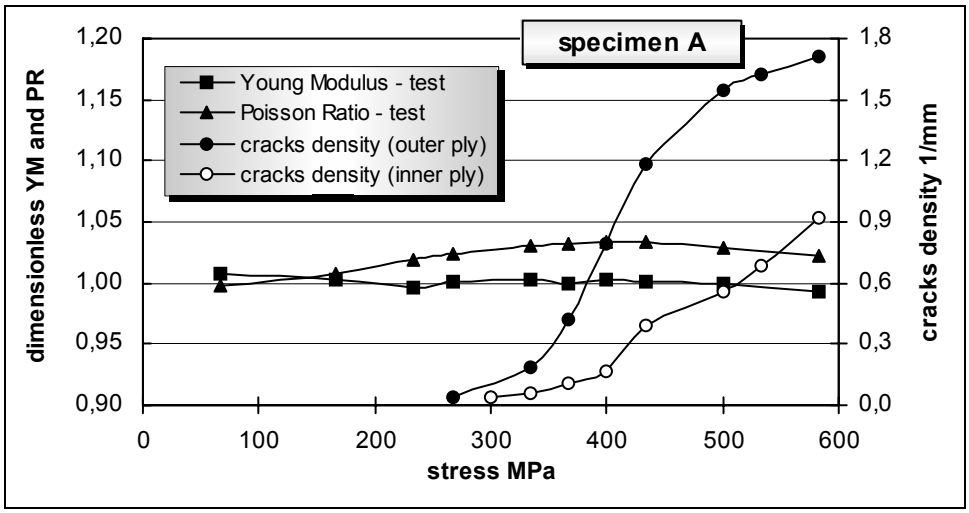

Figure 2.21. Dimensionless YM, PR and cracks density in outer and inner 90 deg plies vs. stress for specimen $[-20/20/90_2/-20/20/90_2/-20/20]_s$

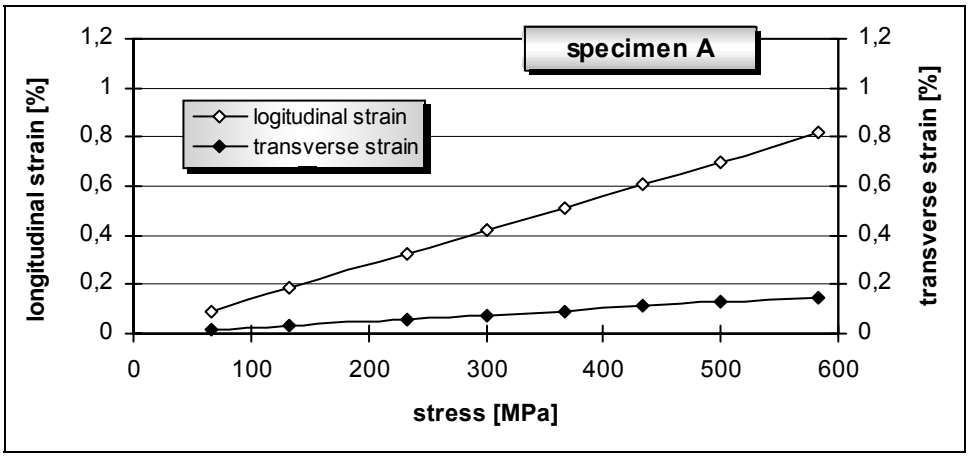

Figure 2.22. Longitudinal and transverse strains vs. stress for specimen $[-20/20/90_2/-20/20/90_2/-20/20]_s$

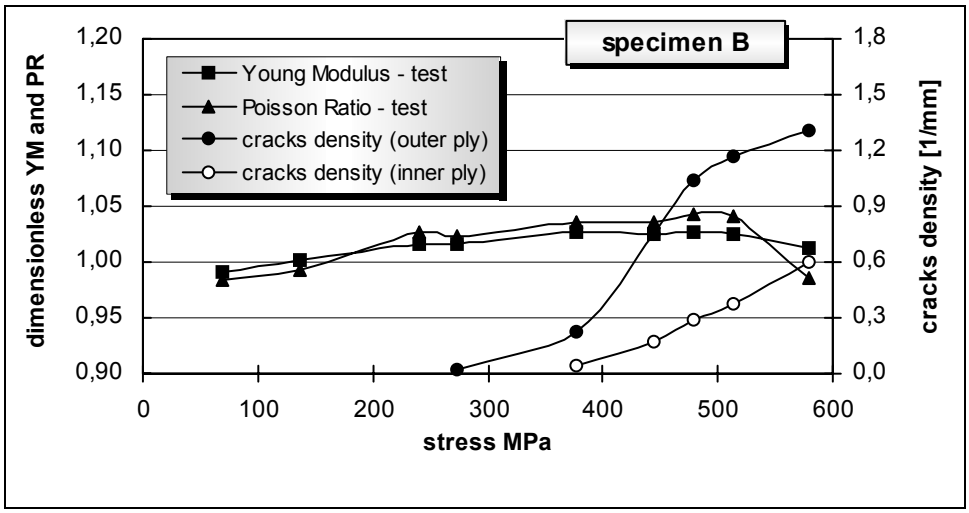

Figure 2.23. Dimensionless YM, PR and cracks density in outer and inner 80 deg plies vs. stress for specimen $[–20/20/–80_2/–20/20/80_2/–20/20]_s$

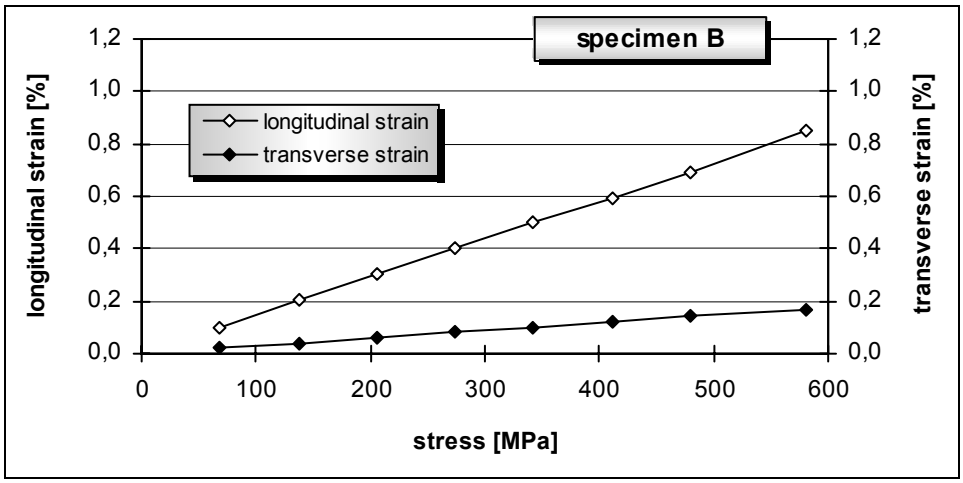

Figure 2.24. Longitudinal and transverse strains vs. stress for specimen $[–20/20/–80_2/–20/20/80_2/–20/20]_s$

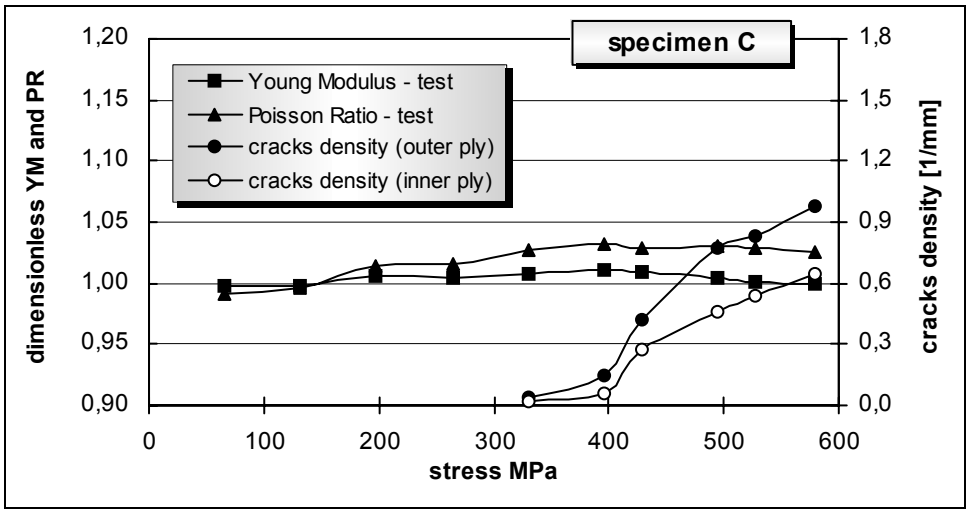

Figure 2.25. Dimensionless YM, PR and cracks density in outer and inner 75 deg plies vs. stress for specimen $[–20/20/–75_2/–20/20/75_2/–20/20]_s$

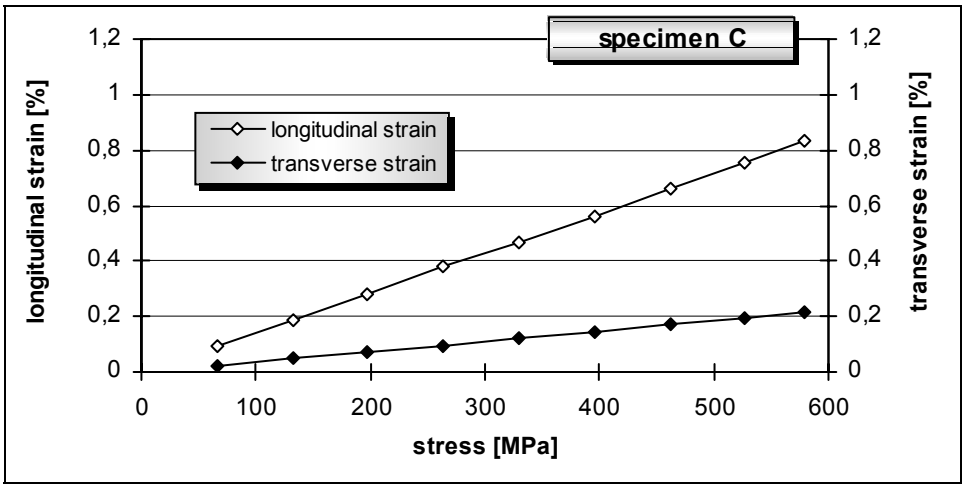

Figure 2.26. Longitudinal and transverse strains vs. stress for specimen $[–20/20/–75_2/–20/20/75_2/–20/20]_s$

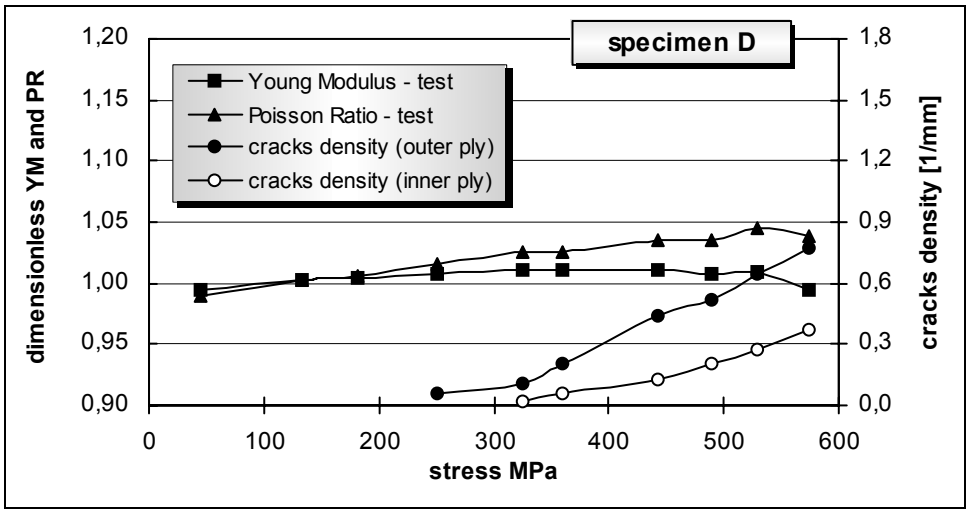

Figure 2.27. Dimensionless YM, PR and cracks density in outer and inner 70 deg plies vs. stress for specimen $[-20/20/-70_2/-20/20/70_2/-20/20]_s$

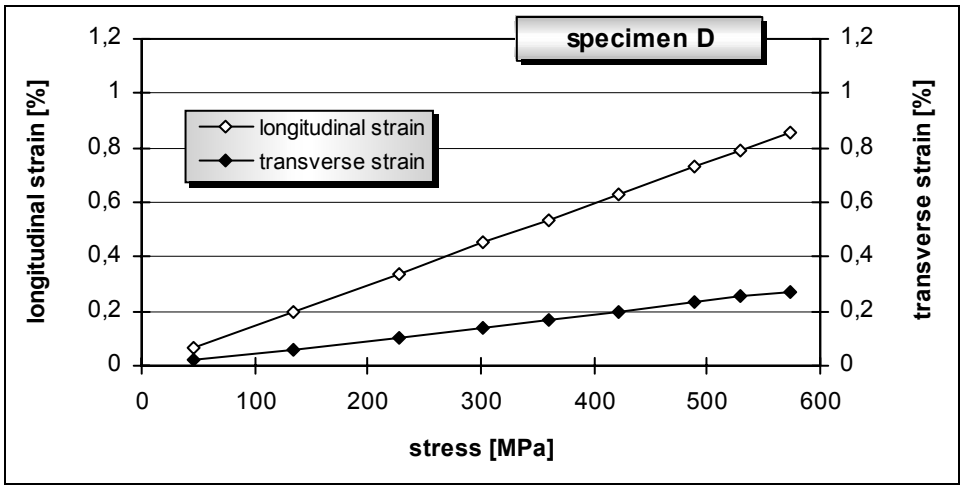

Figure 2.28. Longitudinal and transverse strains vs. stress for specimen $[-20/20/-70_2/-20/20/70_2/-20/20]_s$

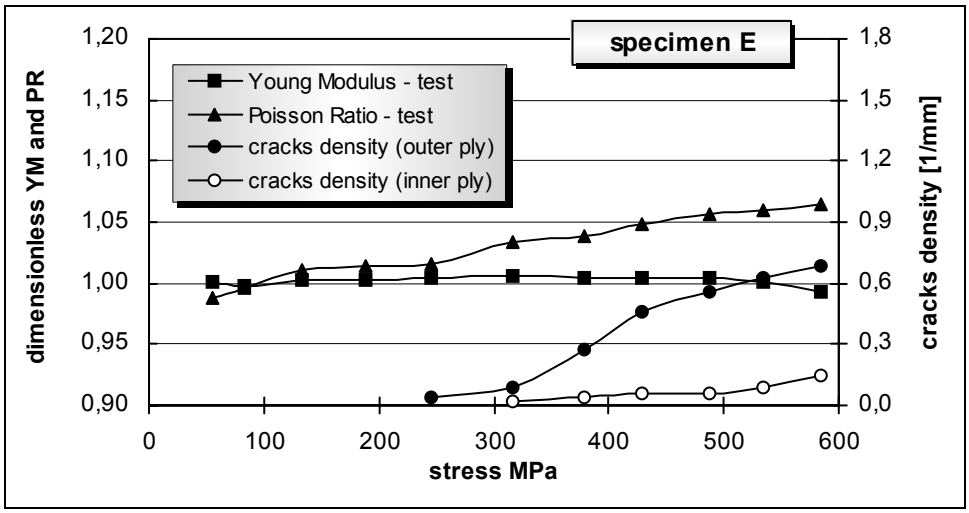

Figure 2.29. Dimensionless YM, PR and cracks density in outer and inner 60 deg plies vs. stress for specimen $[-20/20/-60_2/-20/20/60_2/-20/20]_s$

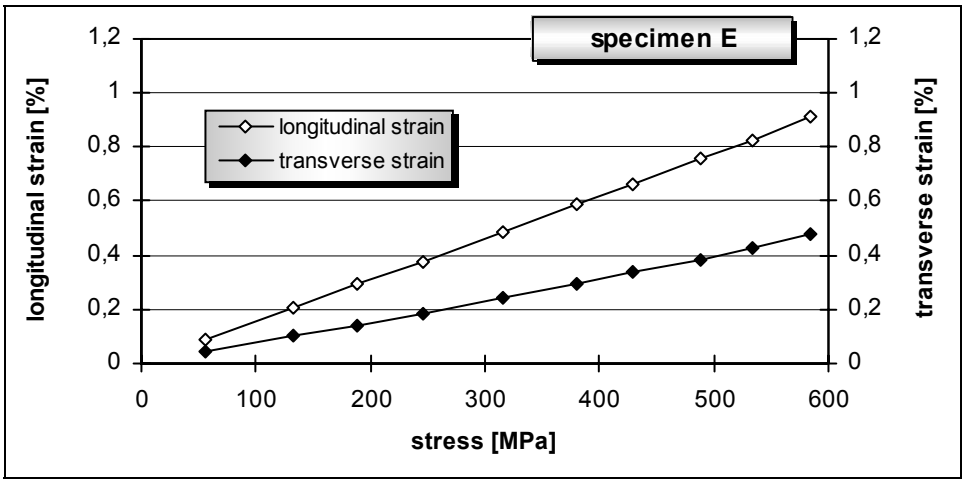

Figure 2.30. Longitudinal and transverse strains vs. stress for specimen $[-20/20/-60_2/-20/20/60_2/-20/20]_s$

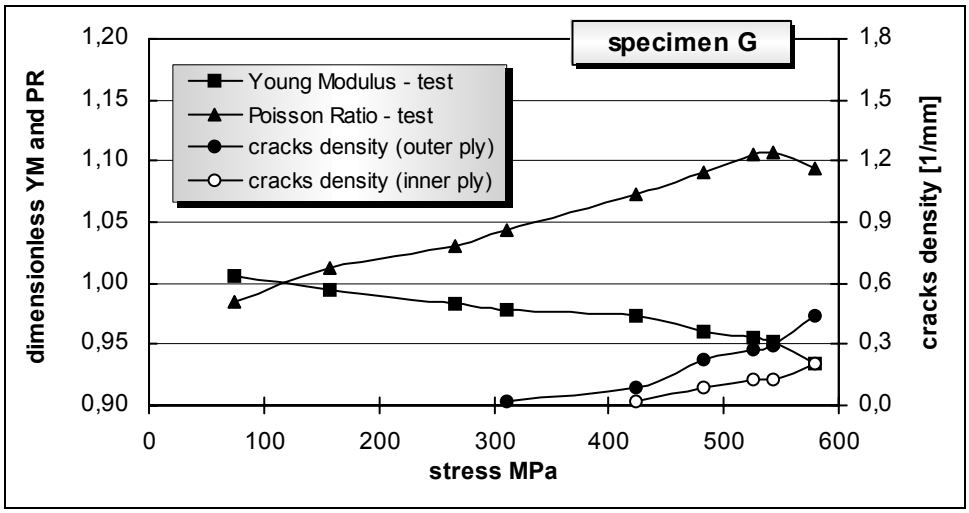

Figure 2.31. Dimensionless YM, PR and cracks density in outer and inner 50 deg plies vs. stress for specimen $[-20/20/-50_2/-20/20/50_2/-20/20]_s$

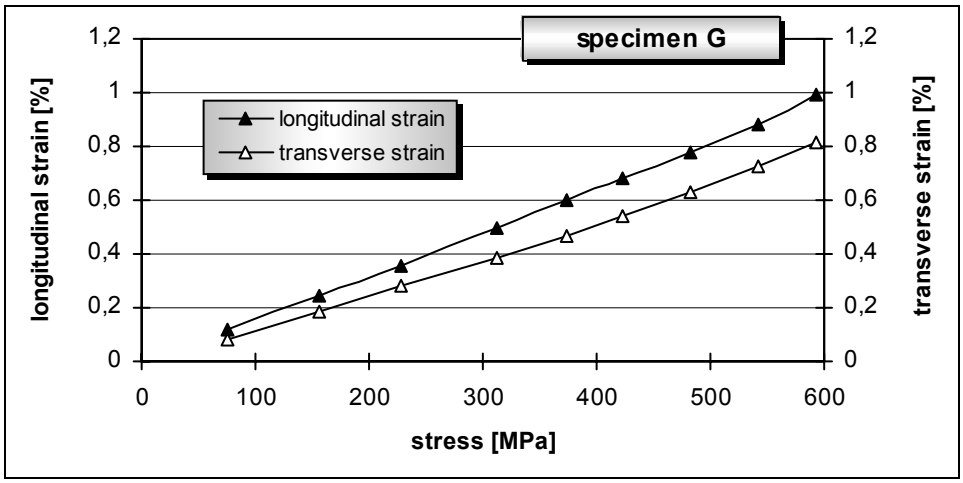

Figure 2.32. Longitudinal and transverse strains vs. stress for specimen $[-20/20/-50_2/-20/20/50_2/-20/20]_s$

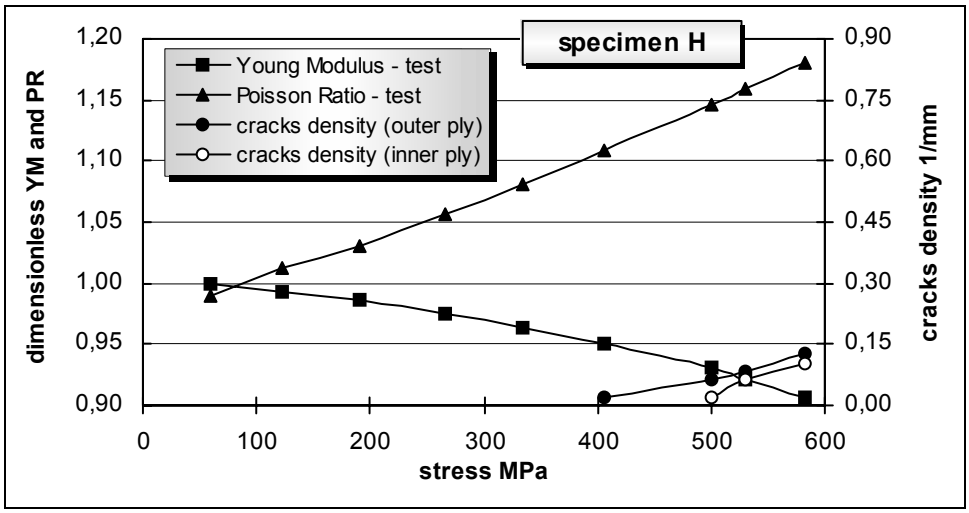

Figure 2.33. Dimensionless YM, PR and cracks density in outer and inner 40 deg plies vs. stress for specimen $[-20/20/-40_2/-20/20/40_2/-20/20]_s$

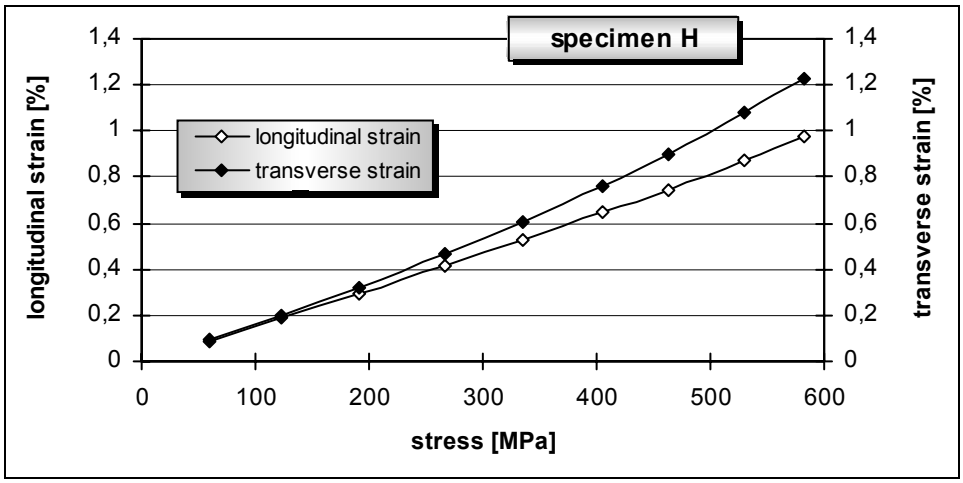

Figure 2.34. Longitudinal and transverse strains versus stress for specimen $[-20/20/-40_2/-20/20/40_2/-20/20]_s$

3. THEORETICAL PREDICTIONS VERSUS EXPERIMENTAL RESULTS

3.1. LAMINATE STIFFNESS CHANGES ESTIMATED IN FRAME OF STANDARD STRENGTH ANALYSIS

The simplest way to estimate the changes of a laminate stiffness, expressed in terms of engineering moduli, is to perform the standard strength analysis of a laminate. Such an analysis is based on the assumption that the elements of stiffness matrix of damaged ply are equal to zero – this method is generally called **P**ly **D**iscount **M**ethod (PDM). There are two approaches within PDM: in the first one it is assumed that all elements of stiffness matrix of damaged ply are equal to zero, while in the second one it is assumed that only chosen elements of stiffness matrix are equal to zero, namely those which are connected with damage mechanism responsible for ply failure. The above two approaches are called: **T**otal PDM (TPDM) and **P**artial PDM (PPDM), respectively. The PDM method must be coupled with one of the number of strength criteria for a single ply (see e.g. [47], [59], [98]). The reason is that laminate's strength analysis is in fact done at constituent plies level. The flow chart of appropriate procedure to perform calculations is shown in Figure 3.1.

An example result of PPDM analysis by utilising the Azzi-Tsai-Hill (ATH) criterion, taken from [37], [39], for specimen $[0/90_2]_s$ made of carbon/epoxy composite Torayca T300/Vicotex 174 is shown in Figure 3.2. In this figure the changes of longitudinal Young's modulus (YM) and Poisson's ratio (PR) are presented together with test data (see also Figure 2.15). The substantial differences, both quantitative and qualitative, are easily visible. It is a general observation that PDM underestimates the stiffness of a damaged laminate. The reason is that even cracked plies can still carry some loading in spite of PDM assumption of zero stiffness of those plies. This underestimation, in the example considered, reaches as much as 15% in the case of Young's modulus and 90% in the case of Poisson's ratio.

Another observation is that PDM leads to somewhat unreasonable prediction of a ”step” change of the engineering moduli instead of gradual one, as it is observed in tests.

Thus, the predictions of strength analysis with regard to the engineering moduli, thought relatively easy (but time consuming) to derive, do not give reasonable estimation of engineering characteristics.

Now, let us compare the tests data presented in a series of figures with successive odd numbers, namely from Figs 2.13–2.33, with the predictions of a theoretical model considered in Part I.

The values of dimensionless longitudinal Young's modulus (the ratio of a current value to the initial one) and Poisson's ratio for the cross-ply specimens (set #2) can be derived from eqs (139) and (141), directly.

For the angle-ply specimens (set #1) the calculations are a little more complex, as engineering moduli of interest must be derived from the general relations given by eq. (125), thus both stiffness matrices $\boldsymbol{A}^o$ and $\boldsymbol{A}^d$ have to be determined following the procedure presented in Part I. The only parameter needed in these calculations which must be taken from tests is the transverse crack density within all cracking plies. In order to construct the diagrams showing the changes of engineering moduli predicted on the basis of the proposed model we have used the values of material constants A_2, A_6, A_{10} given by eq. (150).

The results of calculations are presented in Figs 3.3–3.13, together with experimental data.

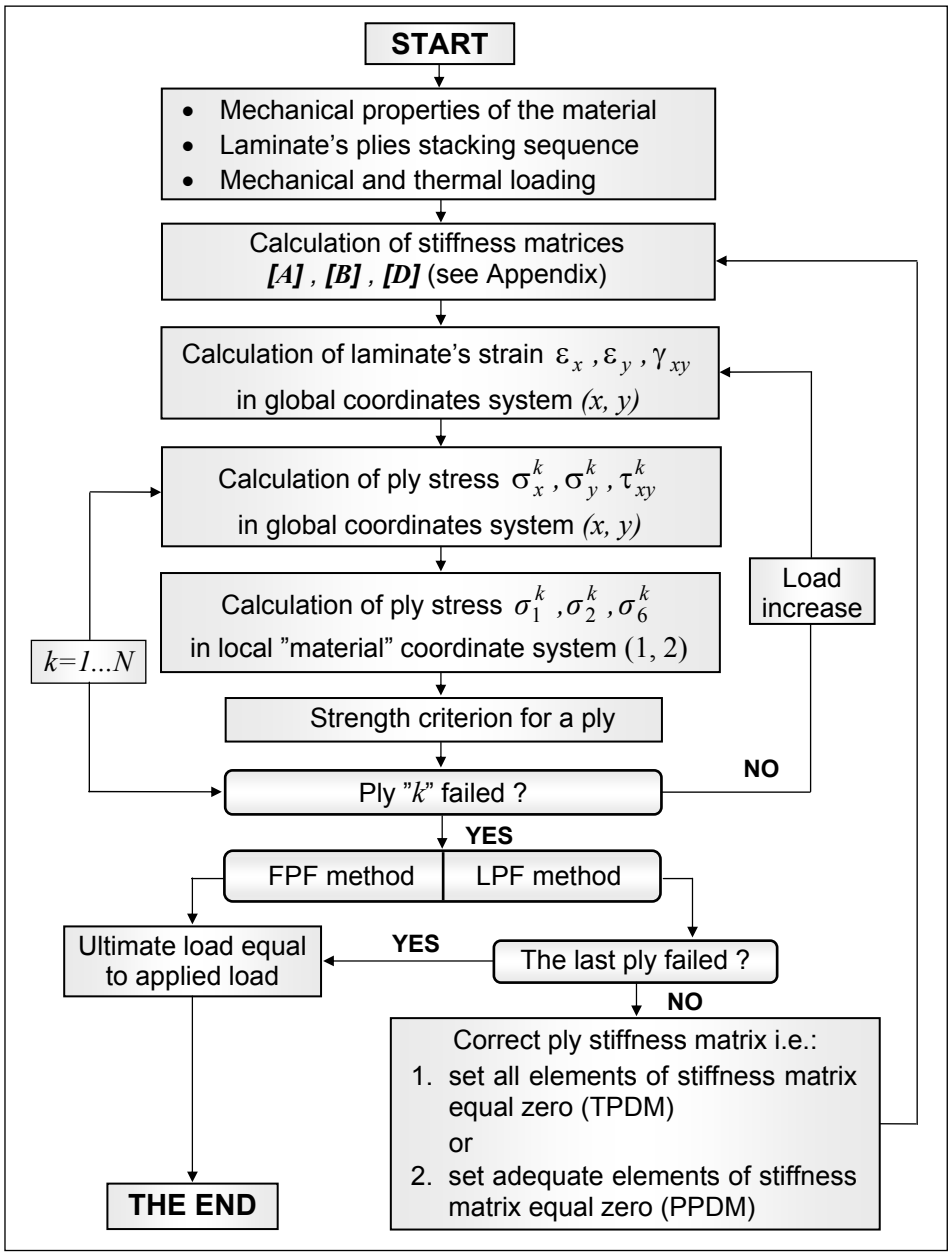

Figure 3.1. Flow chart of strength analysis of a laminate

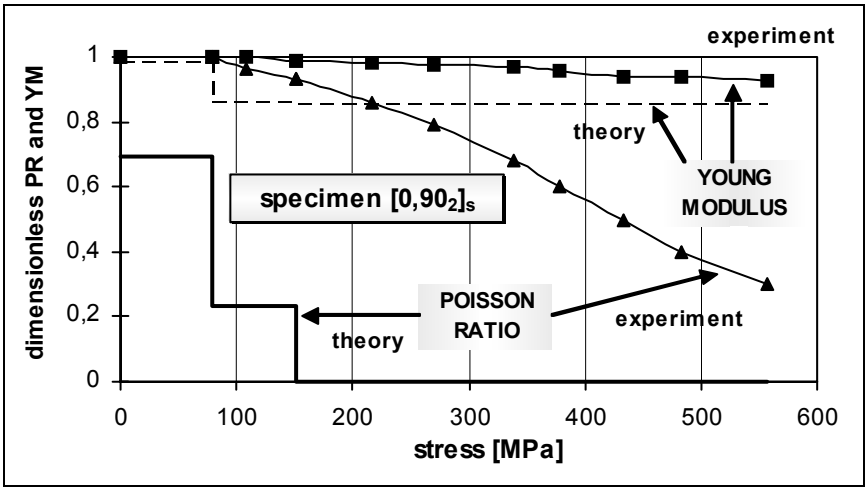

Figure 3.2. Dimensionless YM and PR – theoretical predictions (PPDM and ATH criterion) and test data for the cross-ply laminate $[0/90_2]_s$

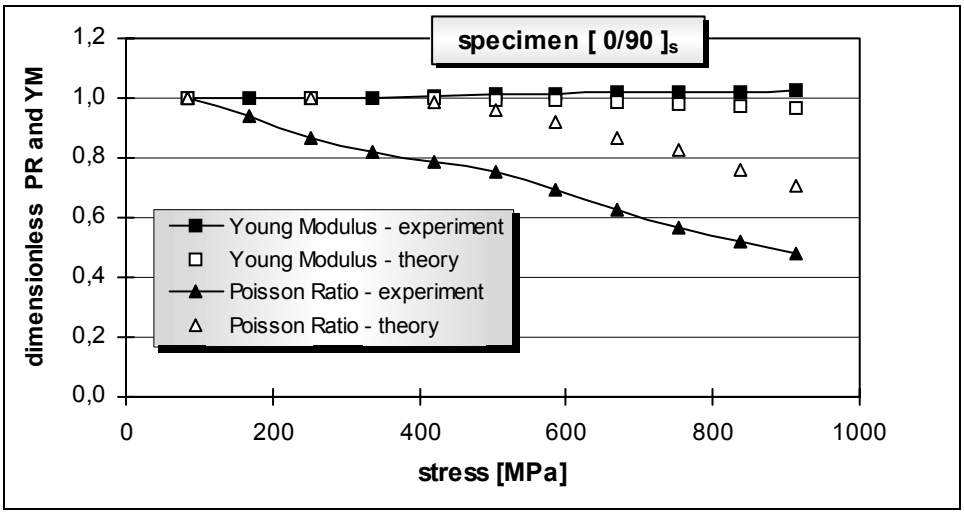

Figure 3.3. Dimensionless YM and PR – model predictions and test data for the cross-ply laminate $[0/90]_s$

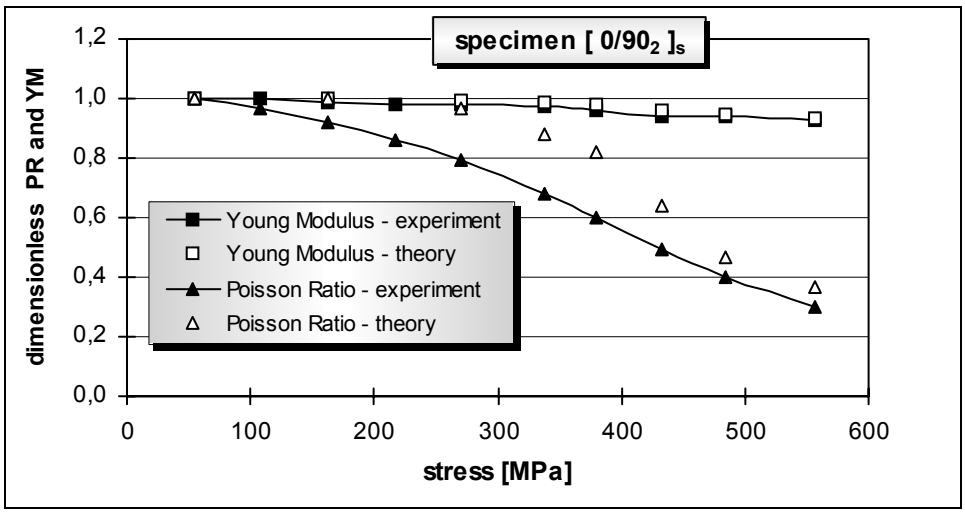

Figure 3.4. Dimensionless YM and PR – model predictions and test data for the cross-ply laminate $[0/90_2]_s$

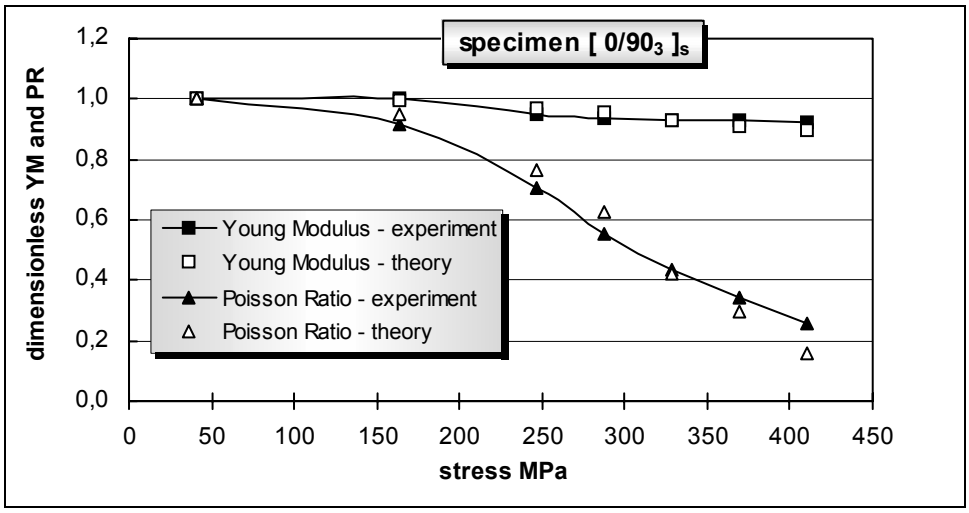

Figure 3.5. Dimensionless YM and PR – model predictions and test data for the cross-ply laminate $[0/90_3]_s$

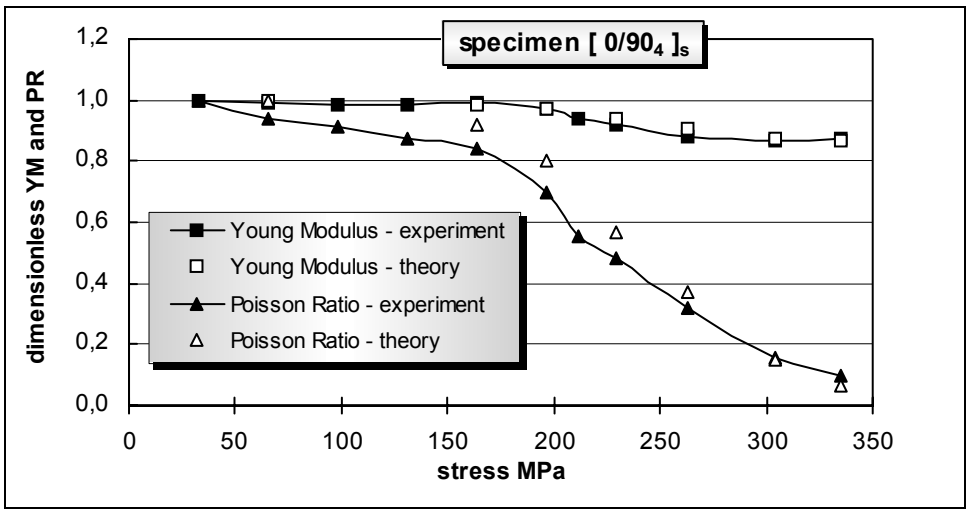

Figure 3.6. Dimensionless YM and PR – model predictions and test data for the cross-ply laminate $[0/90_4]_s$

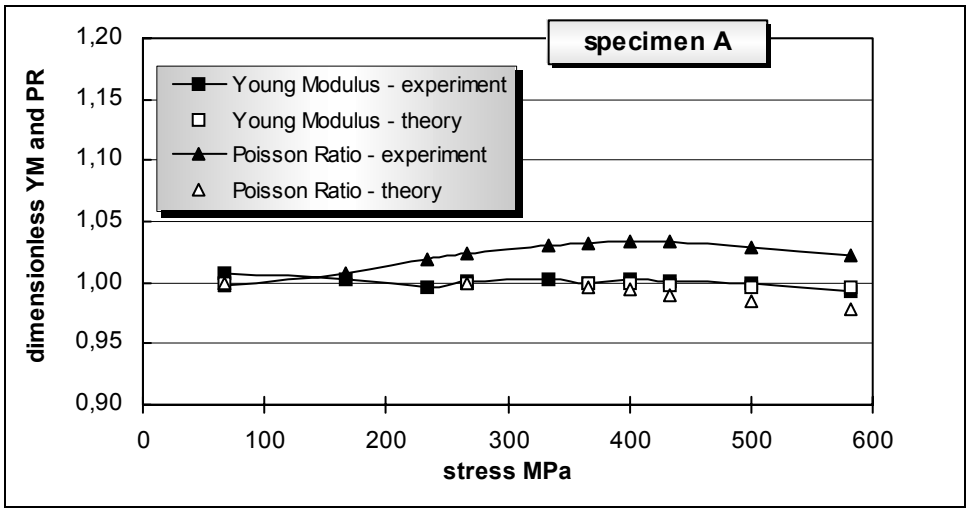

Figure 3.7. Dimensionless YM and PR – model predictions and test data for the angle-ply laminate $[-20/20/90_2/-20/20/90_2/-20/20]_s$

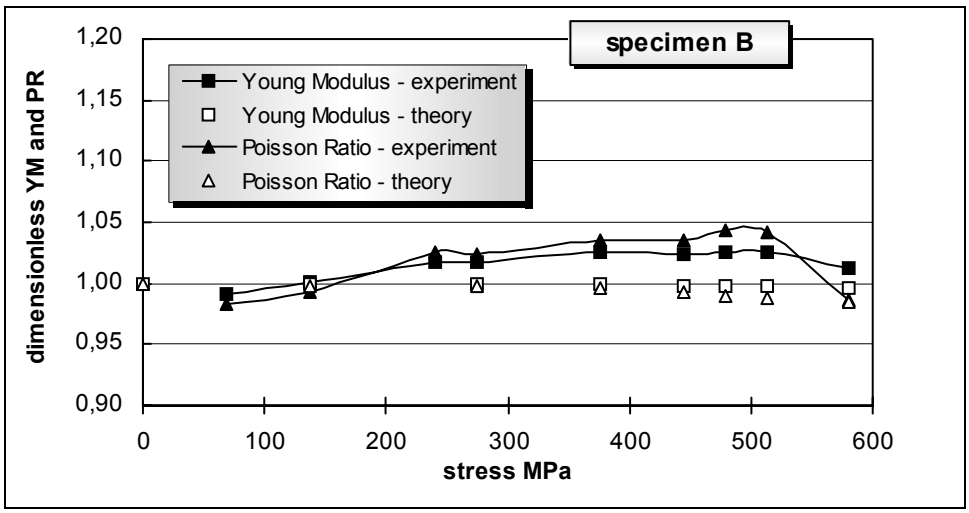

Figure 3.8. Dimensionless YM and PR – model predictions and test data for the angle-ply laminate $[-20/20/-80_2/-20/20/80_2/-20/20]_s$

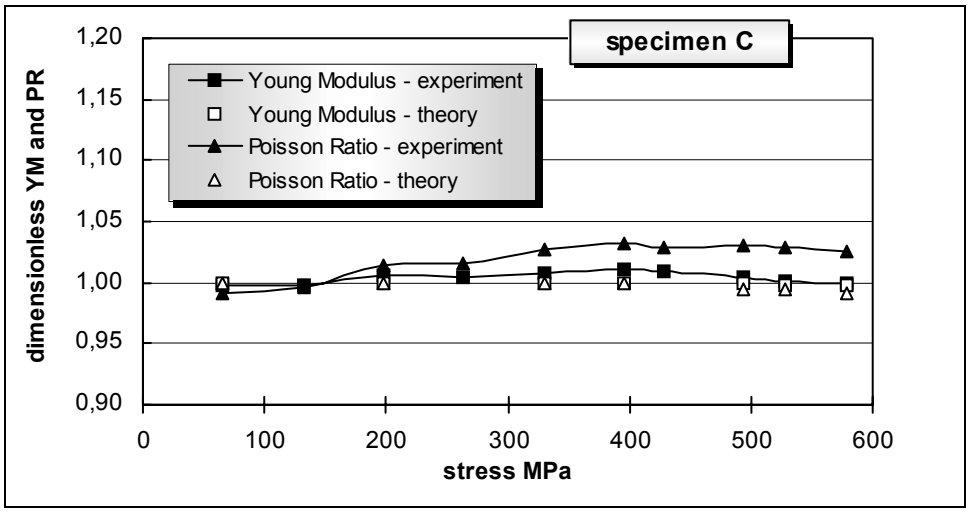

Figure 3.9. Dimensionless YM and PR – model predictions and test data for the angle-ply laminate $[-20/20/-75_2/-20/20/75_2/-20/20]_s$

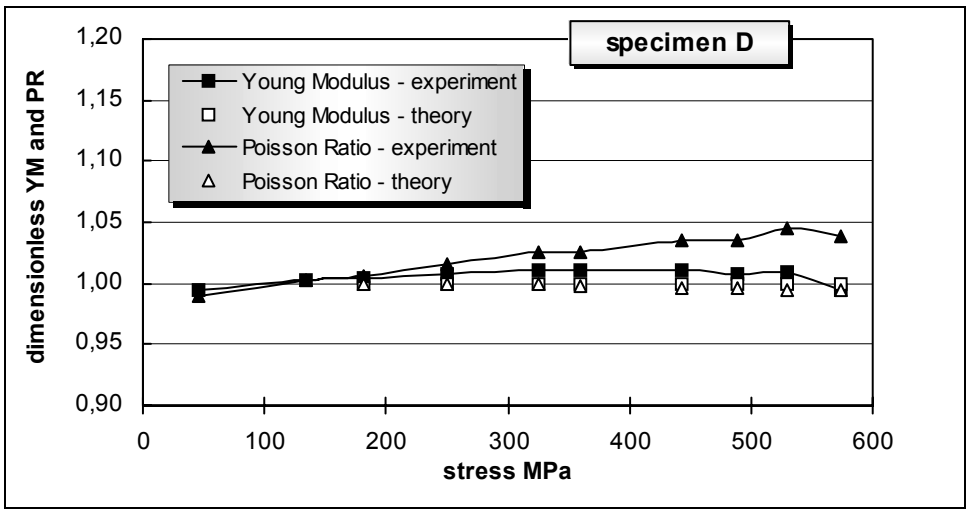

Figure 3.10. Dimensionless YM and PR – model predictions and test data for the angle-ply laminate $[-20/20/-70_2/-20/20/70_2/-20/20]_s$

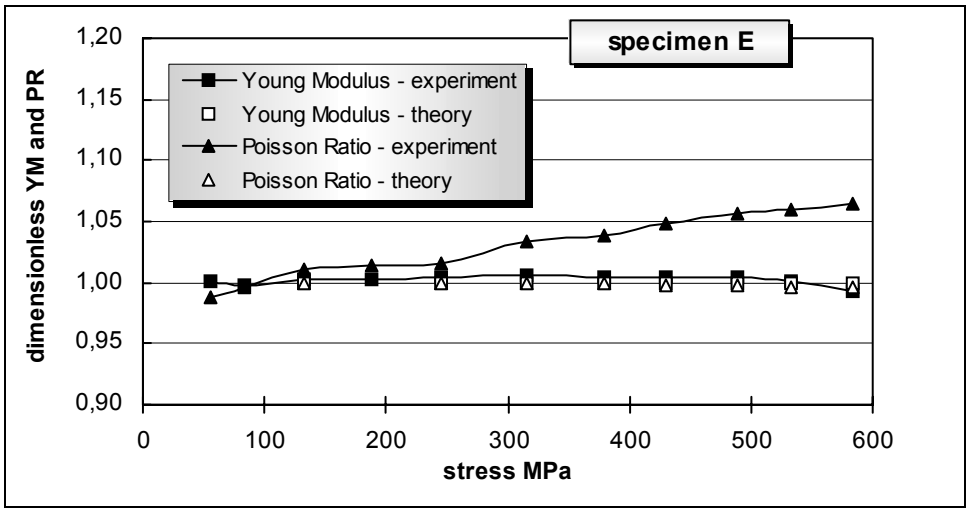

Figure 3.11. Dimensionless YM and PR – model predictions and test data for the angle-ply laminate $[-20/20/-60_2/-20/20/60_2/-20/20]_s$

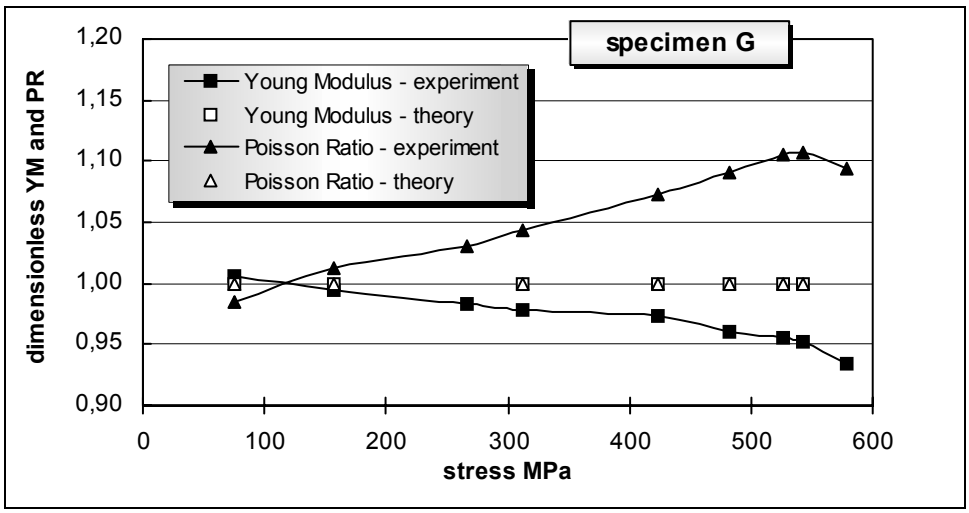

Figure 3.12. Dimensionless YM and PR – model predictions and test data for the angle-ply laminate $[-20/20/-50_2/-20/20/50_2/-20/20]_s$

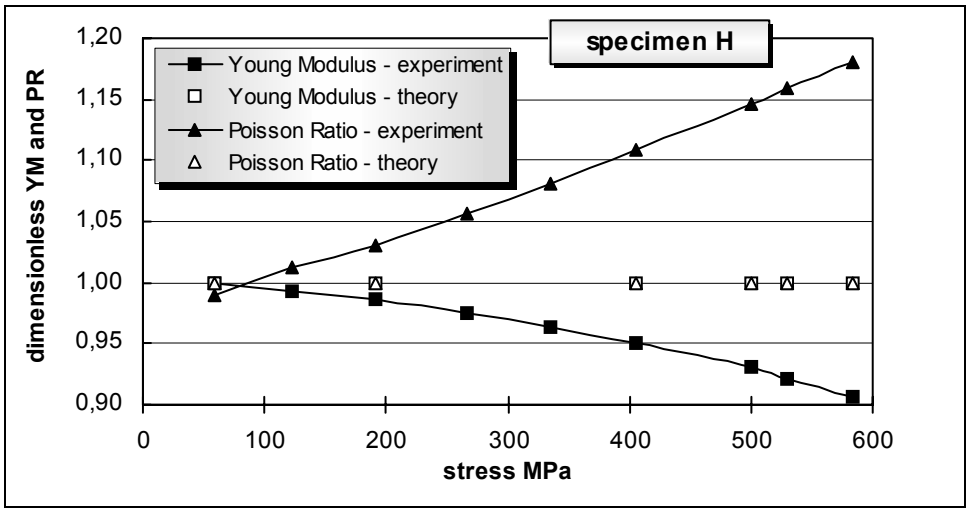

Figure 3.13. Dimensionless YM and PR – model predictions and test data for the for the angle-ply laminate $[-20/20/-40_2/-20/20/40_2/-20/20]_s$

Young's modulus predicted by the proposed theoretical model matches the test data with very good accuracy for each cross-ply specimen and for most of the angle-ply specimens. The difference between theoretical predictions and test data does not exceed in these two cases 10%. The only exceptions are specimens G and H – in that case the theoretical model is not able to predict Young's modulus decrease. Crack densities in both types of specimens are very low, especially in case of specimen H, for which single cracks have been observed only. Thus, the decrease of Young's modulus, observed experimentally, cannot be connected with the theoretically analysed transverse matrix cracking.

The proposed model for a low crack density (or no crack at all) must predict the same result as for a nearly virgin material (or entirely virgin) and, in fact, it does. We can conclude therefore that the observed mismatch does not mean that the model is unreasonable. However, in order to explain the above exceptions it probably needs further refinement and improvement.

It is an open question what the reason of Young's modulus decrease is if not a damage state. Taking into account the fact that the only difference between specimens G, H and the remaining specimens of set #1 is an angle θ one can conclude that the explanation of this phenomenon must be purely geometrical and not related to any damage mechanism.

The fitting of the calculated and measured Poisson's ratio is in general not as good as in the case of Young's modulus, but it is significantly better than that given by the partial ply discount method. It varies from specimen to specimen – the maximum difference is approx. 30%, but in most cases much less.

3.2. CONCLUSIONS

The influence of intralaminar cracks in the carbon/epoxy laminates of two orientations on strength, ultimate strains and engineering characteristics has been investigated.

Experimental data regarding engineering moduli have been compared with the theoretical predictions derived on the basis of the transverse cracking model discussed in Part I of the present publication. The analysis presented in both parts of the paper allows drawing the following conclusions:

- longitudinal strength is not influenced significantly by damage of 90° plies in cross-ply laminates and $\pm\theta_2$ plies in the other orientation considered,
- ultimate longitudinal and transverse strains are nearly independent of damage,
- the threshold stress for matrix cracking initiation is inversely related to the thickness of cracking 90° ply. For cross-ply specimens the threshold stress is approx. $0.4-0.5$ of stress at failure. It means that for the load below the threshold level the cross-ply laminate can be considered as damage-free and, as a result, the stiffness derived from CLT calculations is fully representative for laminate's behaviour,
- the first cracks in angle-ply laminates always initiate in outer plies $\pm\theta$ and the threshold stress for matrix cracking initiation, based on the behaviour of these plies, is somewhat below 0.5 of stress at failure. The value 0.4 can be regarded as a conservative estimation of the ratio of FCA to the ultimate tensile strength,
- the damage mechanisms connected with the formation of intralaminar cracks have never developed in plies inclined to the direction of external load at angle less than approx. 40°,
- for cross-ply orientation both YM and PR are reduced due to damage evolution. YM is much less sensitive to crack density than PR,
- in order to avoid the significant stiffness reduction in the cross-ply laminates under applied load in the laminates' operating range it is reasonable to separate 90° plies in groups of thin plies, instead of grouping them in one thick ply,
- in the case of specimens set # 1 the influence of developing damage on engineering characteristics is insignificant, if any. Despite the presence of damage state the growth of PR is observed. Reduction of YM is noticed for specific orientations only (defined by the angle θ less than approx. 50 °) and is probably caused by the factors other than intralaminar cracks,
- a relatively simple theoretical model of transverse matrix cracking provides quite reasonable estimation of the current values of Young's modulus and Poisson's ratio,
- stiffness changes may not always be an appropriate measure of damage state in composite laminates (it relates especially to angle-ply laminates, but not to cross-ply laminates) contrary to isotropic materials for which it is, generally, an accepted damage measure.

APPENDIX

A.1. FUNDAMENTALS OF THE CLASSICAL THEORY OF LAMINATES

The elastic properties of a single ply are defined, in general, in its principal material axis. In the case of a laminate as a collection of plies of different orientation (the directions of material axis for different plies do not coincide) it is crucial to determine these properties in one, arbitrarily chosen reference coordinate system.

Another substantial issue is to take into account the fact that constituent plies of a laminate do not form a set of separate layers, but form a "new" material in which all plies are bonded together and each of them influences the overall behaviour of the laminate.

The theory that deals with laminates and takes into consideration the above issues is called the **C**lassical **L**aminates **T**heory (CLT) (for details see e.g. [37], [66] and [134]).

The basic tool employed in CLT is the Kirchhoff-Love's hypothesis for thin plates, described elsewhere (e.g. [130]). According to this hypothesis, the strain tensor $\boldsymbol{\varepsilon}$ with restriction to the in-plane case is given by the relation:

$$\boldsymbol{\varepsilon} = \boldsymbol{\varepsilon}^{o} + z\,\boldsymbol{\kappa}^{o} \ , \tag{A.1}$$

where $\boldsymbol{\varepsilon}^{o}$ is the tensor of laminate mid-plane strains and $\boldsymbol{\kappa}^{o}$ is the tensor of mid-plane curvatures, and z denotes the coordinate along axis perpendicular to the laminate plane (through the thickness axis).
An explicit form of eq. (A.1) is as follows:

$$\begin{Bmatrix} \varepsilon_x \\ \varepsilon_y \\ \gamma_{xy} \end{Bmatrix} = \begin{Bmatrix} \varepsilon_x^o \\ \varepsilon_y^o \\ \gamma_{xy}^o \end{Bmatrix} + z \begin{Bmatrix} \kappa_x^o \\ \kappa_y^o \\ \kappa_{xy}^o \end{Bmatrix} . \tag{A.2}$$

The constitutive equation for laminate's k-th ply can be written with the use of (A.1) in the form:

$$\boldsymbol{\sigma}_k = \overline{\boldsymbol{C}}_k \, \boldsymbol{\varepsilon}^o + z \, \overline{\boldsymbol{C}}_k \, \boldsymbol{\kappa}^o \ , \tag{A.3}$$

where:

$$\boldsymbol{\sigma}_k = \begin{Bmatrix} \sigma_x \\ \sigma_y \\ \tau_{xy} \end{Bmatrix}_k \ ,$$

$$\overline{\boldsymbol{C}}_k = \begin{bmatrix} \overline{C}_{11} & \overline{C}_{12} & \overline{C}_{16} \\ \overline{C}_{12} & \overline{C}_{22} & \overline{C}_{26} \\ \overline{C}_{16} & \overline{C}_{26} & \overline{C}_{66} \end{bmatrix}_k \tag{A.4}$$

and $\overline{\boldsymbol{C}}$ denotes the transformed reduced stiffness matrix.

In order to determine the laminate stiffness matrices the concept of average laminate stresses is introduced. The average global stresses (averaged through the laminate thickness) are defined in terms of constituent plies stresses as follows:

$$\overline{\boldsymbol{\sigma}} = \frac{1}{t} \int_{-t/2}^{t/2} \boldsymbol{\sigma}_k \, dz \ , \tag{A.5}$$

where $\overline{\boldsymbol{\sigma}}$ denotes the laminate average stress tensor, $\overline{\boldsymbol{\sigma}}_k$ is the stress tensor for k-th ply and t is the laminate thickness.

It is common to use resultant forces $\boldsymbol{N}$ and moments $\boldsymbol{M}$ (with respect to unit width) instead of average stresses. The following relations define these two vectors:

$$\boldsymbol{N} = \overline{\boldsymbol{\sigma}} \, t = \int_{-t/2}^{t/2} \boldsymbol{\sigma}_k \, dz \ , \tag{A.6}$$

$$\boldsymbol{M} = \int_{-t/2}^{t/2} \boldsymbol{\sigma}_k \, z \, dz \ . \tag{A.7}$$

Taking into account the additivity property of integration, the resultant forces and moments, with the use of notation shown in Figure A.1 can be written in the form:

$$\boldsymbol{N} = \sum_{k=1}^{N} \int_{z_{k-1}}^{z_k} \boldsymbol{\sigma}_k \, dz \ , \tag{A.8}$$

$$\boldsymbol{M} = \sum_{k=1}^{N} \int_{z_{k-1}}^{z_k} \boldsymbol{\sigma}_k \, z \, dz \ . \tag{A.9}$$

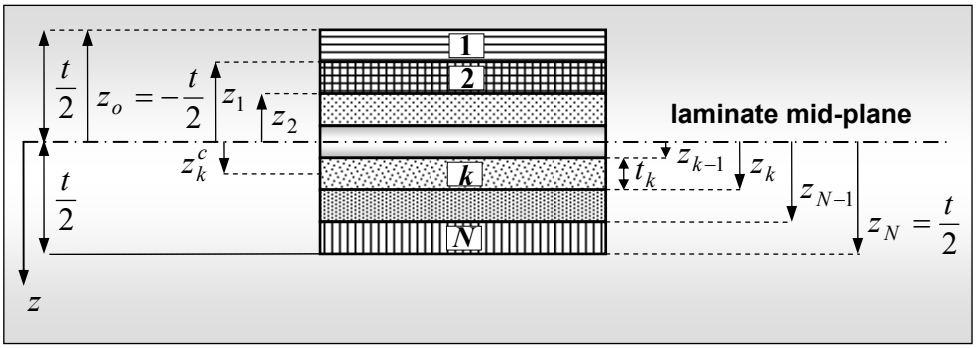

Figure A.1. Laminate cross-section

Notation used in Figure A.1 means: z_k^c – the distance to the centroid of the k-th ply, t_k – the thickness of k-th ply, t – the overall laminate thickness, N – the number of constituent plies.

Equations (A.8) and (A.9) with the use of eq. (A.3) take the following form:

$$\boldsymbol{N} = \sum_{k=1}^{N} \int_{z_{k-1}}^{z_k} \overline{\boldsymbol{C}}_k \, \boldsymbol{\varepsilon}^o \, dz + \sum_{k=1}^{N} \int_{z_{k-1}}^{z_k} \overline{\boldsymbol{C}}_k \, \boldsymbol{\kappa}^o \, z \, dz \ , \tag{A.10}$$

$$\boldsymbol{M} = \sum_{k=1}^{N} \int_{z_{k-1}}^{z_k} \overline{\boldsymbol{C}}_k \, \boldsymbol{\varepsilon}^o \, z \, dz + \sum_{k=1}^{N} \int_{z_{k-1}}^{z_k} \overline{\boldsymbol{C}}_k \, \boldsymbol{\kappa}^o \, z^2 \, dz \ . \tag{A.11}$$

Recalling that the transformed reduced stiffness matrix for any ply does not change across the ply thickness, the strains and curvatures of a laminate mid-plane are common for each ply and they are independent of the coordinate z, we derive after some calculations the following relations:

$$\boldsymbol{N} = \boldsymbol{A}\boldsymbol{\varepsilon}^o + \boldsymbol{B}\boldsymbol{\kappa}^o \ , \tag{A.12}$$

$$\boldsymbol{M} = \boldsymbol{B}\boldsymbol{\varepsilon}^o + \boldsymbol{D}\boldsymbol{\kappa}^o \ , \tag{A.13}$$

which can be written in a short form as follows:

$$\begin{Bmatrix} \boldsymbol{N} \\ \boldsymbol{M} \end{Bmatrix} = \begin{bmatrix} \boldsymbol{A} & \boldsymbol{B} \\ \boldsymbol{B} & \boldsymbol{D} \end{bmatrix} \begin{Bmatrix} \boldsymbol{\varepsilon}^o \\ \boldsymbol{\kappa}^o \end{Bmatrix} \ . \tag{A.14}$$

The matrices $\boldsymbol{A}$, $\boldsymbol{B}$ and $\boldsymbol{D}$ are symmetrical 3×3 matrices with the elements:

$$\boldsymbol{X} = \begin{bmatrix} X_{11} & X_{12} & X_{16} \\ X_{12} & X_{22} & X_{26} \\ X_{16} & X_{26} & X_{66} \end{bmatrix} \quad ; \quad \boldsymbol{X} = \boldsymbol{A} \text{ or } \boldsymbol{B} \text{ or } \boldsymbol{D} \ . \tag{A.15}$$

Matrix $\boldsymbol{A}$ is an extensional stiffness matrix, $\boldsymbol{B}$ is the coupling stiffness matrix and $\boldsymbol{D}$ is called bending stiffness matrix. They are, respectively, given by the relations:

$$\boldsymbol{A} = \sum_{k=1}^{N} \overline{\boldsymbol{C}}_k \, t_k \ , \tag{A.16}$$

$$\boldsymbol{B} = \sum_{k=1}^{N} \overline{\boldsymbol{C}}_k \, t_k \, z_k^c \ , \tag{A.17}$$

$$\boldsymbol{D} = \sum_{k=1}^{N} \overline{\boldsymbol{C}}_k \left(t_k \, z_k^{c\,2} + \frac{t_k^3}{12} \right) . \tag{A.18}$$

Let us confine the further analysis to the in-plane behaviour of the symmetrical laminates. The coupling stiffness matrix is now a zero matrix (it follows directly from the form of eq. (A.17)), therefore the coupling between bending and extension vanishes.

Besides, we assume that the only extensional loading N_x is applied to the laminate which it is a common case in experimental analysis of laminates, based on unidirectional tensile tests, see Figure A.2.

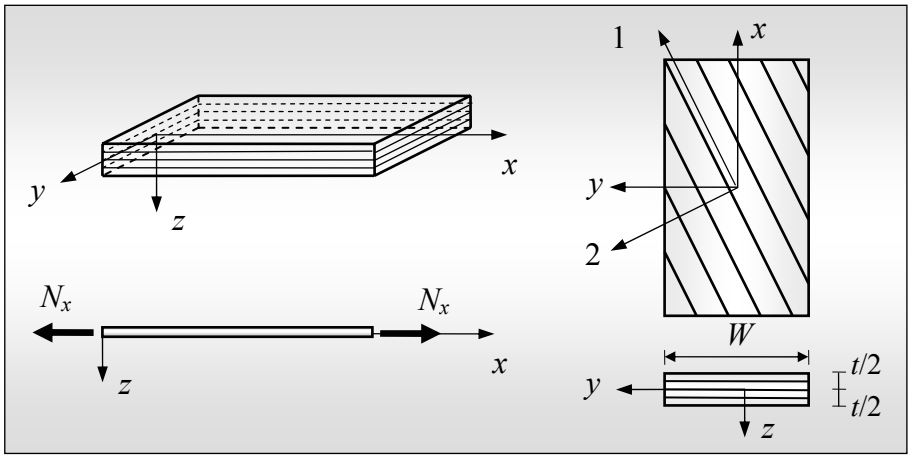

Figure A.2. Laminate under unidirectional tension

Vector $\boldsymbol{M}$ is then, by definition, a zero vector and the curvatures $\boldsymbol{\kappa}^o$ must be equal zero as well, and consequently eq. (A.12) is reduced to the relation:

$$\boldsymbol{N} = \boldsymbol{A}\boldsymbol{\varepsilon}^{o} \ . \tag{A.19}$$

Thus, in the considered case the extensional stiffness matrix $\boldsymbol{A}$ contains complete information on elastic stiffness of a laminate.

Let us notice that in the mechanics of composite laminates it is quite usual to use, the so-called normalised extensional stiffness matrix defined as follows:

$$\frac{\boldsymbol{A}}{t} = \sum_{k=1}^{N} \overline{\boldsymbol{C}}_k \, v_k \ , \tag{A.20}$$

where v_k denotes the volume fraction of k-th ply.

REFERENCES

[1] Abry J. C., Choi Y. K., Chateauminois A., Dalloz B., Giraud G., Salvia M., *In-Situ Monitoring of Damage in CFRP Laminates by Means of AC and DC Measurements*, Composites Science and Technology, Vol. 61, Issue 6, pp. 855–864, 2001.

[2] Abdelal G. F., Caceres A., Barbero E. J., *A Micro-Mechanics Damage Approach for Fatigue of Composite Materials*, Composite Structures, Vol. 56, Issue 4, pp. 413–422, 2002.

[3] Adkins J. E., *Dynamic Properties of Resilient Materials: Constitutive Equations*, Phil. Trans. Roy. Soc. A 250, pp. 519–541, 1958.

[4] Adkins. J. E., *Symmetry Relations for Orthotropic and Transversely Isotropic Materials*, Arch. Rational Mech. Anal., Vol. 4, pp. 193–213, 1959.

[5] Allen, D. H., Harris, C. E., Groves, S. E., *A Thermomechanical Constitutive Theory for Elastic Composites with Distributed Damage I. Theoretical Development*, Int. J. Solids Structures, Vol. 23, pp. 1301–1318, 1987.

[6] Allen, D. H., Harris, C. E., Groves, S. E., *A Thermomechanical Constitutive Theory for Elastic Composites with Distributed Damage II. Application to Matrix Cracking in Laminated Composites*, Int. J. Solids Structures, Vol. 23, pp. 1319–1338, 1987.

[7] Allen D. H., *Homogenization Principles and Their Application to Continuum Damage Mechanics*, Composites Science and Technology, Vol. 61, Issue 15, pp. 2223–2230, 2001.

[8] Araújo A. L., Mota Soares C. M., Moreira de Freitas M. J., Pedersen P., Herskovits J., *Combined Numerical-Experimental Model for the Identification of Mechanical Properties of Laminated Structures, Composite Structures*, Vol. 50, Issue 4, pp. 363–372, 2000.

[9] Araújo dos Santos J. V., Mota Soares C. M., Mota Soares C. A., Pina H. L. G., *Development of a Numerical Model For the Damage Identification on Composite Plate Structures*, Composite Structures, Vol. 48, Issues 1–3, pp. 59–65, 2000.

[10] Azzi, V. D., Tsai, S. W., *Anisotropic Strength of Composites*, Experimental Mechanics, Vol. 5, pp. 283–288, 1965.

[11] Bai QS; Murakami Sumio; Kanagawa Yasushi; Tanaka Kohhei, *A Damage Model for FRP Laminates with Matrix Microcracks and Delamination*, JSMS Original paper, Vol. 46, No.8, pp.981–989, 1997.

[12] Barbero E. J., Lonetti P., *Damage Model for Composites Defined in Terms of Available Data*, Mechanics of Composite Materials and Structures, 8 (4), pp. 299–316, 2001.

[13] Beaumont P. W., R., *The Mechanics of Damage in Structural Composite Materials,* Fracture and Damage Mechanics of Composite Materials, Technomic Publishing AG, 1992.

[14] Benveniste Y., *A New Approach to Application of Mori and Tanaka's Theory in Composite Materials*, Mechanics of Materials, 6, pp. 147–157, 1987.

[15] Berbinau P., Filiou C., Soutis C., *Stress and Failure Analysis of Composite Laminates with an Inclusion under Multiaxial Compression-Tension Loading*, Applied Composite Materials**,** 8 (5), pp. 307–326, 2001.

[16] Boehler J. P., *A Simple Derivation of Representations for Non-Polynomial Constitutive Equations in Some Cases of Anisotropy*, ZAMM 59, pp. 157–167, 1979.

[17] Bressers, J., *Electronic Equivalents Not Plastic Replicas*, Laboratory & Analysis Technology Int., pp. 71–72, 1991.

[18] Bruner Y., Jeulin D., Renard J., Thionett A., *Probabilistic Modelling of Composite Laminate Damage*, Premier Congres Interdisciplinaire sur les Materiaux en France, „Materiaux 2002", Tours, 21–25 Octobre, 2002.

[19] *CERF Report „Gap Analysis for Durability of Fiber Reinforced Polymer Composites in Civil Infrastructure"*, 2001,

Internet: http://www.cerf.org/pdfs/collab/durability/7.pdf.

[20] Chrzanowski M., *Use of the Damage Concept in Describing Creep-Fatigue Interaction under Prescribed Stress*, Int. J. Mech. Sc. Vol. 18, pp. 69–73, 1976.

[21] Chrzanowski M., *Damage Parameter in Continuum Damage Mechanics* (in Polish), Mechanika Teoretyczna i Stosowana, Vol. 16, No. 2, pp. 151–167, 1978.

[22] Chrzanowski M., *Strain Energy Governed Damage Law For a Visco-Plastic Material*, Eng. Trans, 39, 3–4, pp. 389–418, 1991.

[23] Chrzanowski M., *Lectures on Continuum Damage Mechanics*, 1992, **Internet:** http://limba.wil.pk.edu.pl/kwm–edu.html.

[24] Chrzanowski M., German J., *Model of Fracture of a Strip with Hole under Tension*, Eng. Trans. 33, 1–2, pp. 194–203 (in Polish), 1985.

[25] Chrzanowski M., German J., *Creep Crack Propagation in The Presence of Dispersed Damage*, Proc. 9th Congress on Material Testing, pp. 170–174, Budapest 1986.

[26] Chrzanowski M., German J., Grabias M., *Damage Growth in the Presence of Stress Concentrators*, Proc. 1st Workshop on Influence of Local Stress and Strain Concentrators on the Reliability and Safety of Structures, Miskolc, Hungary, pp. 122–130, 1995.

[27] Coleman B. D., Gurtin M. E., *Thermodynamics with Internal State Variables*, J. Chemical Physics, 47, pp. 597–613, 1967.

[28] Deliktas B., Voyiadjis, *Comparison of the Method of Cells with the Mori-Tanaka in Predicting Damaged Elasto-Plastic Behaviour of Laminated Composite Materials*, Fourteenth Engineering Mechanics Conference, ASCE, Austin**,** Texas 2000,

Internet: http://www.ce.utexas.edu/em2000/em2000.pdf.

[29] Desrumaux F., Meraghni F., Benzeggagh M. L., *Micromechanical Modelling Coupled to a Reliability Approach for Damage Evolution Prediction in Composite Materials*, Applied Composite Materials, **7** (4), pp. 231–250, 2000.

[30] Dirikolu Hüsnü M., Aktaş Alaattin, *Analytical and Finite Element Comparisons of Stress Intensity Factors of Composite Materials*, Composite Structures, Vol. 50, Issue 1, pp. 99–102, 2000.

[31] Fiedler B., Hojo M., Ochiai S., Schulte K., Ochi M., *Finite-element Modelling of Initial Matrix Failure in CFRP Under Static Transverse Tensile Load*, Composites Science and Technology, Vol. 61, Issue 1, pp. 95–105, 2001.

[32] Gdoutos E. E., *Fracture Mechanics – an Introduction*, Kluwer Academic Publ., 1993.

[33] German J., Chrzanowski M., *Crack Behaviour in Visco-elastic Body with the Damage Field*, Trans. SMIRT-9 Conf., Vol. L, pp. 489–494, 1987.

[34] German J., *Crack Behaviour in Visco-elastic Body with the Damage Field*, PhD Thesis, Politechnika Krakowska (in Polish), 1987.

[35] German J., *Experimental Analysis of Intralaminar Damage in CFRP Vicotex NCHR 174B Laminates*, Zeszyty Naukowe Politechniki Świętokrzyskiej, Mechanika 56, pp. 175–182 (in Polish), 1995.

[36] German J., *Intralaminar Damage in Fiber-Reinforced Polymeric Matrix Laminates*, in: Materials Ageing and Component Life Extension, Vol. I, ed.: V. Bicego *et al*., Engineering Materials Advisory Services Ltd., U.K. ISBN 0 947817 84 0, pp. 155–164, 1995.

[37] German J., *Fundamentals of the Mechanics of Composite Materials*, Wydawnictwo Politechniki Krakowskiej, ISBN 83–903878–4–0, pp. 282 (in Polish), 1996, **Internet:** http://limba.wil.pk.edu.pl/~jg/kompozyt/.

[38] German J., *A CDM Approach to the Intralaminar Matrix Cracks in Composite Laminates*, Zeszyty Naukowe Politechniki Świętokrzyskiej, Mechanika 62, pp. 147–154 (in Polish), Kielce 1997.

[39] German J., *On Strength of Composite Laminates*, (general lecture), Konferencja Krajowa „Komputerowe wspomaganie projektowania kompozytów do celów cywilnych i wojskowych", Oficyna Wydawnicza Politechniki Warszawskiej, pp. 43–64 (in Polish), Warszawa 1999.

[40] German J., *Stiffness Changes in CFRP Laminates due to Intralaminar Damage*, Zeszyty Naukowe Politechniki Świętokrzyskiej, Mechanika 68, pp. 129–140 (in Polish), Kielce 1999.

[41] German J., *Stiffness Changes in Fiber-Reinforced Polymeric Matrix Laminates Caused by Intralaminar Damage*, Przegląd Mechaniczny, SIMP, 5–6/00, pp. 13–17 (in Polish),Warszawa 2000.

[42] German J., *Stiffness Changes in Fiber-Reinforced Polymeric Matrix Laminates caused by Intralaminar Damage*, ECF 14, Fracture Mechanics Beyond 2000, Vol. I/III, ed.: A. Neimitz *et al*., EMAS Publications U.K., pp. 599–606, 2002.

[43] German J., *Constitutive Relation for an Orthotropic Body with Damage*, Zeszyty Naukowe Politechniki Świętokrzyskiej, Mechanika 78, pp. 153–162, Kielce, 2003.

[44] German J., *Damage Influence on Mechanical Properties of Composite Laminates*, (general lecture), IV Szkoła Kompozytów „Współczesne zagadnienia mechaniki materiałów i konstrukcji kompozytowych", Oficyna Wydawnicza Politechniki Warszawskiej, pp. 103–121 (in Polish), 2003.

[45] German J., *Constitutive Relation for an Orthotropic Body with Damage*, Archive of Mechanical Engineering, (to be published), 2004.

[46] German J., *The Influence of Intralaminar Damage of Fiber-Reinforced Polymeric Matrix Laminates on Their Mechanical Properties*, Engineering Transactions, (to be published), 2004.

[47] Gołaski L., *Failure Criteria for Laminates under Combined Loading Conditions*, Joint Seminary on Failure of Advanced Materials, Paris, (Ed. by D. François, L. Gołaski), Wyd. Politechniki Świętokrzyskiej, pp. 37–61, 1996.

[48] Gudmundson P., Östlund S., *First Order Analysis of Stiffness Reduction Due to Matrix Cracking*, J. Composite Materials, pp. 1009–1030, 1992.

[49] Gudmundson P., Zang W., *An Analytical Model for Thermoelastic Properties of Composite Laminates Containing Transverse Matrix Cracks*, Int. J. Solids Structures, Vol. 30, No 23, pp. 3211–3231, 1993.

[50] Gudmundson P., Alpman J., *Initiation and Growth Criteria for Transverse Matrix Cracks in Composite Laminates*, Composites Science and Technology, Vol. 60, Issue 2, pp. 185–195, 2000.

[51] Gurtin M. E., *Modern Continuum Thermodynamics*, Mechanics Today, ed. Nemat-Nasser, Vol.1, Pergamon Press Inc., 1972.

[52] Hashin Z., *Analysis of Cracked Laminates: A Variational Approach*, Mechanics of Materials, 4, pp. 121–136, 1985.

[53] Hashin Z., *Analysis of Orthogonally Cracked Laminates under Tension*, J. Applied Mechanics, 54, pp. 872–136, 1987.

[54] Hayhurst D. R., Brown P. R., Morrison C. J., *The Role of Continuum Damage in Creep Crack Growth*, Phil. Trans. Roy. Soc. London, A 311, pp. 131–158, 1984.

[55] Heslehurst Rikard B., *Off-axis Transformation of the Composite Laminate Stiffness Properties*, Composite Structures, Vol. 35, No. 4, pp. 369–374, 1996.

[56] Hill R., *A Self Consistent Mechanics of Composite Materials*, J. Mech. Phys. Solids, Vol. 13, pp. 213–222, 1965.

[57] Highsmith A. L., Reifsnider K. L., *Stiffness-Reduction Mechanisms in Composite Laminates*, Damage in Composite Materials, ASTM STP 775, Ed. Reifsnider K. L., American Society for Testing and Materials, pp. 103–117, 1982.

[58] Hoover J., Kujawski D., Ellyin F., *Transverse Cracking of Symmetric and Unsymmetric Glass-Fibre/Epoxy Resin Laminates,* Composites Science and Technology, Vol. 57, pp. 1513–1526, 1997.

[59] Hult, J., Rammerstorfer, F. G., (eds.), *Engineering Mechanics of Fibre Reinforced Polymers and Composite Structures*, Springer-Verlag, Wien - New York, 1994.

[60] Janson J., Hult J., *Fracture Mechanics and Damage Mechanics - a Combined Approach*, J. de Méc. Appl., Vol. 1, No. 1, pp. 69–84, 1977.

[61] Jansson N. E., Larsson R., *A Damage Model for Simulation of Mixed-Mode Delamination Growth*, Composite Structures, Vol. 53, Issue 4, pp. 409–417, 2001.

[62] Jiang Dazhi, Shen Wei, Wang Xingye, *Damage Constitutive Equations and its Application to Fiber Reinforced Composites under Transverse Impact*, Applied Composite Materials, 9 (5), pp. 315–329, 2002.

[63] Joffe R., Varna J., *Analytical Modelling of Stiffness Reduction in Symmetric and Balanced Laminates due to Cracks in 90 Layers*, Composites Science and Technology, Vol. 59, pp. 1641–1652, 1999.

[64] Joffe R., Krasnikovs A., Varna J., *COD-based Simulation of Transverse Cracking and Stiffness Reduction in* $[S/90_n]_s$ *Laminates*, Composites Science and Technology, Vol. 61, Issue 5, pp. 637–656, 2001.

[65] Jose S., Ramesh Kumar R., Jana M. K., Venkateswara Rao G., *Intralaminar Fracture Toughness of a Cross-Ply Laminate and its Constituent Sub-Laminates*, Composites Science and Technology, Vol. 61, Issue 8, pp. 1115–1122, 2001.

[66] Jones R. M., *Mechanics of Composite Materials*, McGraw-Hill Kogakusha Ltd., 1975.

[67] Kachanov L. M., *On the Time to Rupture in Creep Conditions*, Izv. AN SSSR, Otd. Tekhn. Nauk, 8, pp. 26–31 (in Russian), 1958.

[68] Kachanov M., *Continuum Model of Medium with Cracks*, J. of Eng. Mech. Division, Proc. of ASCE, Vol. 106, No EM5, pp. 1039–1051, 1980.

[69] Kashtalyan M., *Investigation of Matrix Cracking and Delamination in Composite Plates with a Hole Under Biaxial Loading*, Research Project, 2001, **Internet:** http://www.eng.abdn.ac.uk/~eng679/

Internet: http://www.eng.abdn.ac.uk/staff/MK.html.

[70] Kashtalyan M., Soutis C., *Modelling Stiffness Degradation due to Matrix Cracking in Angleply Composite Laminates*, Plastics, Rubber and Composites, pp. 482–488, 29, (9), 2000.

[71] Kato Tetsuji, Kageyama Kazuro, Kimpara Isao, Ohsawa Isamu, Kanai Makoto, Abe Satoshi, Masuda Yasuhisa, *Analysis of Initiation and Extension of Transverse Lamina cracking in Multidirectionally Laminate of Composites by Total Force Method-Finite Element Method*, Key Engineering Materials, Vols. 243–244, pp. 69–74, Trans Tech Publication, 2003, **Internet:** http://www.scientific.net.

[72] Kilic H., Haj-Ali Rami, *Elastic-degrading Analysis of Pultruded Composite Structures*, Composite Structures, Vol. 60, Issue 1, pp. 43–55, 2003.

[73] Kuriakose S., Talreja R., *Matrix Cracking in Cross-Ply Laminates Under Bending*, Proceedings of the 17th American Society for Composites Technical Conference, Lafayette, IN, CRC Press, 3848 FAU Blvd., Boca Raton, FL, 33431, Oct. 21–23, 2002.

[74] Kwon Y. W., Craugh L. E., *Progressive Failure Modelling in Notched Cross-Ply Fibrous Composites*, Applied Composite Materials, 8 (1), pp. 63–74, 2001.

[75] Ladevèze P., Lubineau G., *On a Damage Mesomodel for Laminates Micro-Meso Relationships, Possibilities and Limits*, Composites Science and Technology, Vol. 61, Issue 15, pp. 2149–2158, 2001.

[76] Lavoie J. A., *Scaling Effects on Damage Development, Strength, and Stress-Rupture Life of Laminated Composites in Tension*, Ph.D. Thesis, Virginia Polytechnic Institute and State University, 1997,

Internet: http://scholar.lib.vt.edu/theses/available/etd–4131162939721181/unrestricted/etd_full.pdf.

[77] Laws N., Dvorak G. J., Hajazi M., *Stiffness Changes in Unidirectional Composites Caused by Crack Systems*, Mechanics of Materials, 2, pp. 123–137, 1983.

[78] Lekhnitski S. G., *Theory of Elasticity of an Anisotropic Elastic Body*, Holden-Day, San Francisco, 1963.

[79] Lemaitre J., Dufailly J., *Damage Measurements*, Eng. Fracture Mech., Vol. 28, No.5/6, pp.643–661, 1987.

[80] Lemaitre J., *Damage Mechanics*, Summer School on Failure in Structures, under TEMPUS JEP 8098 Fracture Mechanics in Engineering Curricula, Chapter 3, J. German, K. Nowak (Eds.), Wyd. Politechniki Świętokrzyskiej, Kielce, PL ISSN 0239–4979, 1997.

[81] Lim S. G., Hong C. S., *Prediction of Transverse Cracking and Stiffness Reduction in Cross-Ply Laminated Composites*, J. Composite Materials, pp. 695–713, 1989.

[82] Litewka A., *Effective Material Constants for Orthotropically Damaged Elastic Solid*, Arch. Mech., 37, pp. 631–642, 1985.

[83] Litewka A., Bogucka J., Dębiński J., *Analytical and Experimental Study of Damage Induced Anisotropy of Concrete*, Foundations of Civil and Environmental Engineering, No. 2, pp. 101–124, Publishing House of Poznan University of Technology, ISSN 1642–9303, 2002.

[84] Litewka A., Bogucka J., Dębiński J., *Anisotropic Behaviour of Damaged Concrete and Fiber Reinforced Concrete*, Lecture Notes in Applied and Computational Mechanics, Vol. 9, Anisotropic Behaviour of Damaged Materials, Jacek J. Skrzypek, Artur W. Ganczarski (Eds.), pp. 185–219, Springer Verlag, ISBN 3–540–00437–8, 2003.

[85] Liu C. J., Sterk J. C., Nijhof A. H. J., Marissen R., *Matrix-Dominated Damage in Notched Cross-Ply Composite Laminates: Experimental Observations*, Applied Composite Materials, 9 (3), pp. 155–168, 2002.

[86] Liu C. J., Nijhof A. H. J., Ernst L. J., Marissen R., *Progressive Failure Modelling of Transverse Cracking in Cross-ply Laminates with Double-*

Edge-Semicircular Notches, Engineering Transactions, Vol. 50, No. 4, 2002.

[87] Liu S., Nairn J. A., *Fracture Mechanics Analysis of Composite Microcracking: Experimental Results in Fatigue*, Proceedings of the 5th Technical Conference on Composite Materials, American Society of Composites, East Lansing, Michigan, pp. 287–295, June 11–14, 1990.

[88] Liu Yong-mei, *Anisotropic Damage Evolution in Ceramic Matrix Composites*, Ph.D. Dissertation, University of Virginia 1997, **Internet:** http://www.ipm.virginia.edu/process/Con/Pubs/thesis21/chapter5.pdf.

[89] Lombardi A. V., *A Meso-Macro Model for a Damage Tolerance Analysis of Composite Structures*, Composite Structures, Vol. 59, Issue 1, pp. 37–43, 2003.

[90] Lundmark P., Varna J., *Modelling Thermo-Mechanical Properties of Damaged Laminates*, Key Engineering Materials Vols. 251–252, pp. 381–388, Trans Tech Publication, 2003,
Internet: http://www.scientific.net.

[91] Mattei Ch., *Non-destructive Technique for On-Site Stiffness Determination of Composite Laminates*, CSM Materialteknik AB, 2003, **Internet:** www.csm.se/csm_swe/html/processer/ofp/ndt_care/ndt_pdf/stiffnessmeasurement.pdf.

[92] Mori T., Tanaka K., *Average Stress in Matrix and Average Elastic Energy of Materials with Misfitting Inclusions*, Acta Metallurgica, Vol. 21, No. 5, pp. 571–574, 1973.

[93] Muc A., Krawiec Z., *Design of Composite Plates Under Cyclic Loading*, Composite Structures, Vol. 48, Issues 1–3, pp. 139–144, 2000.

[94] Naik N. K., Nemani Bulliraju, *Initiation of Damage in Composite Plates under Transverse Central Static Loading*, Composite Structures, Vol. 52, Issue 2, pp. 167–172, 2001.

[95] Nairn J A., Shoufeng Hu, *The Formation and Effect of Outer-Ply Microcracks in Cross-Ply Laminates: A Variational Approach*, Engineering Fracture Mechanics, 41, pp. 203–221, 1992.

[96] Nairn J. A., *Matrix Microcracking in Composites*, Polymer Matrix Composites, Chapter 13, R. Talreja, J-A. Månson (eds.), Volume 2 of Comprehensive Composite Materials, A. Kelly and C. Zweben, (eds.), Elsevier Science, 2000.

[97] Nairn J. A., *Fracture mechanics of composites with residual stresses, imperfect interfaces, and traction-loaded cracks*, Composites Science and Technology, Vol. 61, Issue 15, pp. 2159–2167, 2001.

[98] Neimitz A., *The Review of the Failure Criteria for Composites*, Joint Seminary on Failure of Advanced Materials, Paris, (Ed. by D. François, L. Gołaski), Wyd. Politechniki Świętokrzyskiej, pp. 5–25, 1996.

[99] Ogihara Shinji, Kobayashi Satoshi, Takeda Nobuo, Kobayashi Akira, *Damage Mechanics Characterization of Transverse Cracking Behavior in High-Temperature CFRP Laminates*, Composites Science and Technology, Vol. 61, Issue 8, pp. 1049–1055, 2001.

[100] Oñate E., Oller S., Botello S., Canet J. M., *Metodos Avanzados de Calculo de Estructuras de Materiales Compuestos*, Cento Internacional de Metodos Numericos en Ingenieria, Barcelona, España, Monografia CIMNE No. 3, 1991.

[101] Pagano N. J., Yuan F. G., *The Significance of Effective Modulus Theory (Homogenization) in Composite Laminate Mechanics*, Composites Science and Technology, Vol. 60, Issues 12–13, pp. 2471–2488, 2000.

[102] Phifer Stephen P., *Quasi-Static and Fatigue Evaluation of Pultruded Vinyl Ester/E-Glass Composites*, M. Sc. Thesis, Virginia Polytechnic Institute and State University, 1998, **Internet:** http://scholar.lib.vt.edu/theses/available/etd–013199–185939/.

[103] Praveen G., Reddy J. N., *Transverse Matrix Cracks in Cross-Ply Laminates: Stress Transfer, Stiffness Reduction and Crack Opening Profiles*, Acta Mechanica, Vol. 130, No. 3–4, pp. 227–248, 1998.

[104] Pyrz R., *Governing Equations for the Steady State Creep in Orthotropic Materials*, Acta Mechanica, 68, pp. 251–263, 1987.

[105] Rabotnov J. N., *On a Mechanism of Delayed Fracture*, Vopr. Proch. Mat. Kontr., Izd. AN SSSR 5-7 (in Russian), 1959.

[106] Rapp H., Wedemeyer P., *Determination of Stiffness Characteristics of ±45 Degree GFRP-Laminates*, Experimental Mechanics; Advances in Design, Testing and Analysis, I.M. Allison (ed.); A.A. Balkema, Rotterdam, 1998.

[107] Rapp H., Research Project Report *„Experimental Determination of the Young's Modulus of ±45° Composite Laminates*", 1997, **Internet:** http://mlbf01.fbm.hs–bremen.de/foerg/emod45/emod_erg.html.

[108] Rebière J.-L., Maâtallah M.-N., Gamby D., *Initiation and Growth of Transverse and Longitudinal Cracks in Composite Cross-ply Laminates*, Composite Structures, Vol. 53, Issue 2, pp. 173–187, 2001.

[109] Rebière J.-L., Maâtallah M.-N., Gamby D., *Analysis of Damage Mode Transition in a Cross-Ply Laminate Under Uniaxial Loading*, Composite Structures, Vol. 55, Issue 1, pp. 115–126, 2002.

[110] Reifsnider K. L., Henneke E. G., Stinchcomb W. W., Duke J. C., *Damage Mechanics and NDE of Composite Laminates*, Mechanics of Composite

Materials, Recent Advances, eds. Z. Hashin and C. T. Herakovich, Pergamon Press, pp. 399–420, 1983.

[111] Reifsnider Kenneth L., *Summary of Activities*, updated in Nov. 2002, **Internet:** www.ctfuelcell.uconn.edu/pdf/CGFCCReifCV.pdf.

[112] Rippert L., Wevers M., Van Huffel S., *Optical and Acoustic Damage Detection in Laminated CFRP Composite Materials*, Composites Science and Technology, Vol. 60, Issue 14, pp. 2713–2724, 2000.

[113] Rivlin R. S., Phil. Trans. Roy. Soc., A 241, 379, 1948.

[114] Rivlin R. S., Ericksen J. L., *Stress-Deformation Relations for Isotropic Materials*, J. Rational Mech. Anal., Vol. 4, pp. 323–425, 1955.

[115] Roy S., Benjamin M., *Modelling of Opening Displacement of Transverse Cracks in Graphite-Epoxy Laminates Using Shear Lag Analysis*, American Society for Composites, Paper 023, Oct. 2002.

[116] Roy S., Benjamin M., *Modelling of Crack Opening Displacement due to Delamination Using First-Order Shear Laminate Theory*, 44th AiAA/ASME/ASCE/AHS Structures, Structural Dynamics and Material Conference, Norfolk, Virginia (AIAA 2003–1603), 2003.

[117] Santhanam Sridhar, *A $[90/0]_s$ Composite Laminate with Part-Through Matrix Cracks in Adjacent Plies*, Composite Structures, Vol. 53, Issue 4, pp. 499–509, 2001.

[118] Seeleuther Ph., Bai J., Baptiste D., François D., *Micromechanical Modelling of Damage Initiation in a Glass/Epoxy Lamina*tes, Joint Seminary on Failure of Advanced Materials, Paris, (Ed. by D. François, L. Gołaski), Wyd. Politechniki Świętokrzyskiej, pp. 27–35, 1996.

[119] Sharma P., Dasgupta A., *Scale-dependent Average Elastic Fields of Spherical and Cylindrical Inhomogeneities in Micropolar Medium and Overall Properties*, GE Research & Development Center, Report 2001CRD130, General Electric Corporation, 2001.

[120] Sih G. C., Chen E. P., *Cracks in Composite Materials*, Martinus Nijhoff Publishers, 1981.

[121] Smith P. A., Wood J. R., *Poisson's Ratio as a Damage Parameter in the Static Tensile Loading of Simple Crossply Laminates*, Comp. Sci. and Tech., 35, pp. 85–93, 1990.

[122] Spencer A. J. M., *Theory of Invariants*, Continuum Physics, ed. A. C. Eringen, Vol.1, Mathematics, Academic Press, pp. 239–353, 1971.

[123] Swenson D., James M., *FRANC2D/L: A Crack Propagation Simulator for Plane Layered Structures*, Short User's Guide, Version 1.4, Kansas State University, Manhattan, Kansas 1997.

[124] Talreja R., *Fatigue of Composite Materials*, Technomic Publishing Company, Lancaster, 1987.

[125] Talreja R., *Damage Development in Composites: Mechanisms and Modelling*, J. Strain Anal., 24, pp. 215–222, 1989.

[126] Talreja R., *Internal Variable Damage Mechanics of Composite Materials, Yielding, Damage, and Failure of Anisotropic Solids*, EGF5 (Ed. by J. P. Boehler), Mechanical Engineering Publications, London, pp. 509–533, 1990.

[127] Talreja R., *Damage Mechanics of Composite Materials Based on Thermodynamics with Internal Variables*, General Lecture, Durability Analysis of Polymer Based Composite Systems, Brussels, 27–31 Aug. 1990.

[128] Talreja R., Yalvac S., Yats L. D., Wetters D. G., *Transverse Cracking and Stiffness Reduction in Cross Ply Laminates of Different Matrix Toughness*, J. Composite Materials, 26, pp. 1644–1663, 1992.

[129] Tanaka Kohhei; Kanagawa Yasushi; Murakami Sumio, *Study on Evolution of Internal Damage in CFRP in Fatigue Process*, JSMS Original paper, Vol. 47, No. 5, pp. 440–446, 1998.

[130] Timoshenko S., Woinowsky-Krieger S., *Theory of Plates and Shells*, 2nd ed., McGraw-Hill, New York 1959.

[131] Toftegaard H., *Fibre Composites Edge Polishing of Fibre Composite Tensile Test Specimens*, Structure, Struers Metallographic News, No.13, pp. 14–15, 1986.

[132] Torquato S., *Modeling of Physical Properties of Composite Materials*, Int. J. of Solids and Structures, 37, pp. 411–422, 2000.

[133] Toyama N., Noda J., Okabe T., *Quantitative damage detection in cross-ply laminates using Lamb wave method*, Composite Materials, Composites Science and Technology, Vol. 63, Issue 10, pp. 1473–1479, 2003.

[134] Tsai S. W., Hahn T., *Introduction to Composite Materials*, I ed. Technomic Publishing Company Inc., 1980.

[135] Vakulenko A. A., Kachanov M. L., *Continuum Theory of Media with Cracks*, Mekh. Tv. Tela, No.4, pp. 159–166, 1971.

[136] Van Paepegem W., Degrieck J., De Baets P., *Finite Element Approach for Modelling Fatigue Damage in Fibre-reinforced Composite Materials*, Composites, Part B, 32 (7), pp. 575–588, 2001.

[137] Van Paepegem W., Degrieck J., *A New Coupled Approach of Residual Stiffness and Strength for Fatigue of Fibre-reinforced Composites*, Int. Journal of Fatigue, 24 (7), pp. 747–762, 2002.

[138] Van Paepegem W., Degrieck J., *Coupled Residual Stiffness and Strength Model for Fatigue of Fibre-reinforced Composite Materials*, Composites Science and Technology, 62 (5), pp. 687–696, 2002.

[139] Van Paepegem W., Degrieck J., *Calculation of damage-dependent directional failure indices from the Tsai-Wu static failure criterion*, Composite Materials, Composites Science and Technology, Vol. 63, Issue 2, pp. 305–310, 2003.

[140] Varna J., Berglund L. A., Talreja R., Jakovics A., *A Study of the Opening Displacement of Transverse Cracks in Cross-Ply Laminates*, Int. J. of Damage Mechanics, Vol. 2, No 3, pp. 272–289, 1993.

[141] Wada Akihiro; Motogi Shinya; Fukuda Takehito, *Prediction of Stiffness Reduction in Composite Laminates Using Damage Mechanics Approach*, JSMS Original paper, Vol. 48, No. 5 pp. 453–458, 1999.

[142] Whitworth H. A., *Evaluation of the residual strength degradation in composite laminates under fatigue loading*, Composite Structures, Vol. 48, Issue 4, pp. 261–264, 2000.

[143] Zang W., Gudmundson P., *Damage Evolution and Thermoelastic Properties of Composite Laminates*, Int. J. Damage Mechanics, Vol. 2, No 3, pp. 290–308, 1993.

[144] Życzkowski M., *An Attempt to Describe Heart Attacks via Continuum Damage Mechanics*, Archives of Mechanics, Vol. 52, No. 4–5, 2000.

SUMMARY

ПОВРЕЖДЕНИЯ СВЯЗУЮЩЕГО ВНУТРИ СЛОЕВ ВОЛОКНИСТЫХ КОМПОЗИТОВ

Резюме

Работа касается повреждений слоистых волокнистых композитов вида: связующие „epoxy”/волокна „carbon”.

Целью работы является исследовать воздействие повреждений на механические свойства слоистых волокнисиых пластиков.

Исследованию подвергаются повреждения проявляющиеся разрывом связующего внутри слоев, заключающиеся в возникновении, так называемых, первоначальных трещин в связующем. Дефекты этого типа были описаны с использованием симметрического тензора повреждений второго ранга в виде предлагаемом Вакуленко и Качановым. Благодаря этому можно принять геометрическое ориентирование дефектов, тщательно связаных с ориентированием слоев состовляюших слоистый композит. Растояние трещин было оценено с помощью механики разрушений линейно-упругой среды.

Чтобы описать изменения механических свойств материала под влиянием развивающихся повреждений, использовано физические соотношения связывающие напряжения, деформации и повреждения. В этой работе применено подход опираясь на инвариантных полиномиальных функциях и нередуцируемых базах интегральности, введеных Адкинсом.

Результаты вычислений, вытекающих из принятой теоретической модели, сравнено с экспериментальными данными, касающимися продольного модула Юнга и коэффициента Пуассона.

Одновременно вычисления сравнено с плотностью трещин слоистых композитов с продольно-поперечной армировкой и композитов с армировкой вида $[-20,+20,-\theta_2,-20,+20,+\theta_2,-20,+20]_s$, образованых из

ленты „prepreg”, типа оксиран/углеродное волокно, с коммерческим названием Vicotex NCHR 174B.

В работе подвергнуто анализу также результаты касающиеся воздействия развивающихся повреждений внутри композитного материала на его прочность.

USZKODZENIA WEWNĄTRZWARSTWOWE LAMINATÓW POLIMEROWYCH ZBROJONYCH WŁÓKNAMI

Streszczenie

Praca dotyczy zagadnienia pękania wewnątrzwarstwowego w kompozytach laminatowych o matrycy polimerowej, utworzonych z dowolnie zorientowanych warstw, z których każda jest jednokierunkowo zbrojona włóknami ciągłymi. Celem pracy było zbadanie wpływu powstających pęknięć na charakterystyki „inżynierskie" kompozytu, a także w pewnym stopniu na jego własności wytrzymałościowe.

Praca podzielona jest na dwie części, z których pierwsza dotyczy modelu teoretycznego, zaś druga zawiera opis wykonanych badań doświadczalnych, analizę uzyskanych wyników i weryfikacje modelu teoretycznego.

W załączniku przedstawiono podstawy klasycznej teorii laminatów, wykorzystanej w budowie modelu teoretycznego.

W pierwszej części pracy przedstawiono model teoretyczny wewnątrzwarstwowego pękania matrycy laminatów, składający się z trzech zasadniczych segmentów.

1. Opis pęknięć matrycy dowolnej warstwy laminatu w układzie tzw. osi materiałowych warstwy (konfiguracja *on-axis*) na gruncie mechaniki uszkodzeń kontynualnych.

   Do opisu stanu uszkodzenia wykorzystano koncepcję tensora uszkodzeń Kaczanowa-Vakulenki (tensor uszkodzeń II rzędu), wiążącego uszkodzenia uśrednione po reprezentatywnej objętości materiału z wektorem nieciągłości przemieszczeń powierzchni pęknięcia. W dalszej analizie ograniczono się do symetrycznej części tensora, opisującej przemieszczenia normalne brzegu pęknięcia.

   Przemieszczenia te wyznaczono dzięki zastosowaniu zaproponowanego w pracy pomysłu „pasma zastępczego". Umożliwia on w przybliżony sposób uwzględnienie tzw. efektu więzów. Występuje on w większości laminatów, gdyż z reguły warstwy uszkadzające się wskutek m.in. pękania matrycy są rozdzielone warstwami o takim zorientowaniu

włókien, które „hamuje" powiększanie się pęknięć wychodzących z warstw sąsiednich. Przy obliczaniu uśrednionego przemieszczenia normalnego brzegu pęknięcia zastosowano również rozwiązania, wynikające z liniowo-sprężystej mechaniki pękania.

2. Budowa związku konstytutywnego dla uszkodzonej pojedynczej warstwy kompozytowej w układzie osi materiałowych (konfiguracja *on-axis*).
   W celu skonstruowania równania konstytutywnego dla indywidualnej, uszkodzonej warstwy w jej osiach materiałowych wykorzystano formalne podejście zaproponowane przez Adkinsa. Zgodnie z tym podejściem, współrzędne tensora naprężenia powiązano z elementami tzw. nieredukowalnej bazy niezmienniczej – właściwej dla materiału o symetrii ortotropowej i dwóch symetrycznych tensorów II rzędu, a mianowicie tensora odkształcenia i tensora uszkodzenia – poprzez odpowiednie funkcje wielomianowe.
   W wyniku zastosowania tej metody otrzymano macierz sztywności dla uszkodzonej warstwy kompozytowej, którą zdekomponowano na macierz sztywności warstwy dziewiczej i macierz sztywności warstwy, związaną wyłącznie z uszkodzeniami matrycy. Współrzędne tej ostatniej macierzy zawierają nieznane stałe materiałowe, wynikające z zastosowanej funkcji wielomianowej, które należało następnie wyznaczyć doświadczalnie.
   W pracy wykazano, że zastosowane czysto matematyczne podejście oparte na równaniu Adkinsa jest formalnie w pełni równoważne podejściu energetycznemu, opartemu na tzw. termodynamice *Colemana-Gurtina* z wewnętrznymi zmiennymi stanu, prowadzącemu do macierzy sztywności poprzez zastosowanie wielomianowej postaci energii swobodnej Helmholtza.
3. Wyznaczenie macierzy sztywności dla laminatu symetrycznego w stanie tarczowym.
   W celu wyznaczenia macierzy sztywności warstwy w dowolnym układzie odniesienia – tzw. transformowanej macierzy sztywności – (konfiguracja *off-axis*) zastosowano klasyczną metodę *Tsaia-Pagano*.
   Globalną macierz sztywności tarczowej laminatu, w którym pewne warstwy mogą być uszkodzone, a inne pozostawać w stanie dziewiczym, wyznaczono w ramach klasycznej teorii laminatów.
   Dzięki takiemu podejściu możliwe jest uwzględnienie sekwencji ułożenia warstw, co różni przyjęty w niniejszej pracy model od innych – stosujących „homogenizację" materiału kompozytowego.

Korzystając z otrzymanej macierzy, określono zależności opisujące stałe inżynierskie kompozytu laminatowego, zawierające nieznane stałe materiałowe związane z istniejącymi uszkodzeniami, które należało wyznaczyć doświadczalnie.

Na podstawie uzyskanych rezultatów doświadczalnych, dotyczących stałych inżynierskich i gęstości szczelin wewnątrzwarstwowych dla jednej wybranej konfiguracji krzyżowej (*cross-ply)* laminatu, wyznaczono wartości liczbowe stałych materiałowych występujących w modelu teoretycznym.

W drugiej części pracy przedstawiono procedury doświadczalne wykorzystane do wyznaczenia niezbędnych w zaproponowanym modelu teoretycznym stałych materiałowych. W części tej pokazano również uzyskane wyniki doświadczalne dotyczące charakterystyk sztywnościowych, wytrzymałościowych i procesu pękania matrycy.

Dokonano także porównania wyników eksperymentalnych z obliczeniami wykonanymi w ramach przyjętego modelu teoretycznego.

Doświadczalna część pracy zawiera kilka zasadniczych elementów.

1. Szczegółowy opis procedury „fabrykacji" wielowarstwowych próbek kompozytowych, wykonanych z taśm „prepreg" *carbon/epoxy* o nazwie handlowej Ciba-Geigy Vicotex NCHR 174B, o modyfikowanej matrycy epoksydowej Vicotex 174, jednokierunkowo zbrojonej włóknami węglowymi Torayca T 300, na którą składają się:
   - sposób budowy próbek o żądanej konfiguracji krzyżowej i kątowej warstw (*cross-ply* i *angle-ply*);
   - technologia laminacji „stosu" warstw prowadząca do uzyskania materiału kompozytowego;
   - metoda przygotowania bocznych krawędzi próbek, poprzez szlifowanie i polerowanie z wykorzystaniem wyspecjalizowanego urządzenia DP-U4/Pedemax 2 i specjalnych materiałów polerskich (papiery szlifujące SiC, aerozole diamentowe DP, tkaniny polerujące DP-Dur, tarcze diamentowe Petrodisc-M, ciecze smarujące DP-Blue Lubricant) firmy STRUERS A/S Denmark. Zastosowana metoda pozwoliła uzyskać „jasne", lustrzane powierzchnie boczne próbek, umożliwiające mikroskopową obserwację procesu pękania wewnątrz określonych warstw próbki kompozytowej;
   - sposób umieszczania elektrooporowych czujników tensometrycznych na powierzchni próbek kompozytowych.

2. Szczegółowy opis procedury prowadzenia badań doświadczalnych na wytworzonych próbkach, obejmującej:
   - zestawienie stanowiska badawczego, składającego się z hydraulicznej maszyny wytrzymałościowej Instron sterowanej oprzyrządowaniem i oprogramowaniem firmy Hewlett-Packard, cyfrowych mostków pomiarowych firmy Brüel & Kjaer, plotterów „x–y" firmy Roland – rejestrujących graficznie zależność „siła *versus* przemieszczenie" oraz przesuwnego mikroskopu optycznego sprzężonego z kamerą firmy Canon, umożliwiających rejestrację pola szczelin wewnątrzwarstwowych na wybranym odcinku kontrolnym powierzchni bocznej próbki,
   - program obciążenia – obciążenie rozciągające, monotonicznie narastające z szybkością na tyle małą, aby możliwa była mikroskopowa obserwacja i zliczanie *in situ* powstających szczelin wewnątrzwarstwowych.
3. Opracowanie uzyskanych w trakcie badań wyników, a w szczególności:
   - przeprowadzenie analizy wytrzymałości podłużnej próbek w zależności od konfiguracji kątowej tworzących je warstw i ich grubości, a także porównanie wyników z przykładowymi, klasycznymi obliczeniami wytrzymałościowymi kompozytów laminatowych,
   - przeprowadzenie analizy zależności podłużnego modułu Younga i współczynnika Poissona od wielkości obciążenia,
   - przeprowadzenie analizy wpływu bieżącej (tzn. odpowiadającej aktualnej wielkości obciążenia) średniej gęstości szczelin wewnątrzwarstwowych na uzyskane doświadczalnie wartości wytrzymałości podłużnej i wymienione wcześniej podstawowe charakterystyki sprężyste.
4. Weryfikacja modelu teoretycznego poprzez porównanie wyników obliczeń wg modelu z wynikami doświadczeń.
   Korzystając z wyznaczonych na podstawie wyników doświadczalnych, a dotyczących jednej wybranej konfiguracji próbki, stałych materiałowych, wprowadzonych w modelu teoretycznym – na podstawie zależności otrzymanych z tego modelu, obliczono stałe inżynierskie dla innych konfiguracji laminatów (tak krzyżowych, jak i kątowych).
   Porównanie rezultatów teoretycznych z doświadczalnymi wykazało ich dobrą zgodność, szczególnie w przypadku laminatów krzyżowych (w tym przypadku można mówić o znakomitej zgodności). Niezależnie od konfiguracji laminatu lepszą zgodność wyników uzyskano w

przypadku podłużnego modułu sprężystości, w przypadku współczynnika Poissona była ona nieco gorsza.

Dla dwu konfiguracji laminatów kątowych model teoretyczny nie był w stanie prawidłowo opisać wyników doświadczalnych, co należało wiązać z tym, że zmiana charakterystyk sprężystych nie była w tych przypadkach stowarzyszona z niemal niewystępującym pękaniem matrycy.